

## **General Disclaimer**

### **One or more of the Following Statements may affect this Document**

- This document has been reproduced from the best copy furnished by the organizational source. It is being released in the interest of making available as much information as possible.
- This document may contain data, which exceeds the sheet parameters. It was furnished in this condition by the organizational source and is the best copy available.
- This document may contain tone-on-tone or color graphs, charts and/or pictures, which have been reproduced in black and white.
- This document is paginated as submitted by the original source.
- Portions of this document are not fully legible due to the historical nature of some of the material. However, it is the best reproduction available from the original submission.

NASA TECHNICAL  
MEMORANDUM

NASA TM X- 72746

NASA TM X- 72746

(NASA-TM-X-72746) HUMAN COMFORT RESPONSE TO  
RANDOM MOTIONS WITH A DOMINANT LONGITUDINAL  
MOTION (NASA) 88 p HC \$4.75 CSCL 05E

N75-32746

Unclass  
G3/53 41159

HUMAN COMFORT RESPONSE TO RANDOM MOTIONS  
WITH A DOMINANT LONGITUDINAL MOTION

Ralph W. Stone, Jr.

July 1975



This informal documentation medium is used to provide accelerated or special release of technical information to selected users. The contents may not meet NASA formal editing and publication standards, may be revised, or may be incorporated in another publication.

NATIONAL AERONAUTICS AND SPACE ADMINISTRATION  
LANGLEY RESEARCH CENTER, HAMPTON, VIRGINIA 23665

1. Report No. NASA TM X-72746	2. Government Accession No.	3. Recipient's Catalog No.	
4. Title and Subtitle  HUMAN COMFORT RESPONSE TO RANDOM MOTIONS WITH A DOMINANT LONGITUDINAL MOTION		5. Report Date July 1975	
6. Performing Organization Code			
7. Author(s)  Ralph W. Stone, Jr.		8. Performing Organization Report No.	
9. Performing Organization Name and Address  NASA Langley Research Center Hampton, VA 23665		10. Work Unit No. 504-09-21-02	
		11. Contract or Grant No.	
12. Sponsoring Agency Name and Address  National Aeronautics and Space Administration Washington, D.C. 20546		13. Type of Report and Period Covered Technical Memorandum	
		14. Sponsoring Agency Code	
15. Supplementary Notes			
16. Abstract  Subjective ride comfort response ratings have been measured on the Langley Visual Motion Simulator with longitudinal acceleration inputs with various power spectra shapes and magnitudes. The results show only little influence of spectra shape on comfort response. The effects of magnitude on comfort response indicate the applicability of psychophysical precepts for comfort modeling.			
17. Key Words (Suggested by Author(s)) (STAR category underlined)  Ride quality, simulations, response modeling <u>Star Category 05</u>		18. Distribution Statement  Unclassified - Unlimited	
19. Security Classif. (of this report)  Unclassified	20. Security Classif. (of this page)  Unclassified	21. No. of Pages 87	22. Price* \$4.75

\*Available from The National Technical Information Service, Springfield, Virginia 22151

STIF/NASA Scientific and Technical Information Facility, P.O. Box 33, College Park, MD 20740

HUMAN COMFORT RESPONSE TO  
RANDOM MOTIONS WITH A DOMINANT LONGITUDINAL MOTION

By Ralph W. Stone, Jr.

SUMMARY

The effects of random longitudinal accelerations on passenger ride comfort response were examined on the Langley Visual-Motion Simulator. The effects of power spectral density shape and frequency ranges from 0 to 2 Hz were studied. This paper presents the data obtained. There existed during this study motions in all other degrees of freedom, as well as the intended longitudinal motion, because of the characteristics of the simulator. These unwanted motions may introduce some interactive effects which should be considered in any analysis of the data.

INTRODUCTION

An increase in short-haul operations using short take-off and landing aircraft is expected (ref. (1)). Such operations, which are at low altitudes and with relatively low wing loading aircraft, will probably lead to conditions of flight where the ride quality will be degraded compared to that experienced in current jet aircraft operations. Accordingly, the consideration of ride comfort will probably become increasingly important. Understanding and defining the problems of passenger acceptance, and developing methods and systems for aircraft design that will allow for acceptable ride comfort, are encompassed in a NASA program (ref. (2)). This program includes the simultaneous measurement of subjective ride comfort responses and vehicle motions made on both scheduled airlines and simulators.

Much data have been obtained and ride comfort indices and acceptance ratings have been developed based on human exposures to the full six degree of freedom motion of aircraft (refs. (3), (4), (5), (6), and (7), for example). The interactions of the various degrees of freedom of motion as they affect human comfort responses is not known. The nature of these interactions is important to the understanding of the total comfort response. In addition, data available for subjective comfort responses to single degree of freedom motions exist primarily for sinusoidal oscillations at specific frequencies (ref. (8)).

The influence of single degree of freedom motions having random oscillations typical of those of aircraft in turbulence also is not known. Typical airplane response to turbulence have power spectra shape that decreases rapidly beyond 1 to 2 Hertz. However, some response motions of the airplane (particularly the angular motion) have a somewhat flatter power spectra shape. It is not known if these different spectral shapes will have a significant

influence on the ride comfort. Consequently, a program to measure human comfort response ratings in single degree of freedom random motions and the interactions of these motions in two, three, and six degrees of freedom using two types of power spectra shapes and three frequency ranges is in progress at the NASA Langley Research Center. References (9) and (10) present the data obtained for the studies of the subjective ride comfort response to random vertical and transverse accelerations, respectively. The present paper presents the subjective ride comfort response ratings obtained when using oscillations in the longitudinal degree of freedom on the Visual-Motion Simulator at Langley (fig. 1).

#### SYMBOLS

$\sigma_{R_s}$	standard deviation of ride quality rating
g	acceleration due to gravity
Hz	frequency, cps

#### TESTS AND TEST CONDITIONS

The investigation was initiated to measure human comfort response ratings to single degree of freedom motions and to multiple degree of freedom motions using random motions like those experienced in airplane flight. A program was developed using 14 separate simulator "flights," each flight consisting of 24 segments. Each of the segments consisted of either a single degree of freedom motion, a two-, three-, or six-degree of freedom motion. The segments for the six single degrees of freedom (vertical, transverse, longitudinal acceleration and pitch, roll and yaw rates) were scattered throughout six flights. Any one single degree of freedom was contained within only two of the six flights. The various two degrees of freedom segments were similarly scattered throughout four flights. The various three degrees of freedom segments were scattered throughout two flights, and six degrees of freedom similarly in two flights.

As mentioned previously, typical airplane responses to turbulence have power spectra that decreases rapidly beyond 1 to 2 Hertz. However, some responses, particularly for angular motions, have flatter power spectra. In order to investigate the effect of spectral shape and the frequency distribution of the response power on ride comfort, six power spectral density distributions were developed to drive the simulator. There were two general groups, the first termed "typical," having variation with frequency like those experienced on typical aircraft and the second termed "flat" with shallower decreases at the high frequencies. In each group, three distinct frequency distributions were used; the first with peak power centered between 0 and 1 Hz, the second between 0 and 2 Hz, and the third between 1 and 2 Hz.

The six power spectra shapes were tailored by filtering the output of a random number generator. The nominal shapes of these spectra are shown in figure 2. In designing the spectra shapes to suit the simulator characteristics the "flat" spectra were not as flat as was intended and in figure 2 appear similar to those of the "typical" spectra. However, the "flat" spectra have more power in the 1 to 3 Hz range than the typical spectra for conditions with the same peak power. This increase in power, over the typical spectra, ranges from 35 percent for the 1 to 2 Hz spectra to 170 percent for the 0 to 1 Hz spectra.

The nominal spectra shown in figure 2 are normalized to have a peak of 1. For the actual motions on the simulator the magnitude was raised for each spectra type by adjusting the gain of the input signal. Four magnitudes were examined for each of the six spectra shapes. Thus, the 24 flight segments were developed for use in the study.

The Langley Visual-Motion Simulator (VMS) is primarily used for piloted flight, stability, control, and display studies, and does not contain a passenger compartment. The passengers used in this study sat in the pilot's compartment and rode passively, the controls and instruments being inoperative for these experiments. Figure 3 is an interior view of the cockpit. Two passengers rode each experimental "flight."

The normal operational envelope of motion frequencies and magnitudes of the VMS are presented in reference (2). The largest practicable input frequency is about 3 Hz. As noted in references (6) and (7), the major energy in aircraft motions is in the region of 2 Hertz and less.

The VMS is a large mechanical device with six hydraulically operated telescoping legs and associated switching valves. The desired motions are developed by extending the legs in a prescribed manner. In order to obtain the desired motions without exceeding the mechanical limitations of the simulator, various control and limiting systems were incorporated. The simulator, as a dynamic device, has its own natural frequencies and damping, and thus exerts an effect on the resulting motion. For precise development of a single degree of freedom, the six legs would have to move synchronously. Because of friction in the hydraulic systems and valves, and variations in the hydraulic pressure, it was not possible to produce the precise conditions necessary for one degree of freedom. Therefore, the motions developed by the simulator had the longitudinal acceleration as the dominant motion with various lesser amounts of the other five degrees of freedom present. For these same reasons, the motions were not precisely duplicated even for identical computer inputs. As a result of the dynamic characteristics of the simulator, the actual motion power spectra experienced by the subjects was somewhat different than the nominal spectra used as input to the computer. The four different magnitudes mentioned previously were supposed to be alike for each input spectra shape; however, because of the dynamic response characteristics of the simulator, it provided different RMS values of the longitudinal accelerations for the different spectra shapes.

Each "flight" was flown four to five times so that 8 to 10 subjects experienced each motion. As these "flights" were not precisely duplicated, the data discussed in the "Data" section of this paper are the average values of the four or five "flights" used. The standard deviation of the longitudinal accelerations from the average values for the various segments in terms of percent of the average values is 6.39 percent. The maximum deviation was 11.06 percent. The actual output of the simulator for a test segment representing most nearly the average output for a given input segment and, therefore, the motions essentially experienced by the subjects are presented in figures 4 to 9. Those include time histories for all six degrees of freedom, histograms of the longitudinal acceleration, and power spectral densities of the longitudinal accelerations for the 24 segments of "flight" as follows:

Figure	Spectra shape	Frequency range
4	Typical	0-1 Hz
5	"	0-2 Hz
6	"	1-2 Hz
7	Flat	0-1 Hz
8	"	0-2 Hz
9	"	1-2 Hz

The four segments of motion in each figure are for progressively increasing values of longitudinal acceleration.

The reference axis used was relative to the seated passengers and is shown in figure 10. The longitudinal accelerations used for this paper were along the longitudinal axis shown in figure 10. The actual motions of the simulator, as experienced by the passengers, were measured by an inertial instrument package containing three linear accelerometers, one aligned with each axis, and three rate gyros also aligned with each axis.

As noted previously, 24 segments of flight were used in examining the longitudinal degree of freedom. These 24 segments were randomly scattered in two "flights." Each flight was 36 minutes long and consisted of 24, one- and one-half minute segments. The subjects rated a 20-second portion in the center of each segment. A computer-driven buzzer system was used to identify this center portion of the segments. The subjects were instructed to consider only this 20-second segment of "flight" when making their comfort response rating. The subjects rated the segments on a seven-statement scale, as follows:

- Very comfortable
- Comfortable
- Somewhat comfortable
- Acceptable
- Somewhat uncomfortable
- Uncomfortable
- Very uncomfortable

Many subjective ride comfort indices have been based on a five-point numerical scale (see refs. (4) and (7), for example). Accordingly, for analysis purposes the seven-statement rating scale was converted to numerical values for a five-point scale as follows:

- 1 = Very comfortable
- 2 = Comfortable
- 2-1/2 = Somewhat comfortable
- 3 = Acceptable
- 3-1/2 = Somewhat uncomfortable
- 4 = Uncomfortable
- 5 = Very uncomfortable

For the data presented herein, average numerical ratings for the 8 to 10 subjects based on this scale and standard deviations from these averages are used.

The subjects, in general, were supplied by the Hampton Institute and consisted of a relatively broad spectra of people. For the total program, 138 passenger "flights" were made using a total of 98 persons. No person rode the same flight twice. A general profile of the persons used on these "flights" is shown in table I.

#### DATA

The mean RMS values for all six degrees of freedom of the four or five "flights" performed for each input segment along with the mean subjective ride comfort response ratings ( $R_s$ ) are shown in table II. The standard deviation of the response ratings for the passenger group on each "flight" segment are also shown in table II. Cross-correlation coefficients for the various motion components are shown in table III. The four segments of motion on tables II and III for each spectra shape are for progressively increasing values of RMS longitudinal acceleration.

As noted previously, the data presented herein are for longitudinal motion inputs and the existence of the other motion components in tables II and III are the result of simulator characteristics. Until data is available for each degree of freedom of motion and for combined motions, it will not be clear how significant the existence of the other motion components are in the subjective ride comfort responses presented in this paper. The longitudinal RMS accelerations varied from about 1.07 to 7.28 times larger than the vertical or transverse RMS accelerations that occurred. These can be compared because they are similar types of stimulation to the longitudinal RMS acceleration. Because the angular RMS velocities are a different form of stimulation than the linear accelerations, no comparison as to their relative significance to the longitudinal RMS acceleration can be directly made. It should be noted that the values range from about 0.59 to 1.60 degrees per second and have an average value of 0.917 degrees per second. Estimates of thresholds of perception of angular velocity (see refs. (11) and (12)) range from about 0.5 to 4.0 degrees per second. The values of RMS angular velocity that existed in the experiment to

study the response to longitudinal motion are therefore near the estimates of thresholds of perception and may not have had important influences on the comfort responses of this paper. Any analysis made of the data presented herein should maintain cognizance of the existence and possible influence of motion in the degrees of freedom other than longitudinal.

The subjective ride comfort responses presented on table II have an average standard deviation for all 24 segments of 0.579. This compares favorably with other experiences as, for example, the average standard deviation of the ride quality index for the results of reference (7) is 0.758 units of response rating. The value of 0.579 for this longitudinal acceleration study is somewhat smaller than that for the vertical and transverse motions of references (9) and (10), respectively.

As expected, there is a progressive increase in response ratings with increasing longitudinal acceleration. The variation (table II) is not, however, a linear function of longitudinal acceleration. The subjective ride comfort responses are therefore plotted against the  $\log_{10}$  of the RMS longitudinal accelerations for typical power spectra in figure 11 and for flat power spectra in figure 12. Thus plotted, the data show a nearly linear variation of the response, with the  $\log_{10}$  of the acceleration stimulus. This observation implies that the comfort response to RMS longitudinal accelerations conforms to the laws of psychophysical responses, wherein the response varies with the  $\log_{10}$  of the stimulus (ref. (13)).

#### CONCLUDING REMARKS

A study has been made on the Langley Visual-Motion Simulator to examine the influence of random longitudinal accelerations on human subjective ride comfort responses. The effects of two general shapes of power spectral density of the longitudinal acceleration for three frequency ranges in the 0 to 2 Hz region were examined. The data obtained in this study are presented in this paper. Although this study was made basically to examine the influence of random longitudinal accelerations, because of the characteristics of the simulator there occurred in the study some amounts of motion in all other degrees of freedom. Analysis of these data must maintain cognizance of this fact. The response data appear to vary linearly with the  $\log_{10}$  of the longitudinal RMS accelerations indicating congruity with psychophysical law.

## REFERENCES

1. DOT TST-10-4, NASA SP-265. Joint DOT-NASA Civil Aviation Research and Development Policy Study, March 1971.
2. NASA TM X-2620. Symposium on Vehicle Ride Quality Held at Langley Research Center, Hampton, Virginia, July 6-7, 1972, October 1972.
3. Jacobson, Ira D.: Environmental Criteria for Human Comfort - A Study of the Related Literature. NASA CR-132424, University of Virginia, Charlottesville, Virginia, February 1974.
4. Jacobson, Ira D.; and Richards, Larry G.: Ride Quality Evaluation II: Modelling of Airline Passenger Comfort. Memorandum Report 403217, University of Virginia, Charlottesville, December 1974.
5. Gruesbeck, Marta G.; and Sullivan, Daniel F.: Aircraft Motion and Passenger Comfort Data From Scheduled Commercial Airline Flights. University of Virginia, Charlottesville, Virginia, May 1974.
6. Stephens, David G.: Development and Application of Ride-Quality Criteria. NASA TM X-72008, September 1974.
7. Stone, Ralph W., Jr.: Ride Quality - An Exploratory Study and Criteria Development. NASA TM X-71922, February 1974.
8. International Organization for Standardization, International Standard ISO/DIS 2631. Guide for the Evaluation of Human Exposure to Whole-Body Vibration. 1972.
9. Stone, Ralph W., Jr.: Human Comfort Response to Random Motions With a Dominant Vertical Motion. NASA TM X-72691, May 1975.
10. Stone, Ralph W., Jr.: Human Comfort Response to Random Motions With a Dominant Transverse Motion. NASA TM X-72694, May 1975.
11. Stewart, John D.: Human Perception of Angular Acceleration and Implications in Motion Simulation, AIAA Paper No. 70-350, 1970.
12. Ormsby, Charles C.: Model of Human Dynamic Orientation. NASA CR-132537, 1974.
13. Stevens, S. S.: Neural Events and Psychophysical Law. Science, Vol. 170, pp. 1043-1050. 1970.

TABLE I. - PASSENGER PROFILE FOR  
VMS RIDE QUALITY PROGRAM

Total Passengers - 98 Persons

Sex Distribution

	Number	%
Males	47	48
Females	51	52

Age Distribution

	Number	%	Sex	
			Male	Female
18-25 yrs	55	56	44%	56%
26-45 yrs	30	31	47%	53%
46 → yrs	13	13	69%	31%

TABLE II.- MEAN RMS VALUES OF MEASURED MOTION COMPONENTS WITH LONGITUDINAL ACCELERATION INPUTS AND MEAN RIDE COMFORT RESPONSES.

Longitudinal acc. g	Transverse acc. g	Vertical acc. g	Pitching velocity deg/sec	Rolling velocity deg/sec	Yawing velocity deg/sec	R <sub>s</sub>	R <sub>s</sub>
<b>(a) Typical 0-1 Hz inputs</b>							
0.0164	0.0078	0.0064	0.6830	1.0804	0.5968	1.812	0.753
.0326	.0103	.0085	.8083	1.2972	.7033	2.938	.417
.0655	.0135	.0110	.8813	1.4321	.7611	3.375	.517
.0734	.0136	.0107	.7948	1.3374	.6978	3.875	.582
<b>(b) Typical 0-2 Hz inputs</b>							
0.0141	0.0089	0.0075	0.8004	1.2506	0.6972	2.000	0.534
.0315	.0091	.0076	.6963	1.0887	.6020	2.812	.259
.0598	.01272	.0108	.7272	1.1566	.5705	3.625	.232
.0900	.01822	.01459	.9390	1.6012	.7524	4.312	.753
<b>(c) Typical 1-2 Hz inputs</b>							
0.0098	0.0078	0.0067	0.7013	1.1381	0.6138	1.562	0.821
.0291	.0092	.0094	.7754	1.2379	.6642	3.125	.443
.0545	.0125	.0127	.8400	1.3301	.6771	4.000	.463
.0798	.0160	.0163	.8549	1.4049	.6009	4.375	.694

TABLE II. - MEAN RMS VALUES OF MEASURED MOTION COMPONENTS WITH LONGITUDINAL ACCELERATION INPUTS AND MEAN RIDE COMFORT RESPONSES (CONTINUED).

Longitudinal acc. g	Transverse acc. g	Vertical acc. g	Pitching velocity g	Rolling velocity g	Yawing velocity g	R <sub>s</sub>	$\sigma_{R_s}$
<b>(d) Flat 0-1 Hz inputs</b>							
0.0138	0.0079	0.0066	0.7009	1.1005	0.6052	2.562	0.563
.0301	.0091	.0079	.7339	1.1304	.6195	2.625	.582
.0727	.0137	.0111	.9570	1.4898	.7767	3.688	.651
.0866	.0148	.0119	.9012	1.3508	.7236	4.250	.463
<b>(e) Flat 0-2 Hz inputs</b>							
0.0120	0.0078	0.0063	0.6869	1.0697	0.5992	2.000	0.534
.0315	.0102	.0093	.6247	1.2978	.6827	2.938	.496
.0571	.0124	.0114	.8453	1.3425	.6782	3.688	.372
.0835	.0160	.0145	.5628	1.4144	.7551	4.375	.694
<b>(f) Flat 1-2 Hz inputs</b>							
0.0086	0.0080	0.0070	0.7508	1.1769	0.6591	2.375	1.482
.0275	.0091	.0098	.7528	1.1908	.6331	2.625	.834
.0510	.0120	.01418	.9424	1.4200	.7362	3.312	.438
.0790	.0155	.01833	.9422	1.4175	.6660	3.875	1.061

TABLE III.- CROSS-CORRELATION COEFFICIENTS OF MOTION COMPONENTS WITH LONGITUDINAL ACCELERATION INPUTS.

Longitudinal -Vertical	Longitudinal -Pitch	Transverse -Roll	Transverse -Yaw	Vertical -Pitch	Roll -Yaw
<b>(a) Typical 0-1 Hz inputs</b>					
0.3424	0.3745	0.6528	0.8023	0.8468	0.8908
.2919	.3142	.6532	.7768	.8136	.8979
.0479	-.0352	.3134	.5189	.5738	.7441
.0309	-.1417	.2236	.4229	.5838	.7147
<b>(b) Typical 0-2 Hz inputs</b>					
0.4551	0.4716	0.7471	0.8650	0.8850	0.9210
.2707	.1426	.5133	.7032	.6997	.8403
.1764	-.0995	.2673	.4816	.5243	.7500
.1264	-.2678	.6330	.2947	.3866	.4491
<b>(c) Typical 1-0 Hz inputs</b>					
0.5401	0.6463	0.6621	0.8353	0.8513	0.8854
.2976	.1744	.6352	.7919	.6609	.8841
.2393	-.1208	.2289	.5140	.4541	.7277
.1392	-.2919	.1123	.3638	.4187	.7124

TABLE III.- CROSS-CORRELATION COEFFICIENTS OF MOTION COMPONENTS WITH  
LONGITUDINAL ACCELERATION INPUTS (CONTINUED).

Longitu. <sup>l</sup> inal -Vertical	Longitudinal -Pitch	Transverse -Roll	Transverse -Yaw	Vertical -Pitch	Roll -Yaw
<b>(d) Flat 0-1 Hz inputs</b>					
0.5137	0.5495	0.7940	0.8906	0.9119	0.9544
.2982	.1993	.5806	.7690	.7605	.8905
.0612	-.0693	.4113	.5935	.7044	.8362
.1335	-.0950	.1991	.1120	.5522	.6976
<b>(e) Flat 0-2 Hz inputs</b>					
0.5134	0.5227	0.7387	0.8715	0.8930	0.9411
.3382	.2131	.6405	.8177	.7679	.9015
.2778	.0468	.4096	.5786	.6466	.8241
.1769	-.02664	.1416	.4301	.4221	.6583
<b>(f) Flat 1-2 Hz inputs</b>					
0.6993	0.7681	0.8191	0.9179	0.9268	0.9559
.2977	.1419	.6400	.8186	.6654	.8944
.2396	-.0164	.5260	.7210	.5706	.8787
.1860	-.3156	.1258	.4624	.2819	.6672

PRECEDING PAGE BLANK NOT FILMED

ORIGINAL PAGE IS  
OF POOR QUALITY

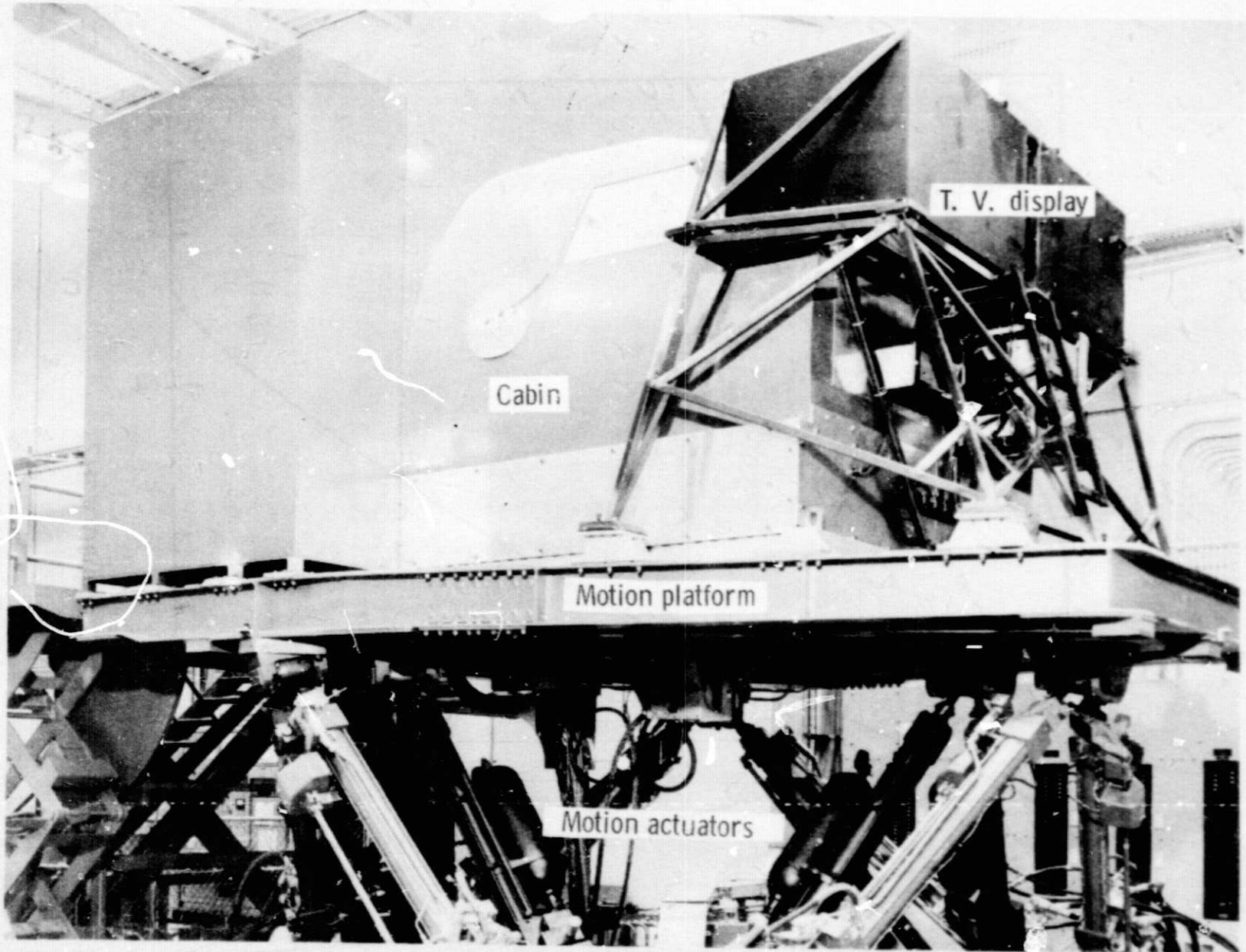
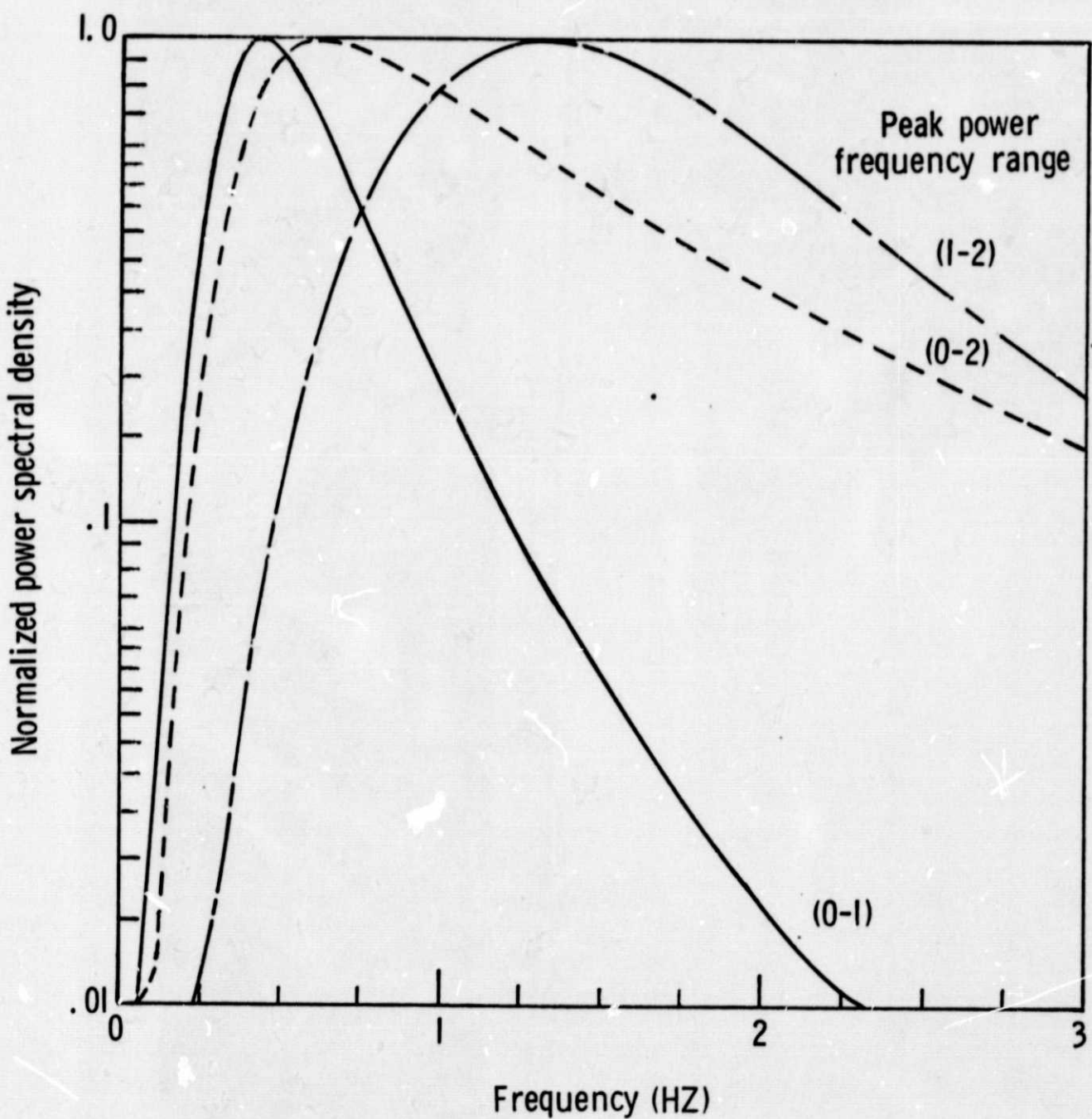
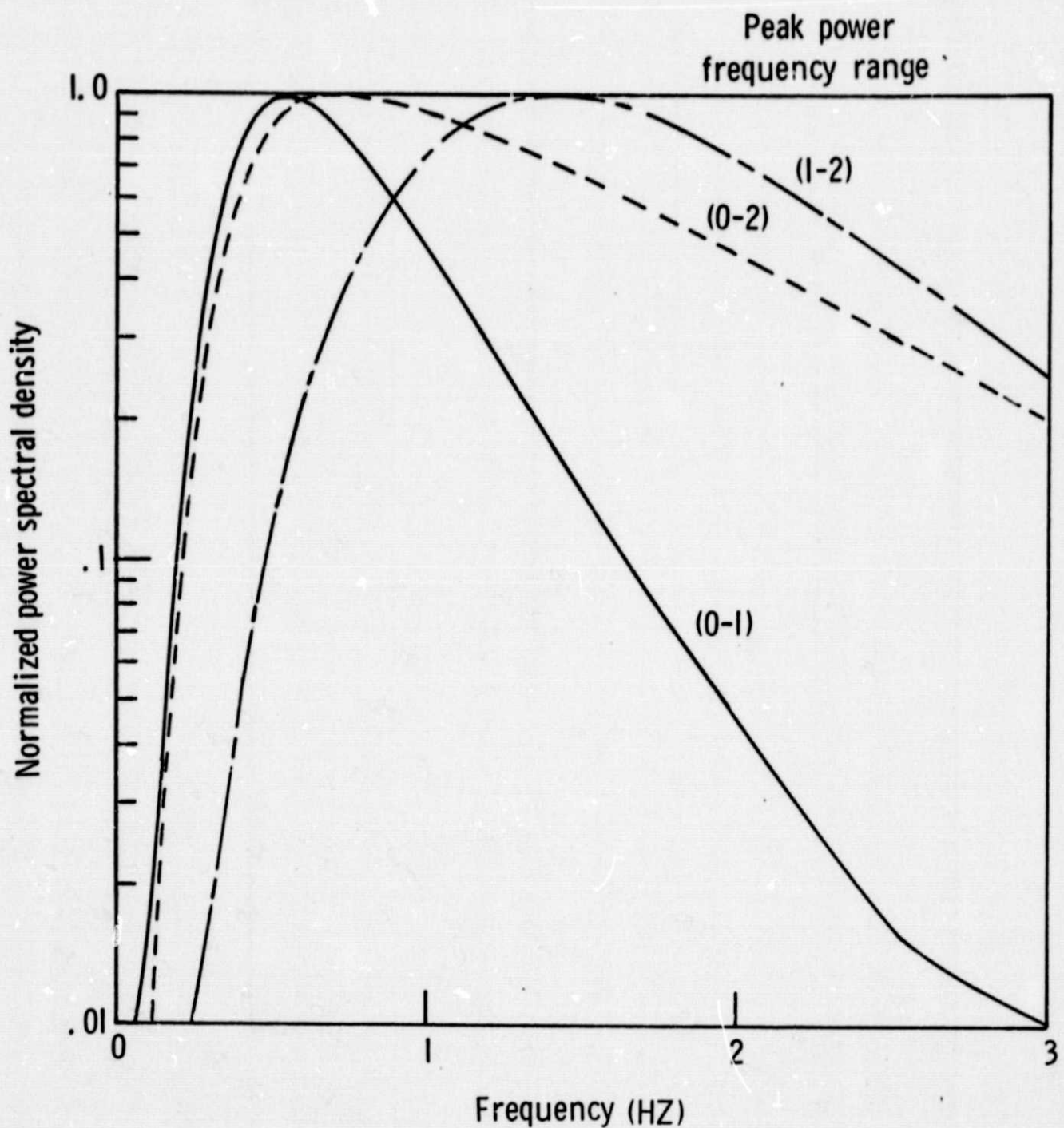


Figure 1.- Langley six-degree-of-freedom visual-motion simulator.



(a) Typical spectra.

Figure 2.- Nominal power spectra of motion components.



(b) Flat spectra

Figure 2.- Concluded.

ORIGINAL PAGE IS  
OF POOR QUALITY

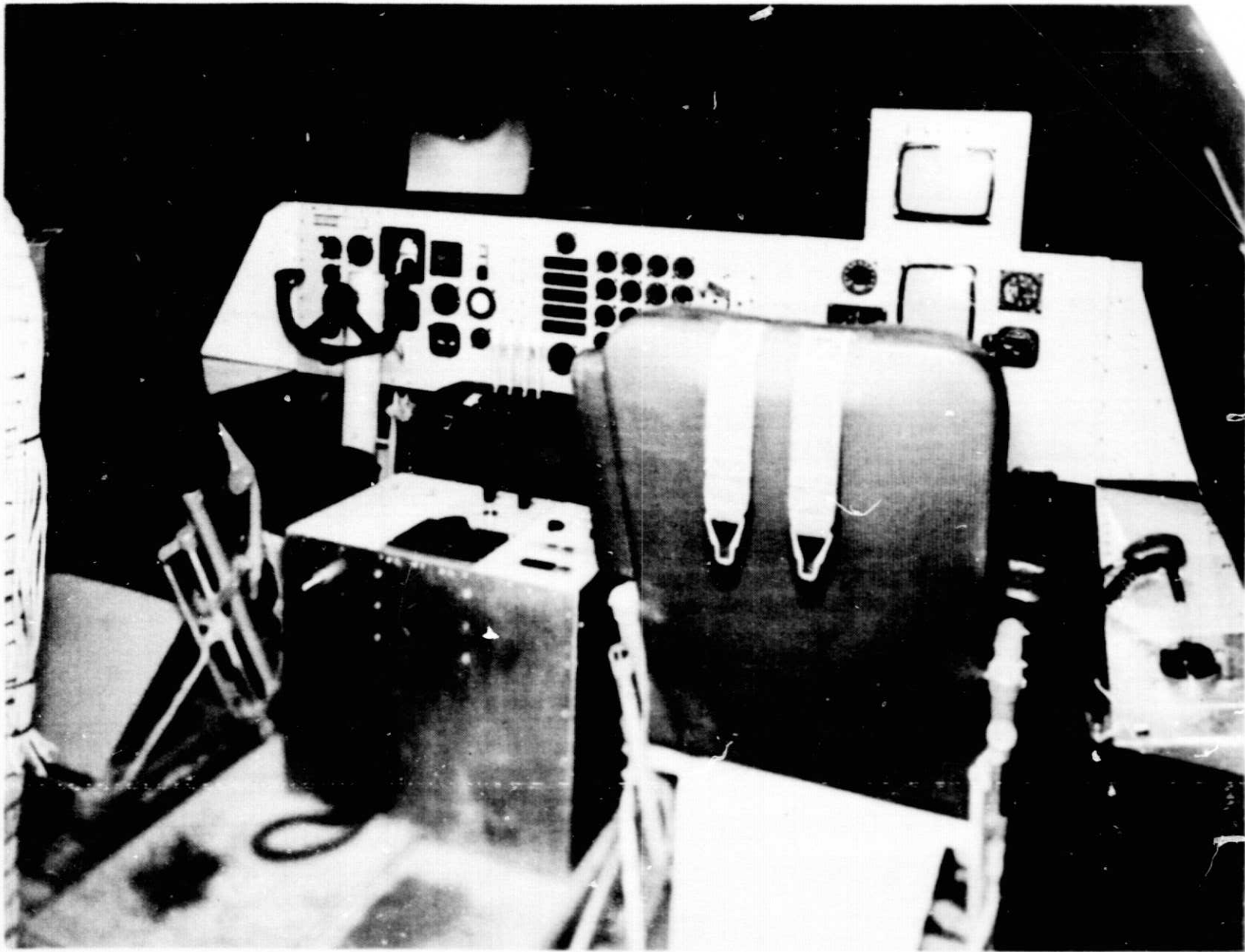


Figure 3.- Interior of Langley Six-Degree-of-Freedom, Visual Motion Simulator.



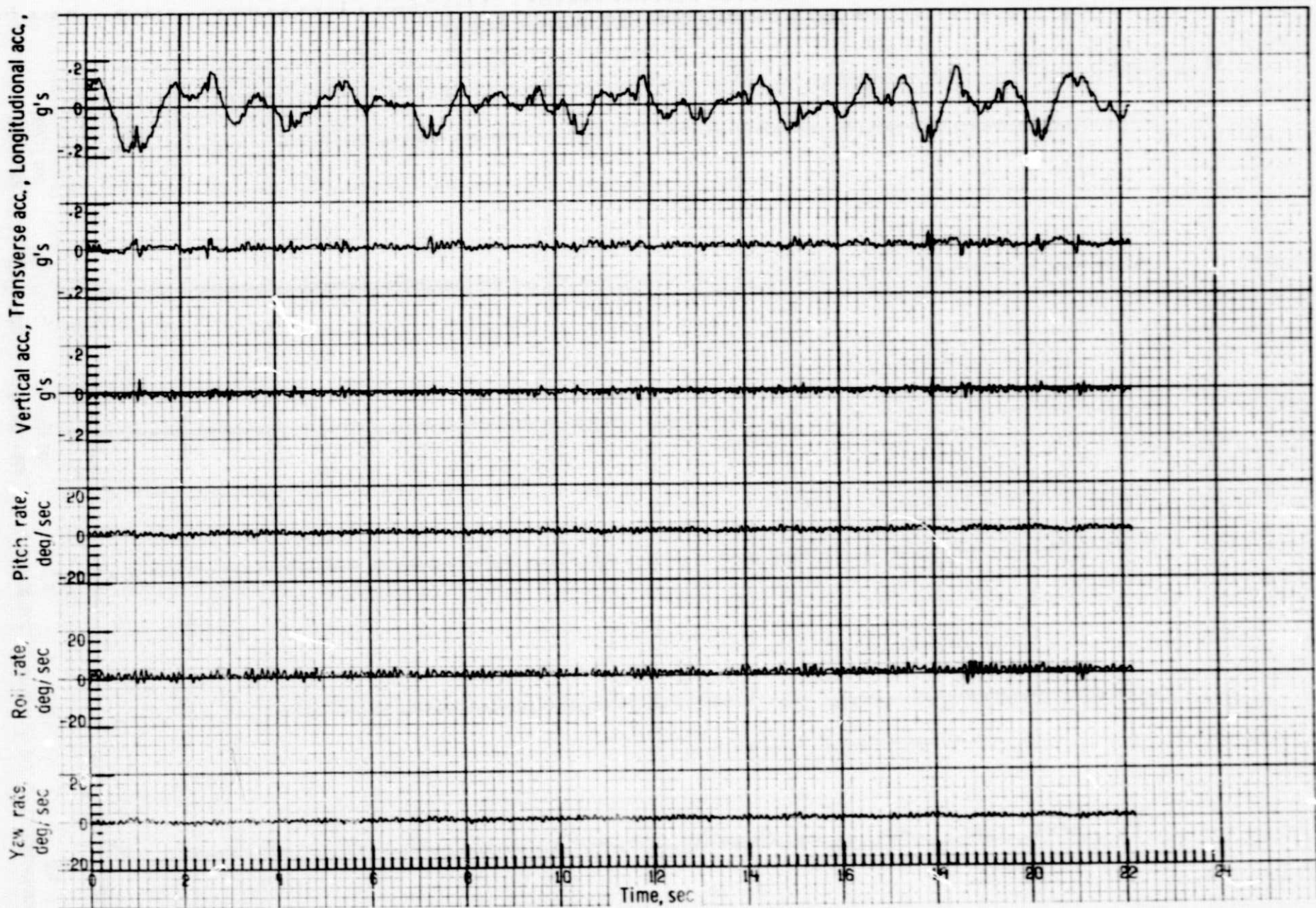
(a) Time histories (RMS longitudinal acc. 0.0164 g).

Figure 4. Measured motion characteristics using longitudinal acc.  
with typical 0-1 Hz inputs.



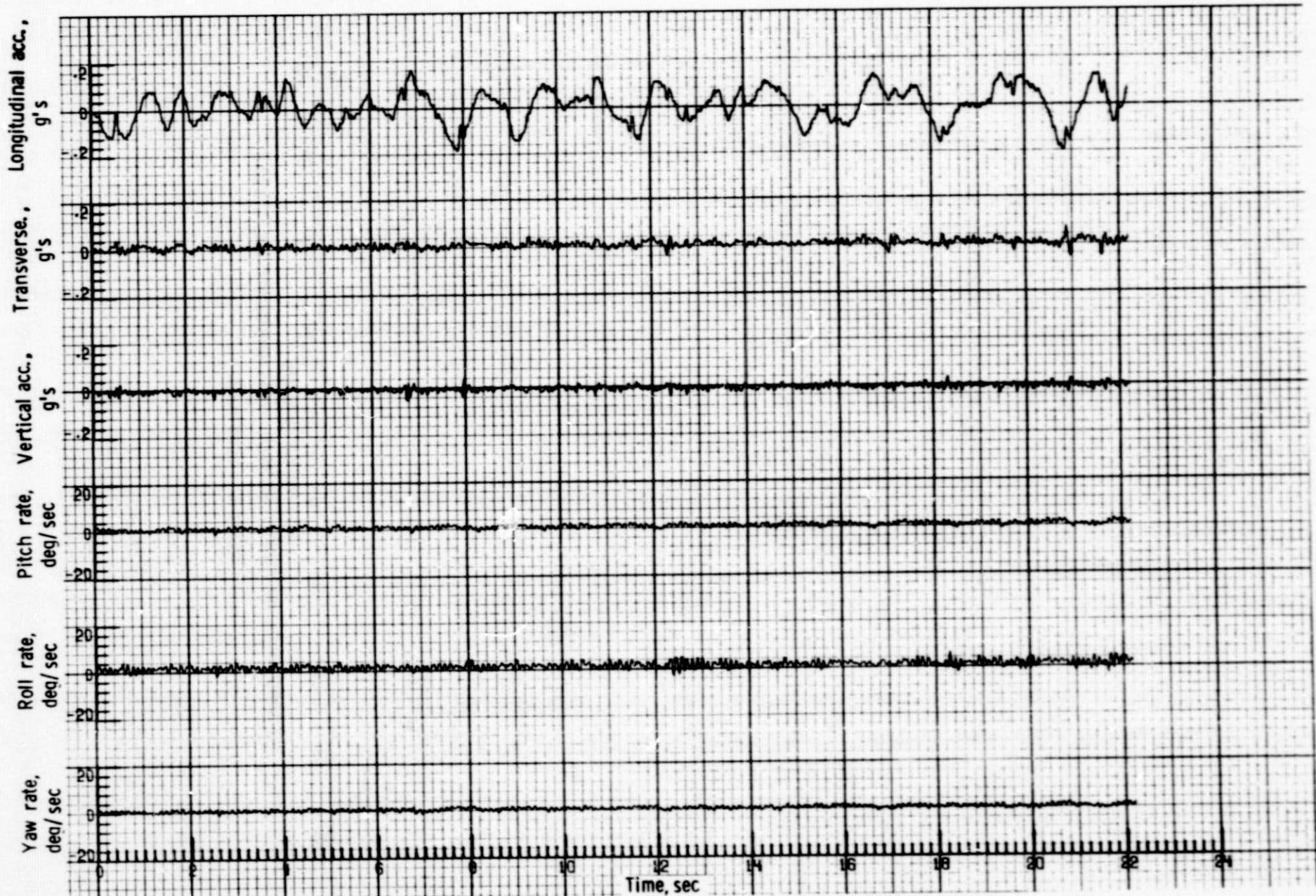
(a) Time histories (RMS longitudinal acc. 0.0326 g).

Figure 4 - Continued.



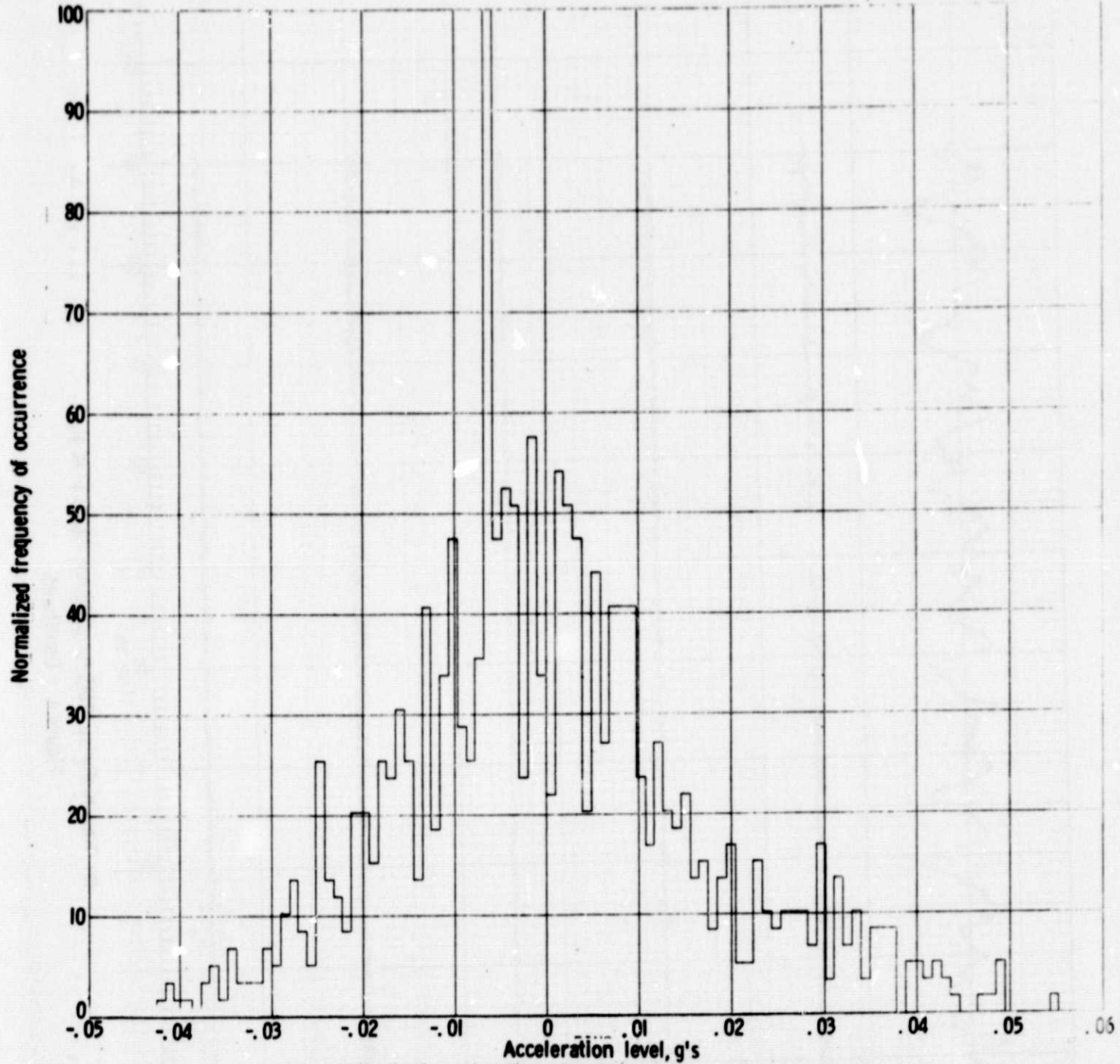
(a) Time histories (RMS longitudinal acc. 0.0655 g).

Figure 4 - Continued.



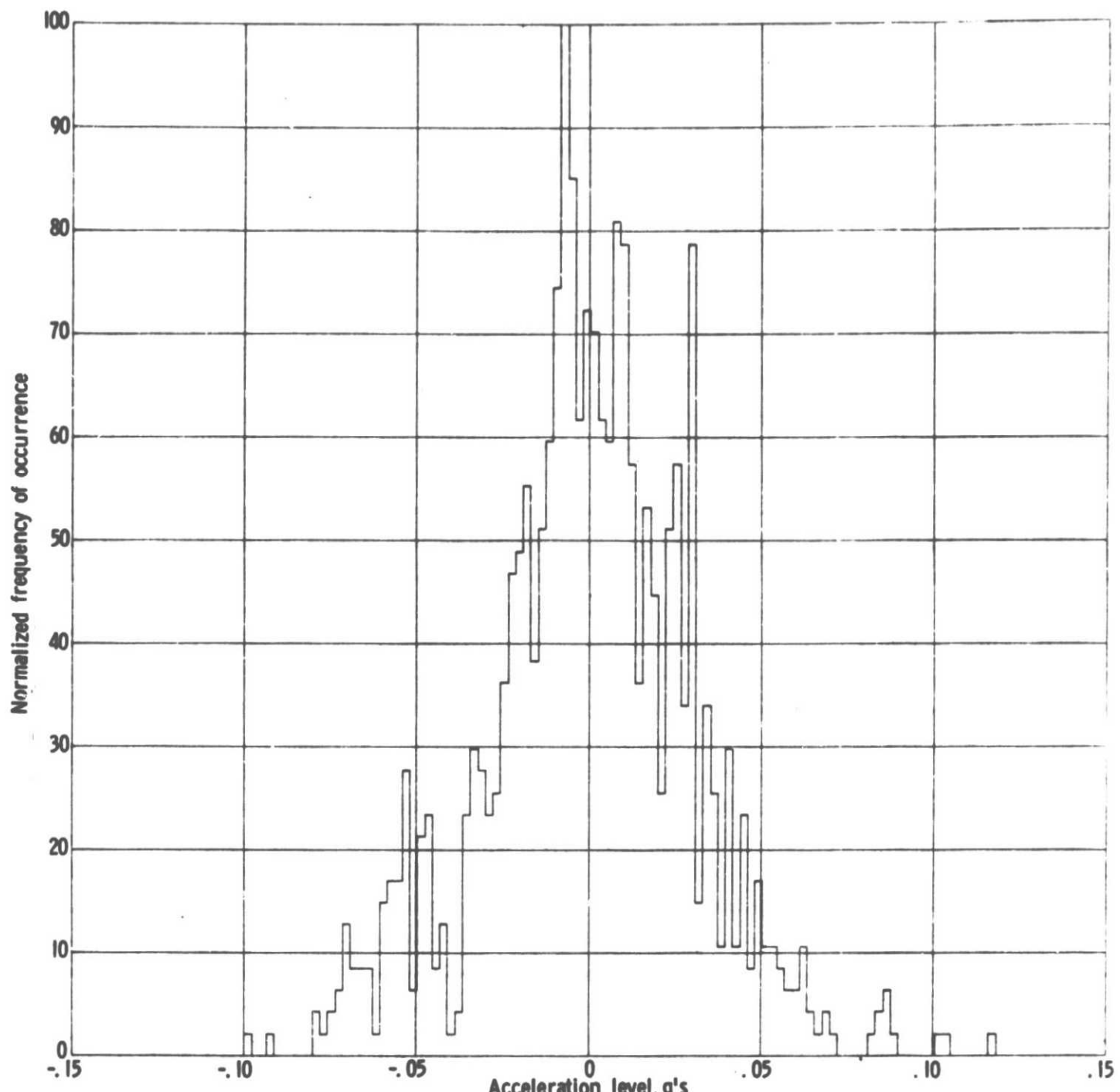
(a) Time histories (RMS longitudinal acc. 0.0734 g).

Figure 4 - Continued.

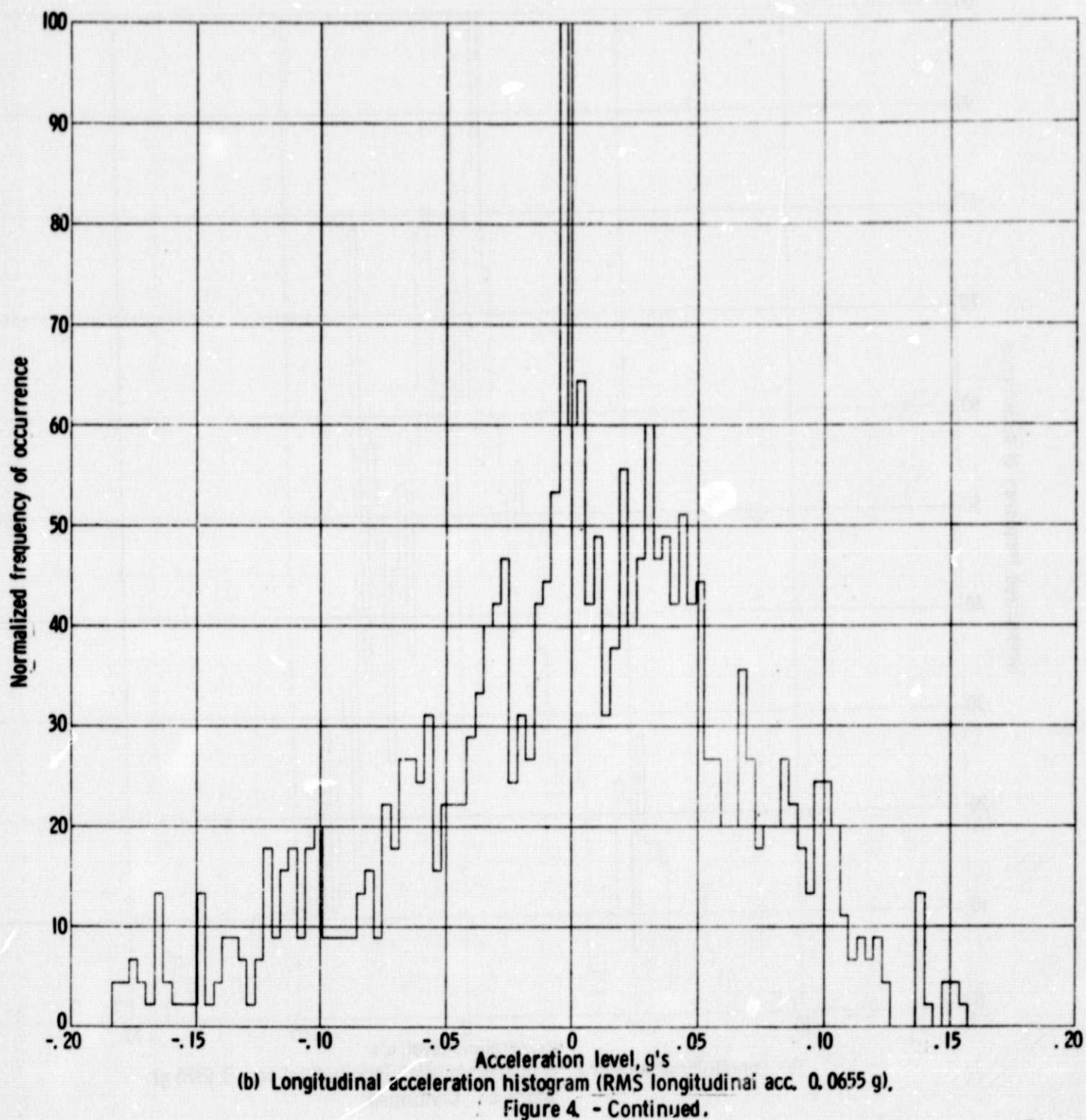


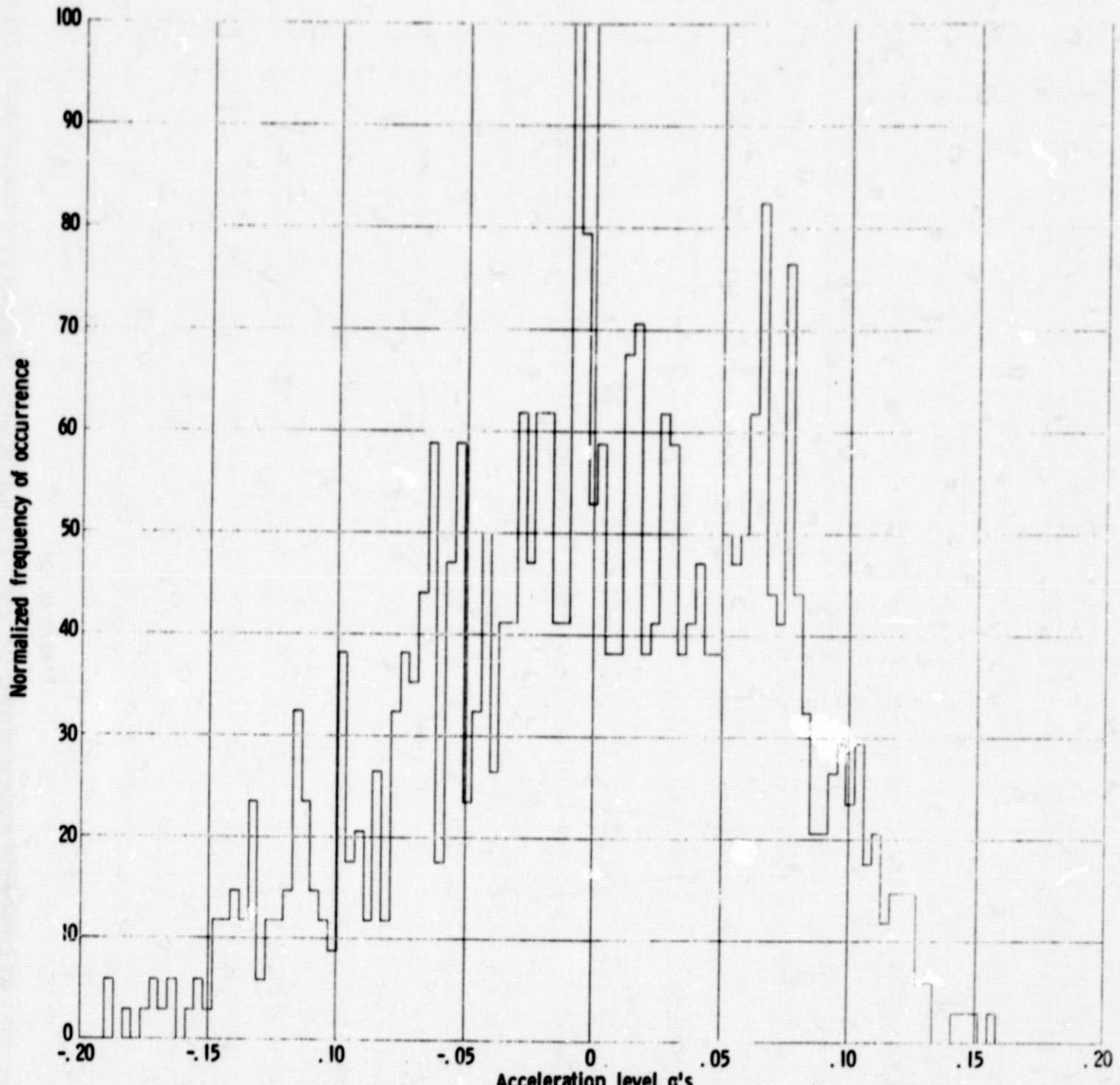
(b) Longitudinal acceleration histogram (RMS longitudinal acc. 0.0164 g).

Figure 4. - Continued.



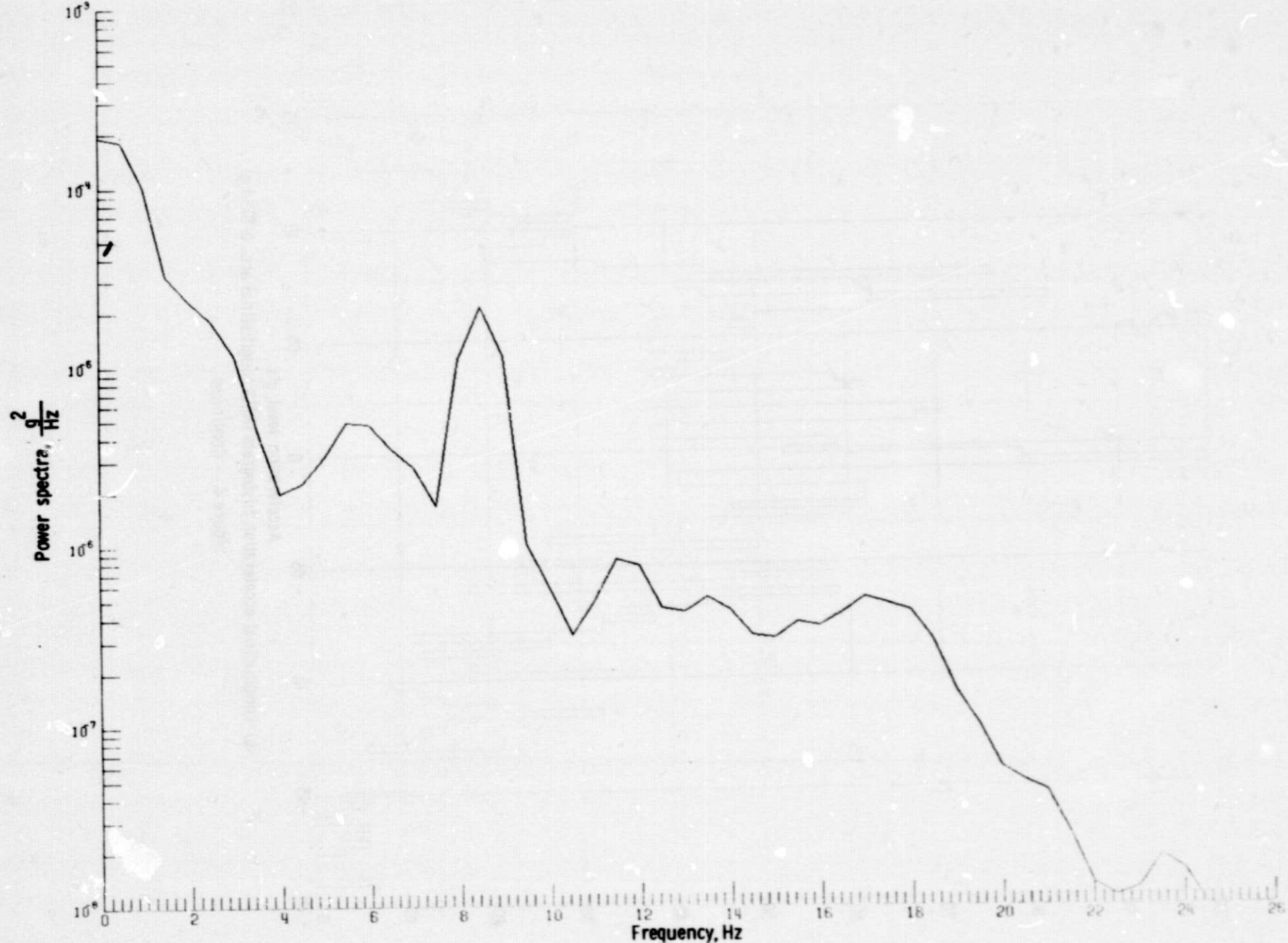
(b) Longitudinal acceleration histogram (RMS longitudinal acc. 0.0326 g).  
Figure 4. - Continued.





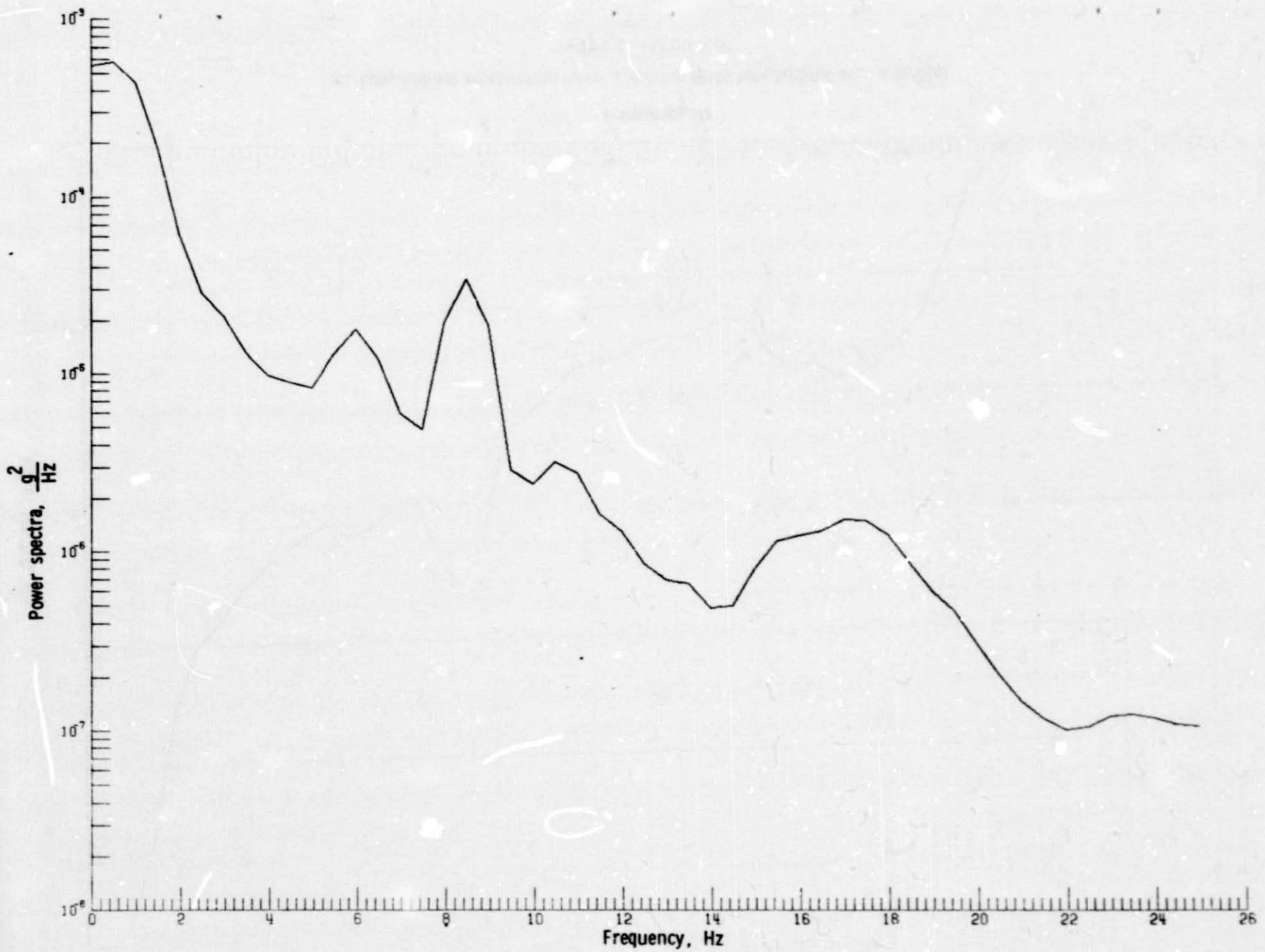
(b) Longitudinal acceleration histogram (RMS longitudinal acc. 0.0734 g)

Figure 4. - Continued



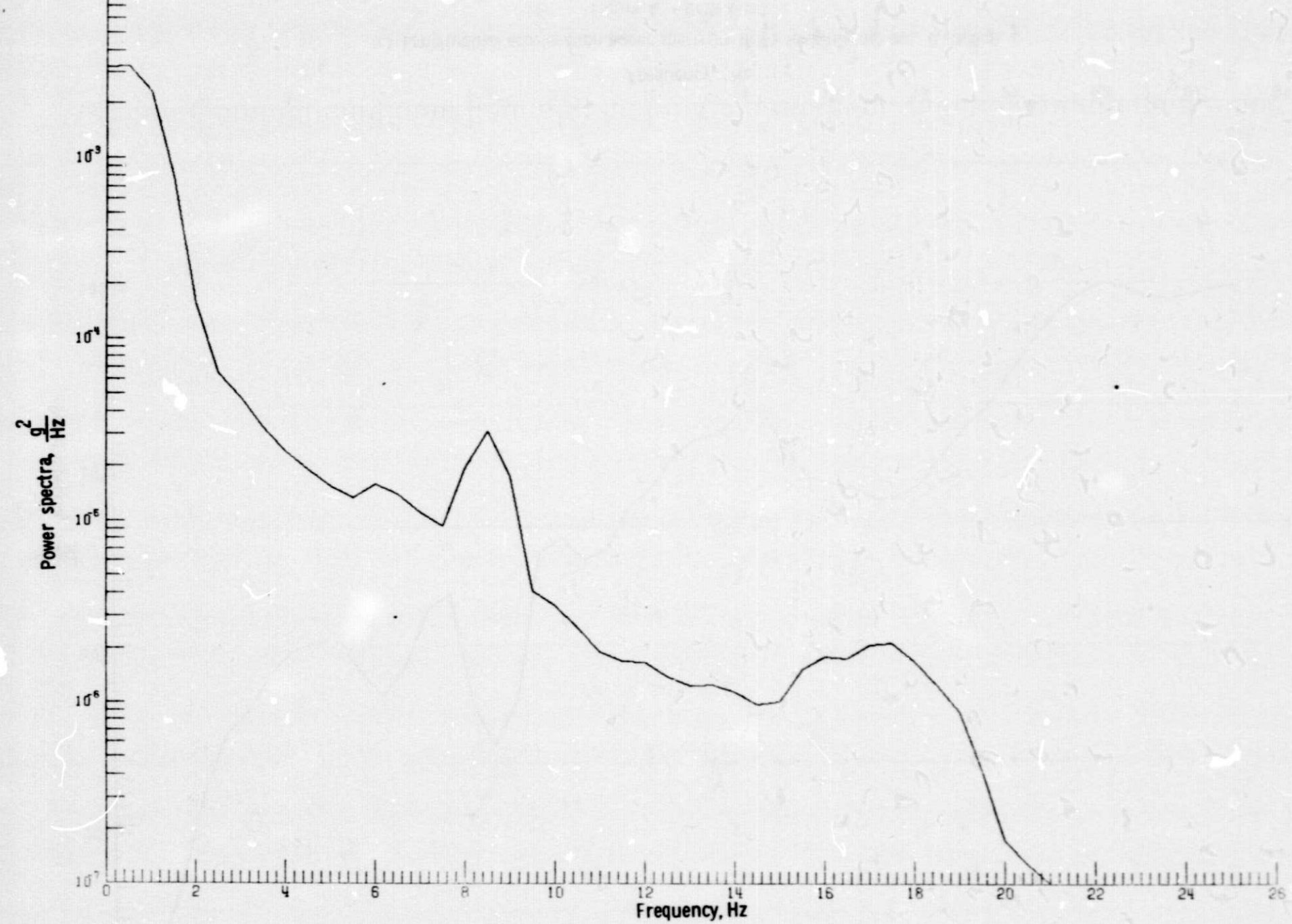
(c) Longitudinal acceleration power spectrum (RMS longitudinal acc. 0.0164 g).

Figure 4 - Continued.



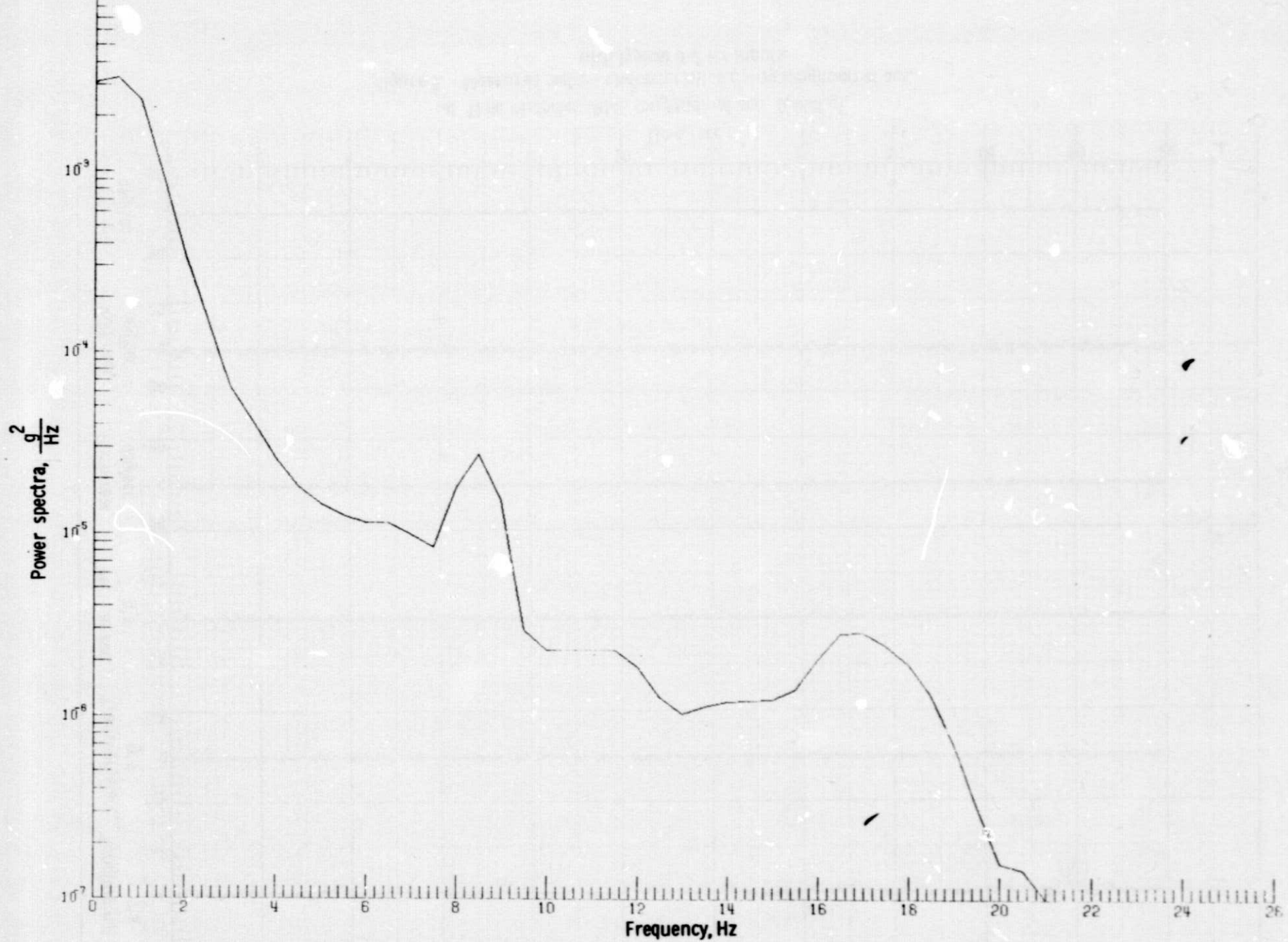
(c) Longitudinal acceleration power spectrum (RMS longitudinal acc. 0.0326 g).

Figure 4. - Continued .



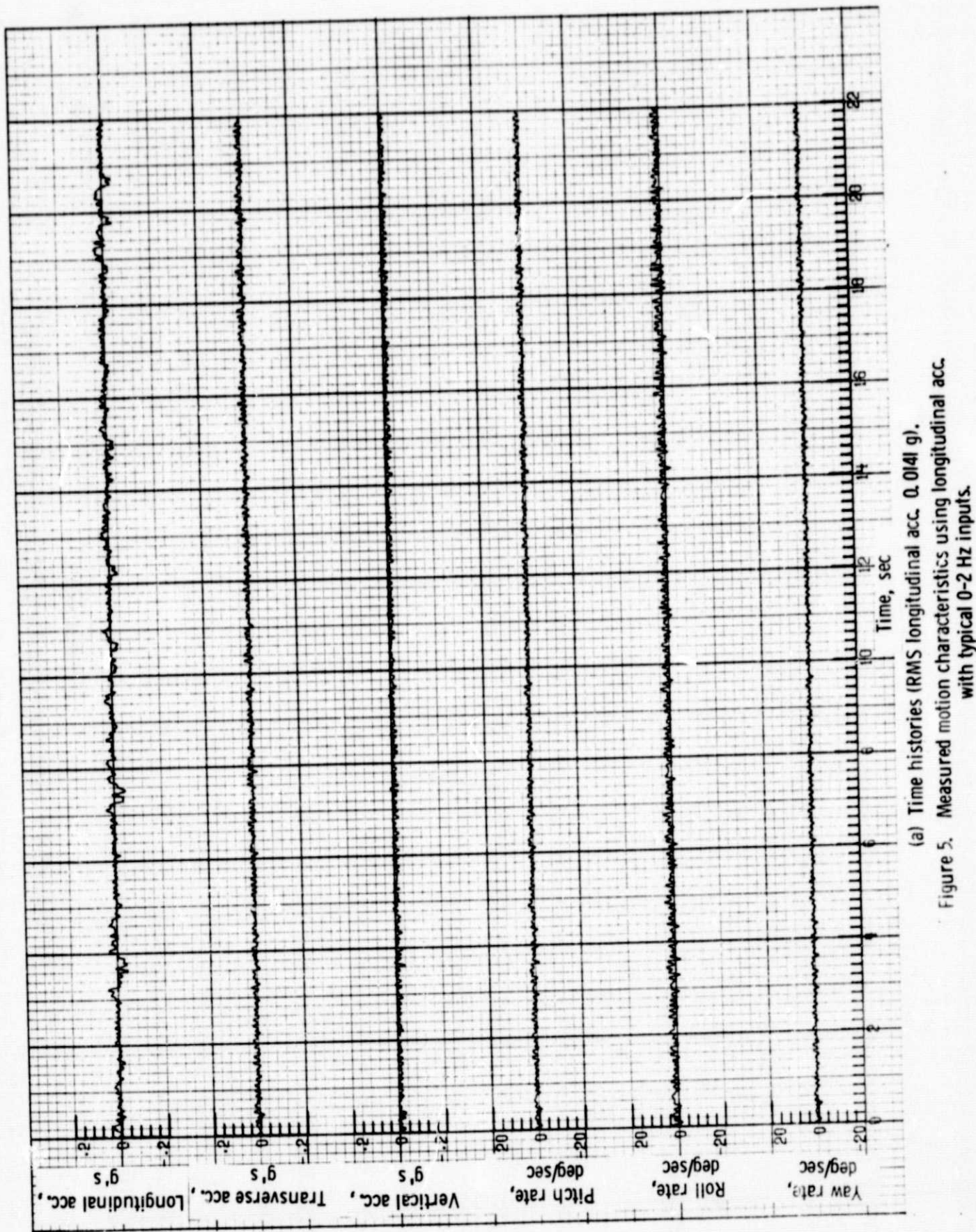
(c) Longitudinal acceleration power spectrum (RMS longitudinal acc. 0.0655 g).

Figure 4. - Continued.



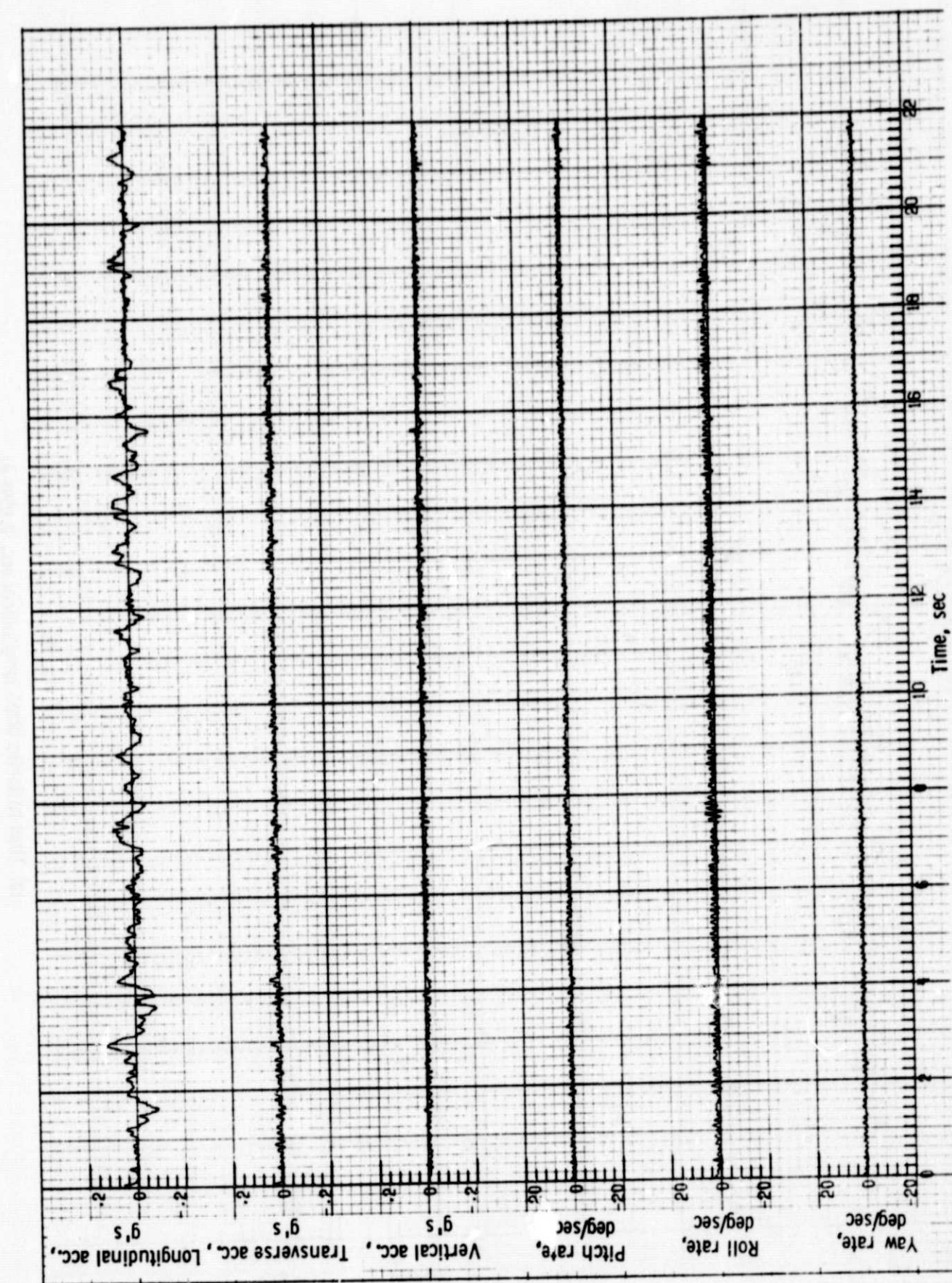
(c) Longitudinal acceleration power spectrum (RMS longitudinal acc. 0.0734 g).

Figure 4 - Concluded.



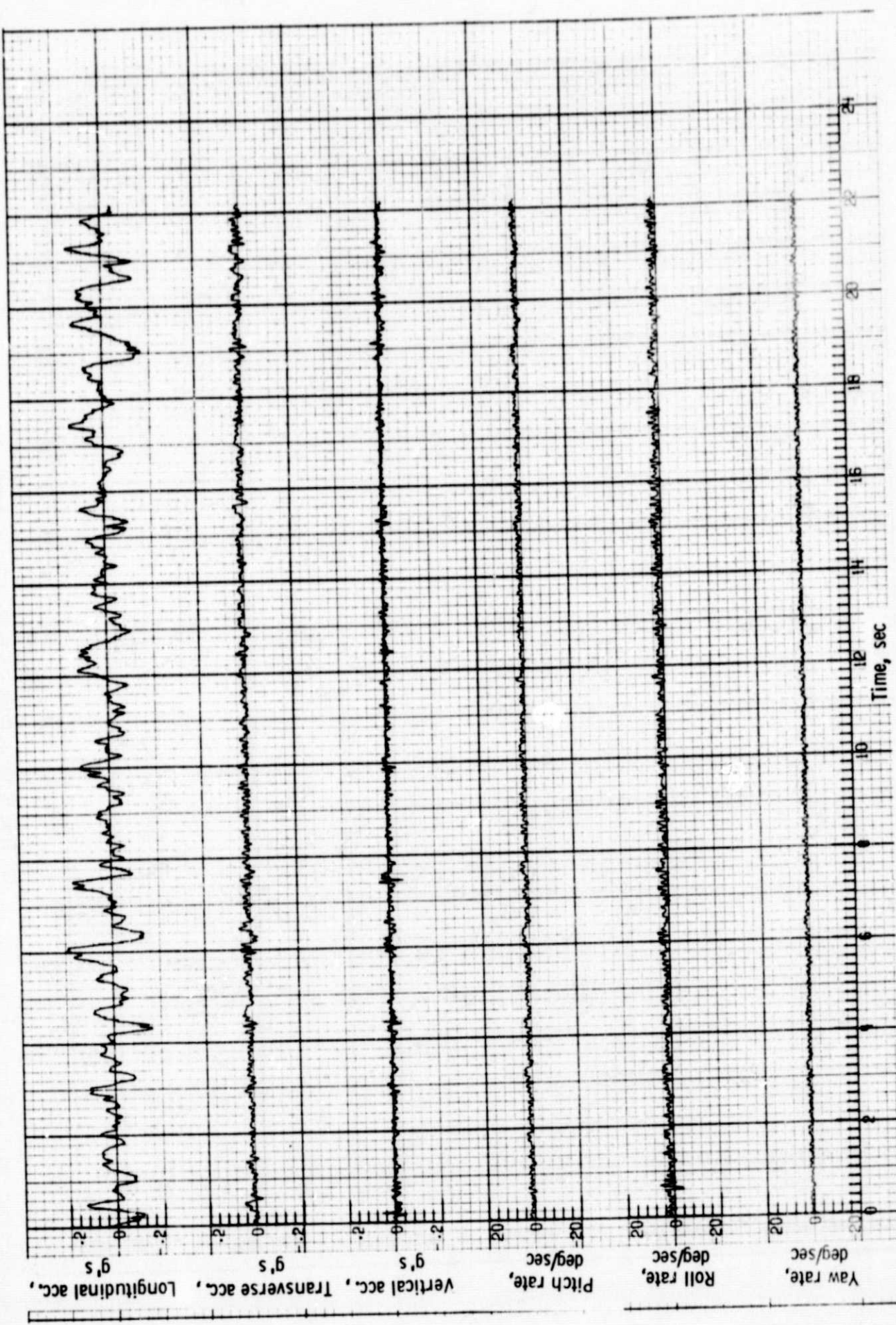
(a) Time histories (RMS longitudinal acc. 0.0141 g).

Figure 5. Measured motion characteristics using longitudinal acc. with typical 0-2 Hz inputs.



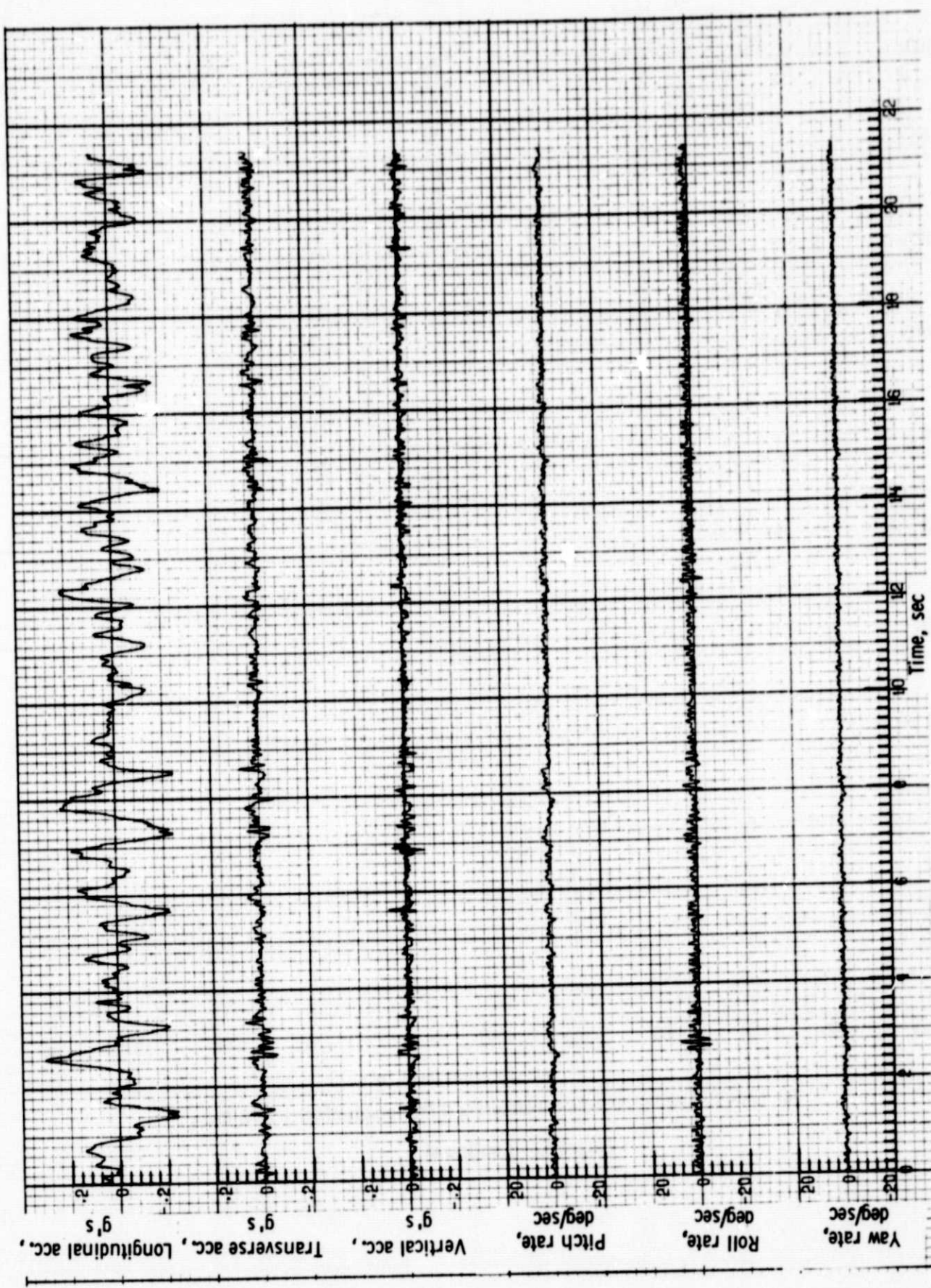
(a) Time histories (RMS longitudinal acc. 0.0315 g).

Figure 5. - Continued.



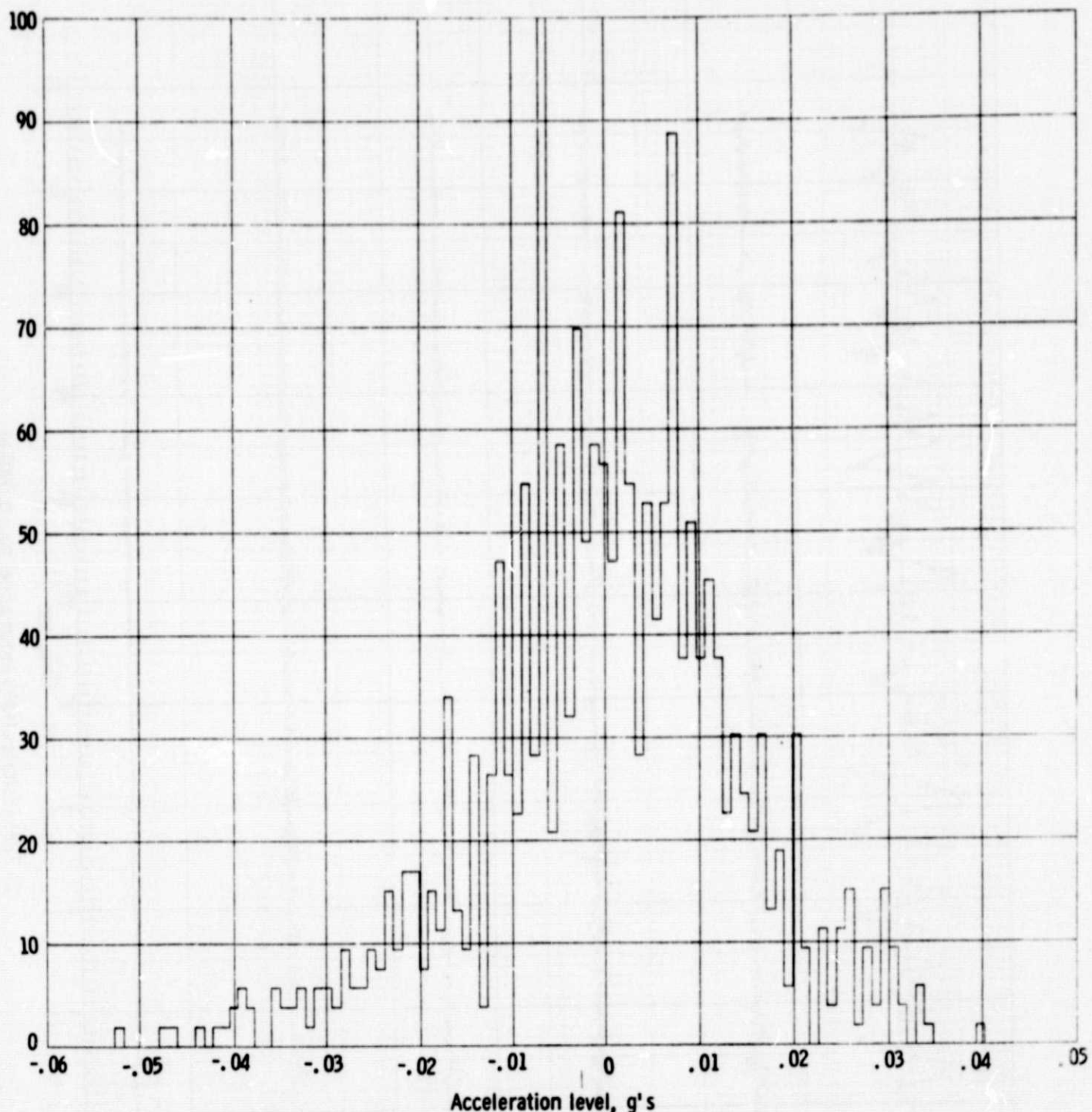
(a) Time histories (RMS longitudinal acc. 0.0598 g).

Figure 5. - Continued.



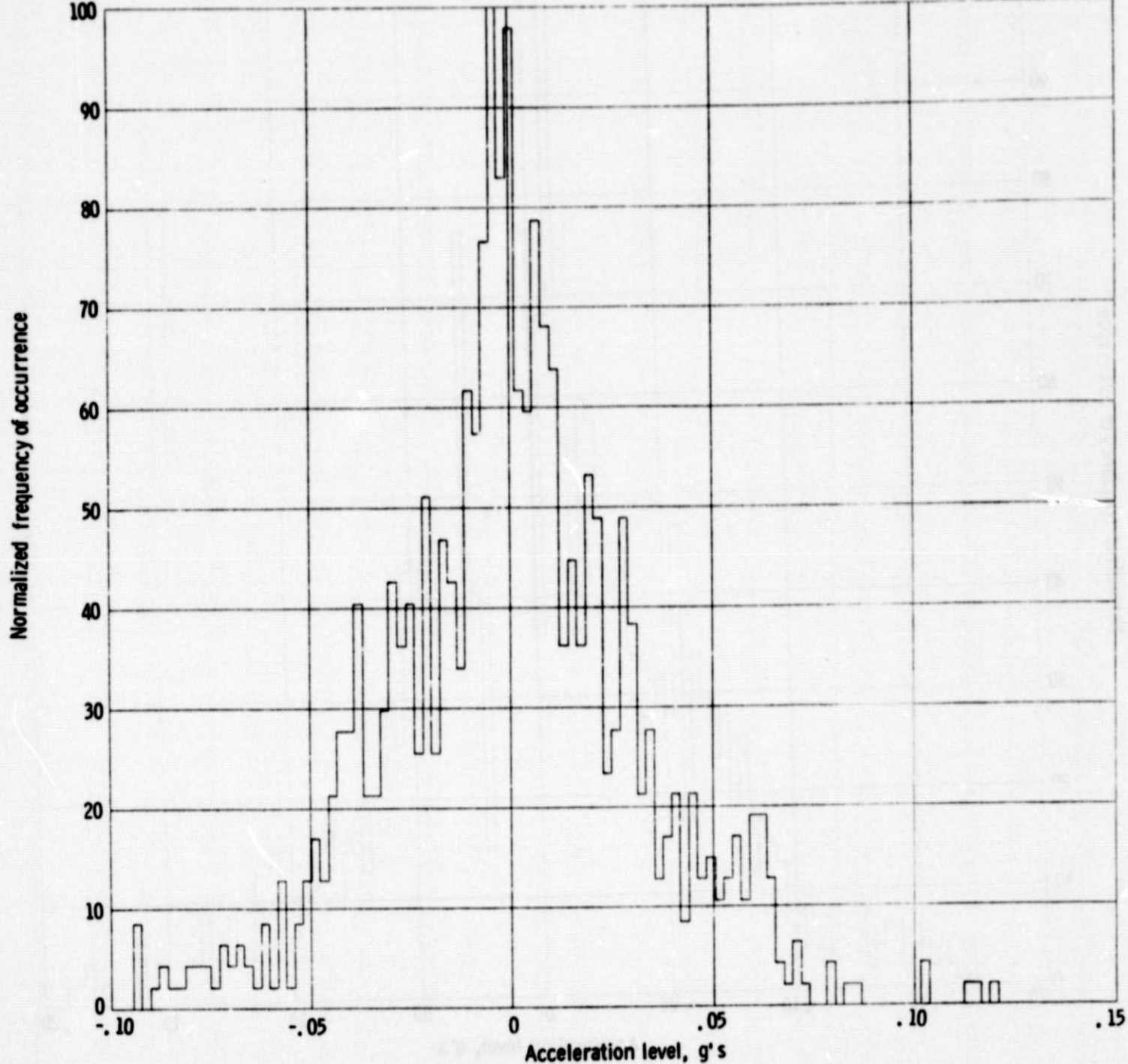
(a) Time histories (RMS longitudinal acc. 0.0900 g).

Figure 5 - Continued.



(b) Longitudinal acceleration histogram (RMS longitudinal acc. 0.0141 g).

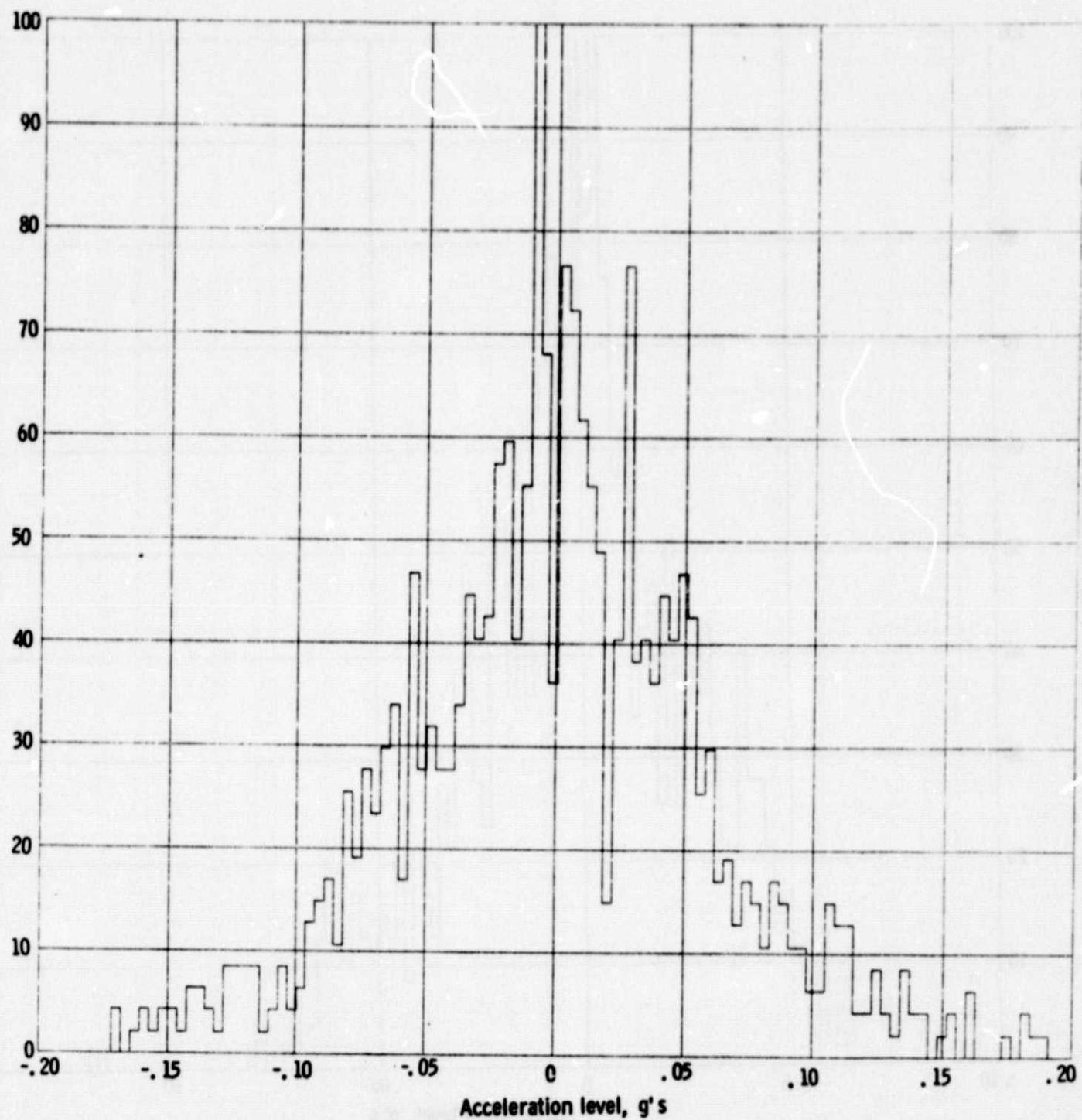
Figure 5. - Continued.



(b) Longitudinal acceleration histogram (RMS longitudinal acc. 0.0315 g.).

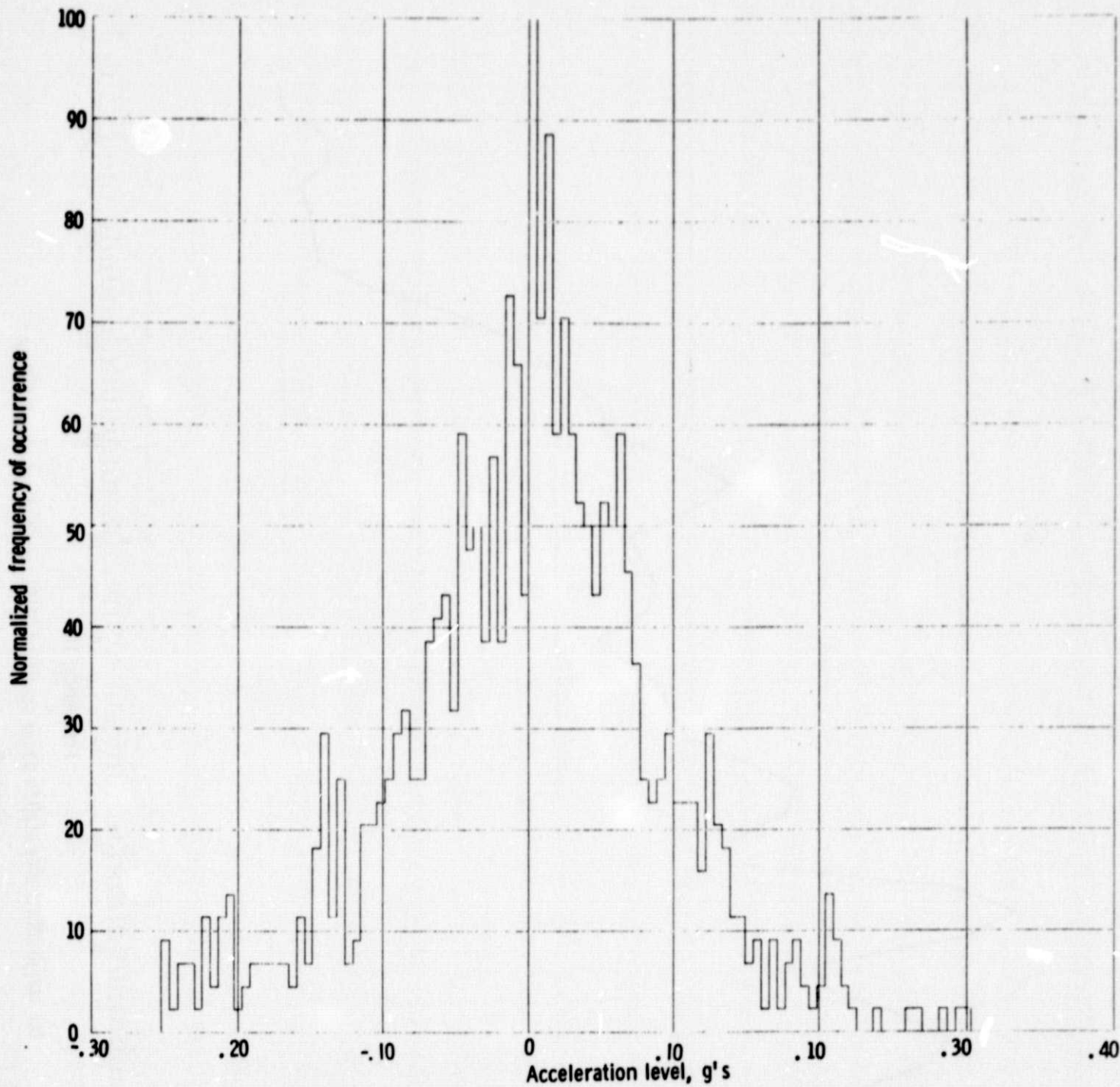
Figure 5. - Continued.

Normalized frequency of occurrence



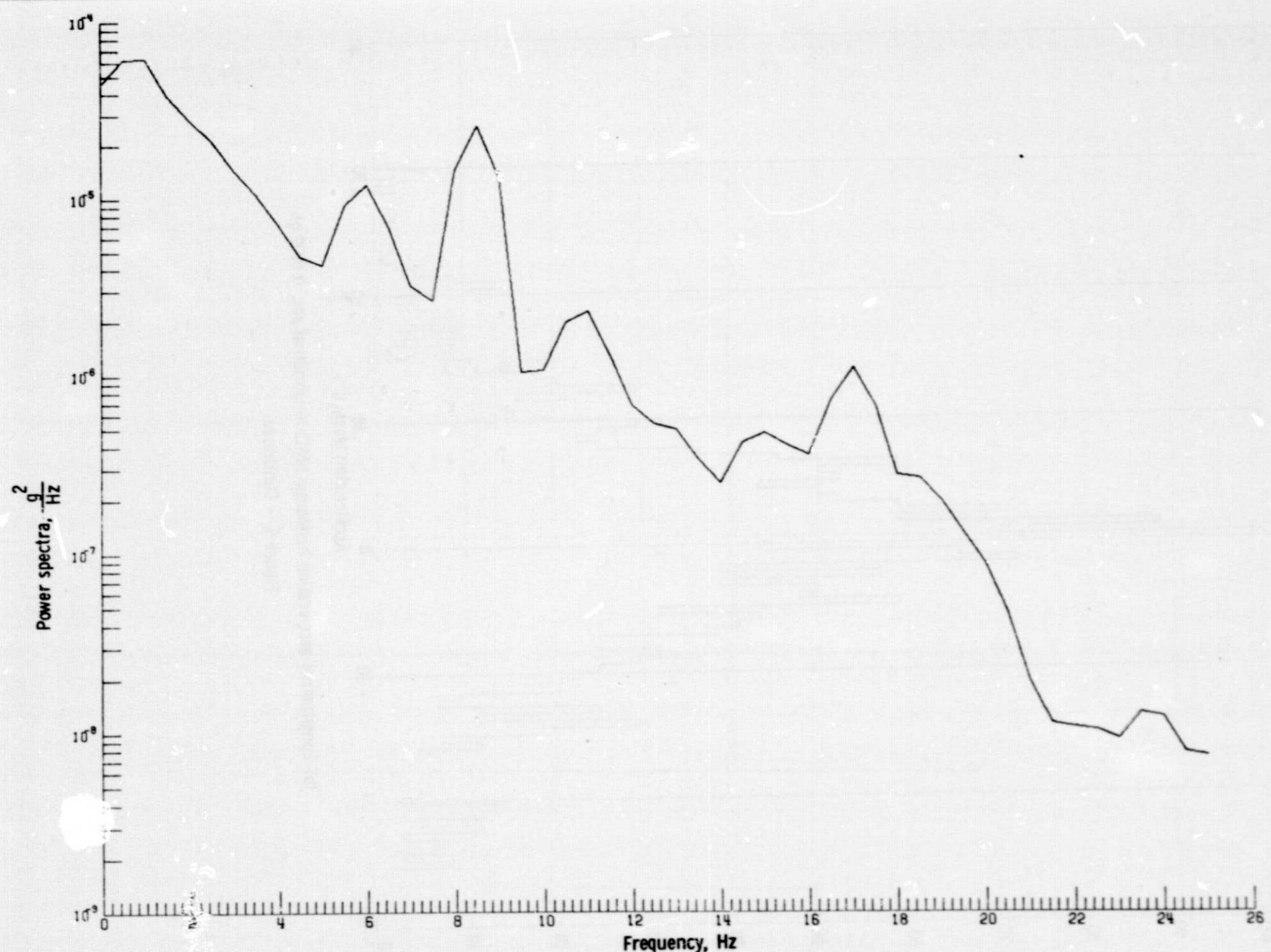
(b) Longitudinal acceleration histogram (RMS longitudinal acc. 0.0598 g).

Figure 5. - Continued.



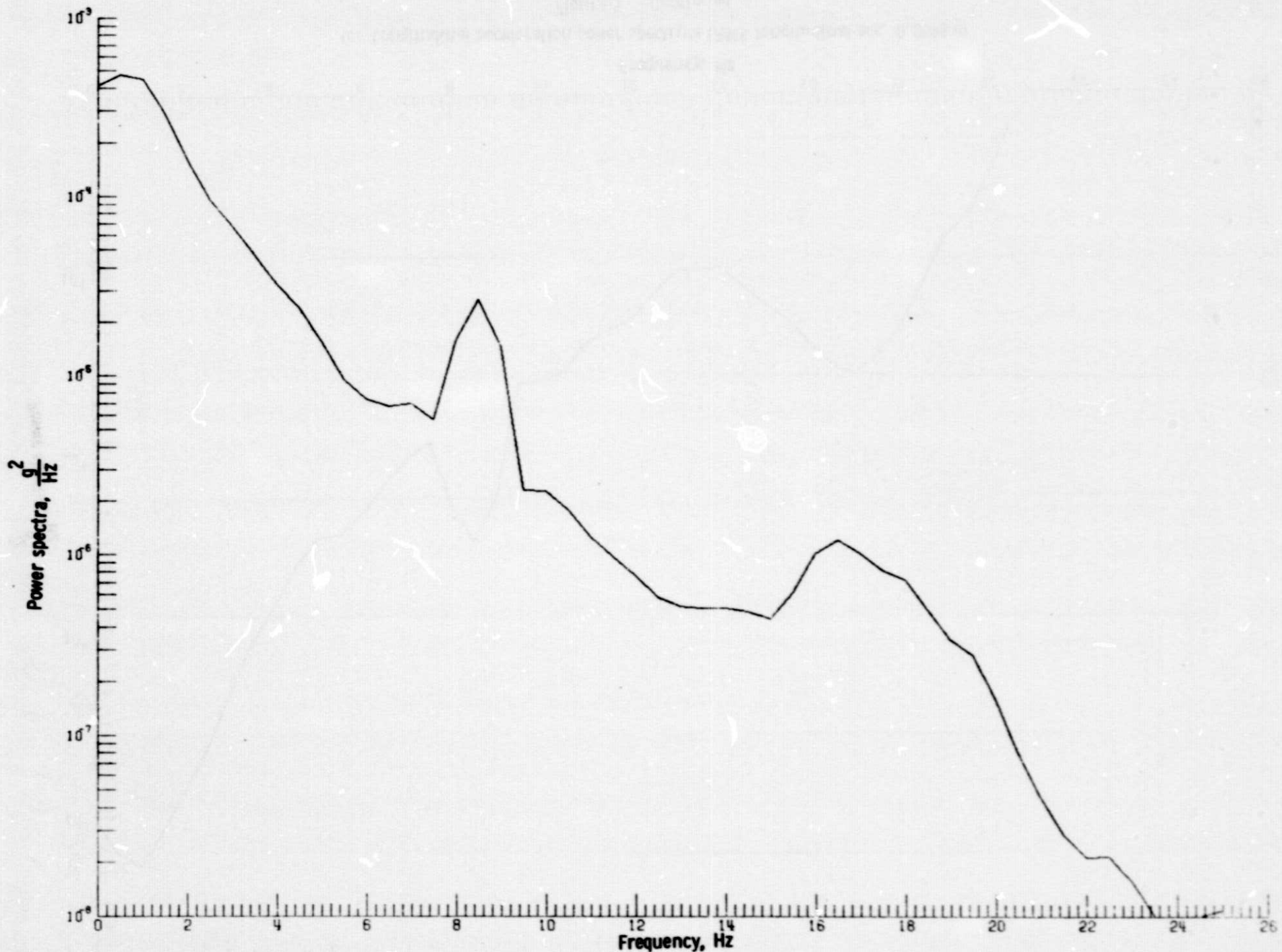
(b) Longitudinal acceleration histogram (RMS longitudinal acc. 0.0900 g).

Figure 5. - Continued.



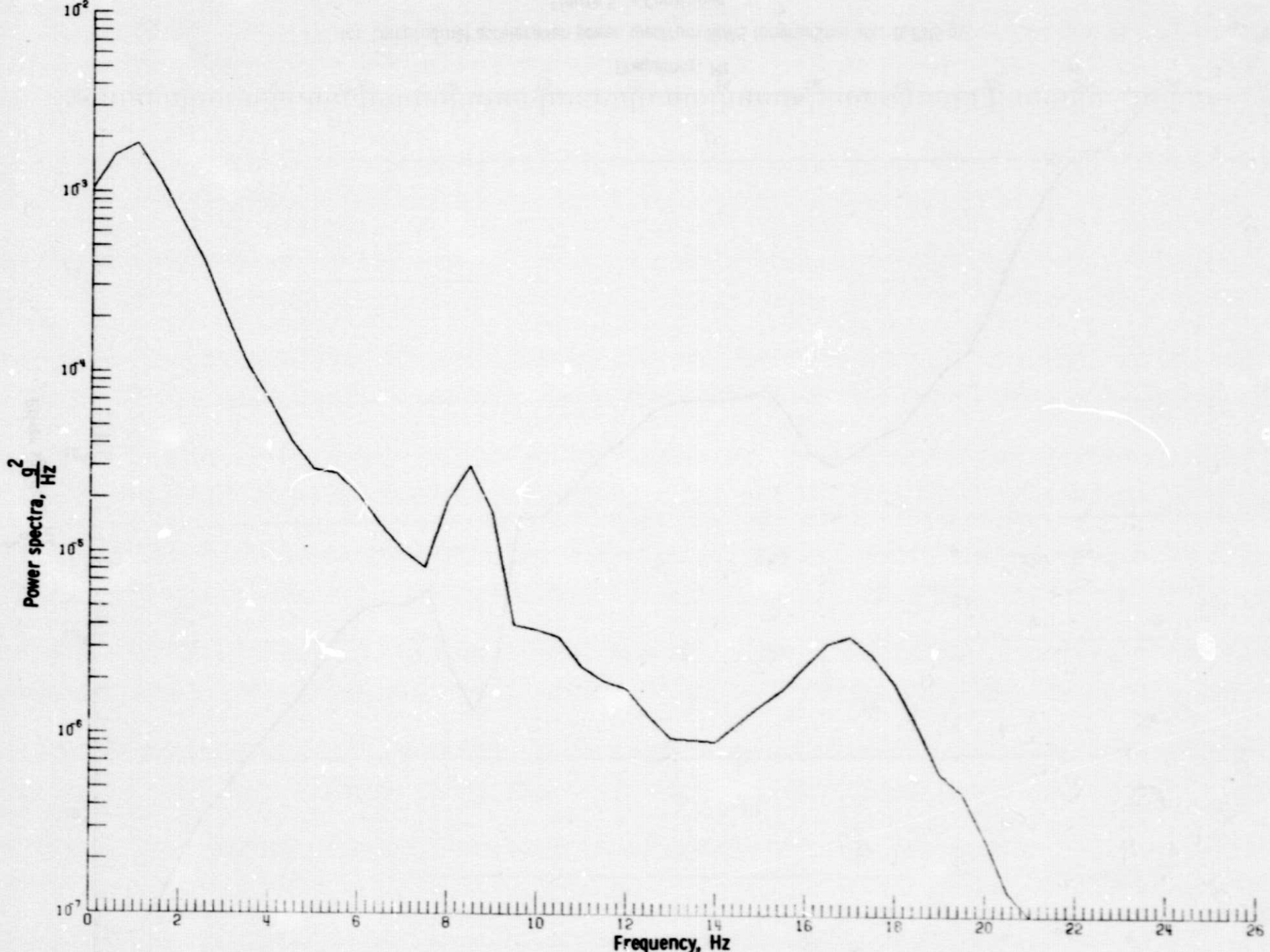
(c) Longitudinal acceleration power spectrum (RMS longitudinal acc. 0.0141 g).

Figure 5. - Continued.



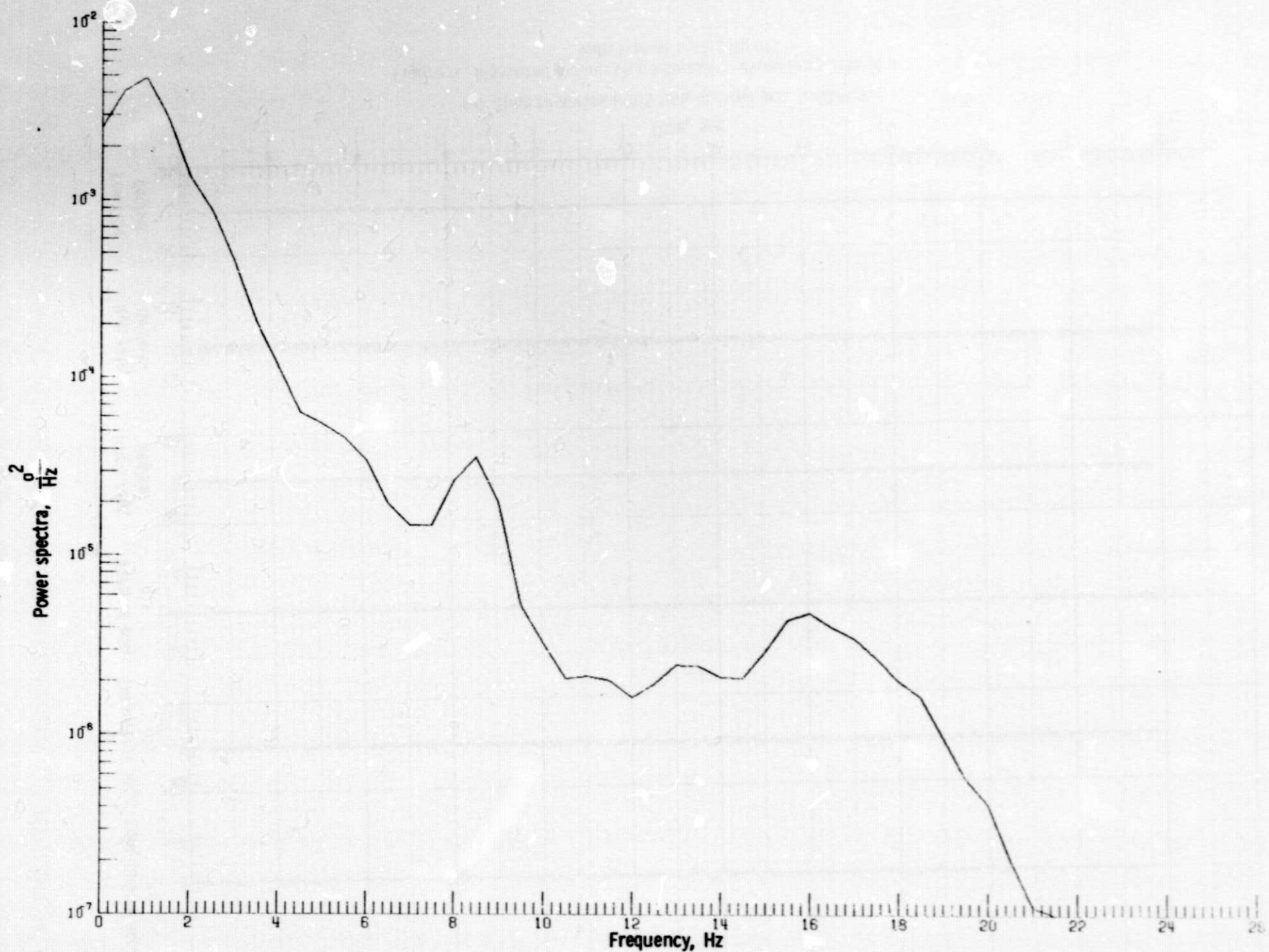
(c) Longitudinal acceleration power spectrum (RMS longitudinal acc. 0.0315 g).

Figure 5. - Continued.



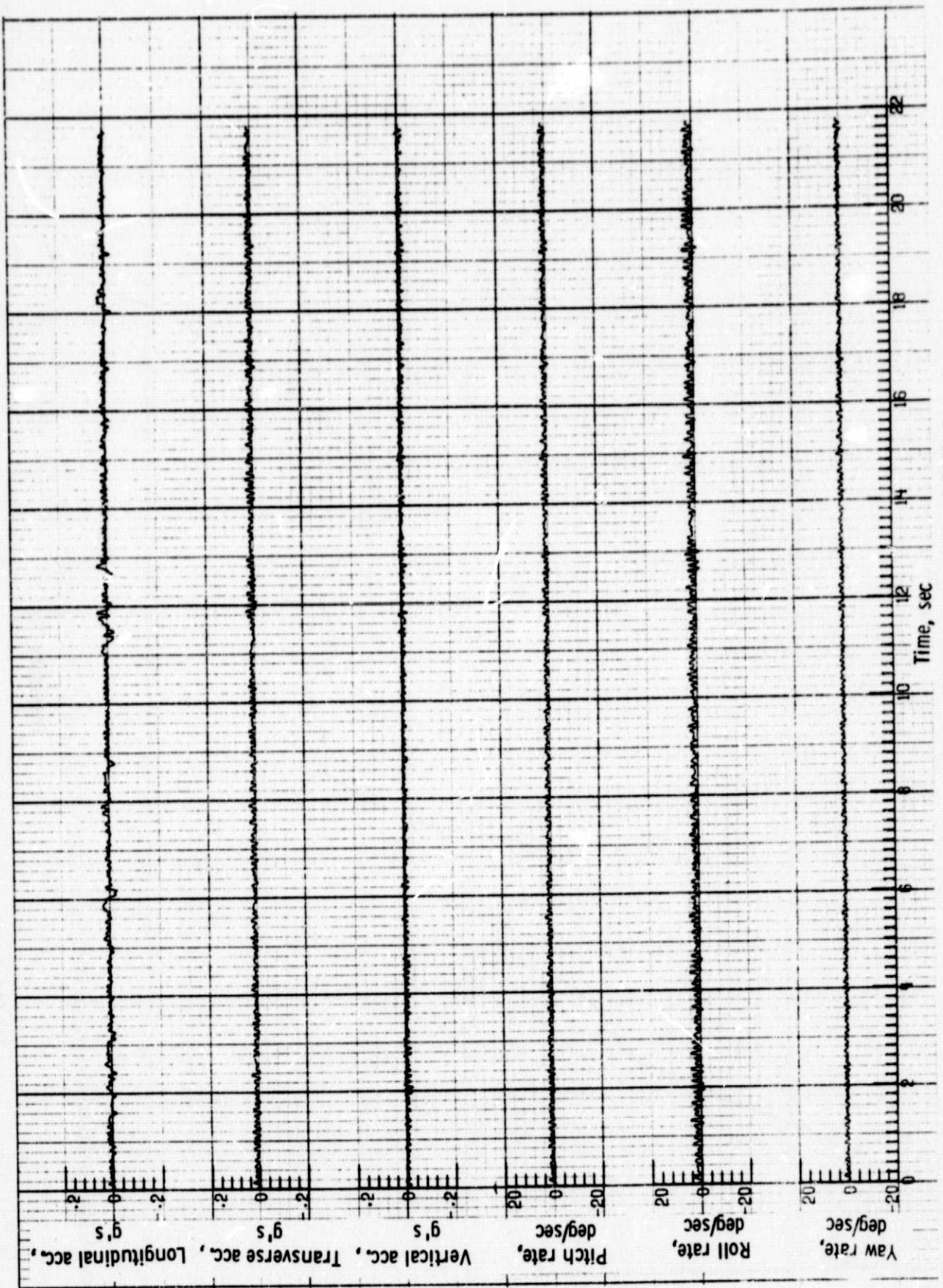
(c) Longitudinal acceleration power spectrum (RMS longitudinal acc. 0.0598 g)

Figure 5. - Continued



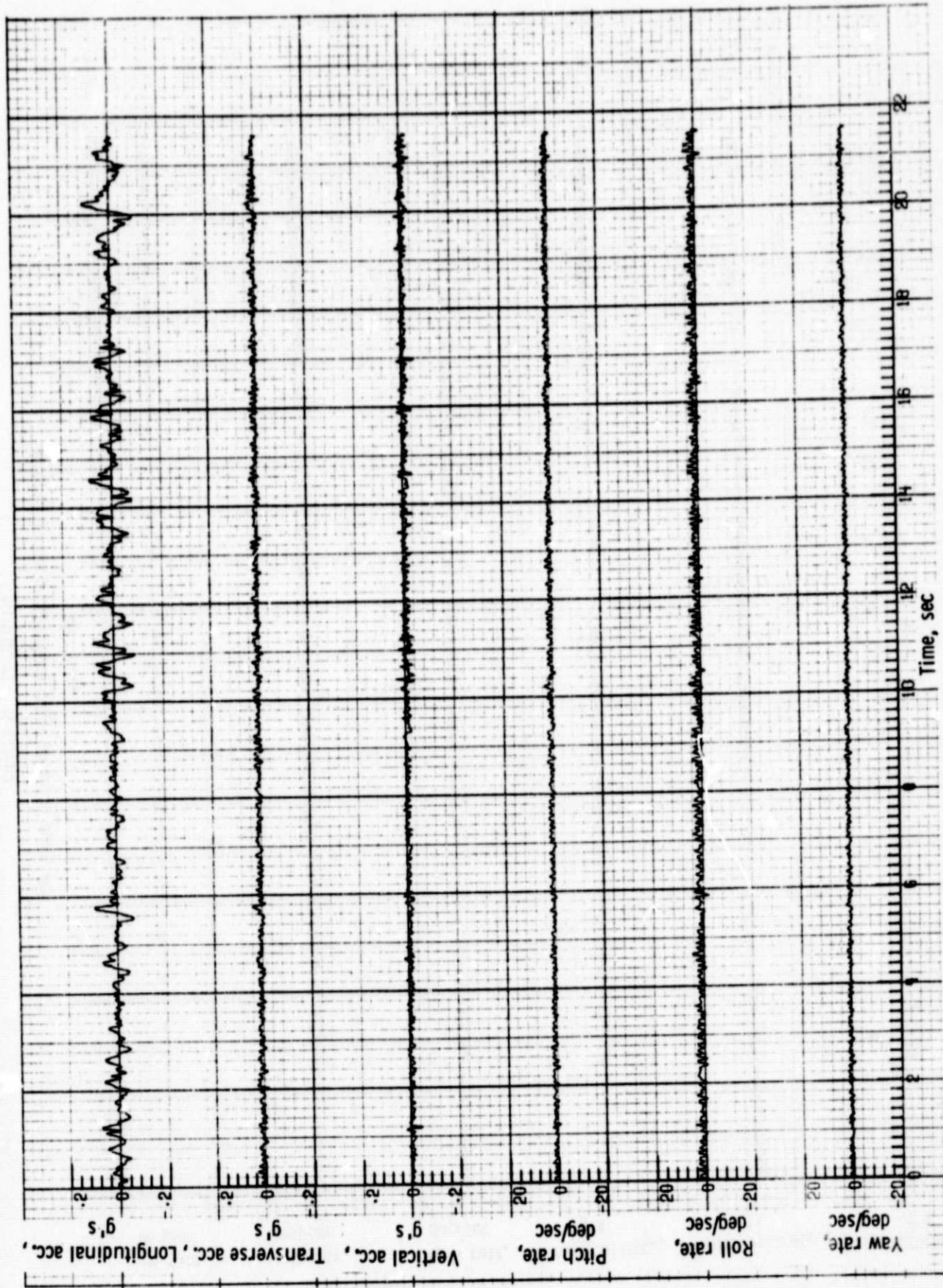
(c) Longitudinal acceleration power spectrum (RMS longitudinal acc. 0.0900 g).

Figure 5. - Concluded.



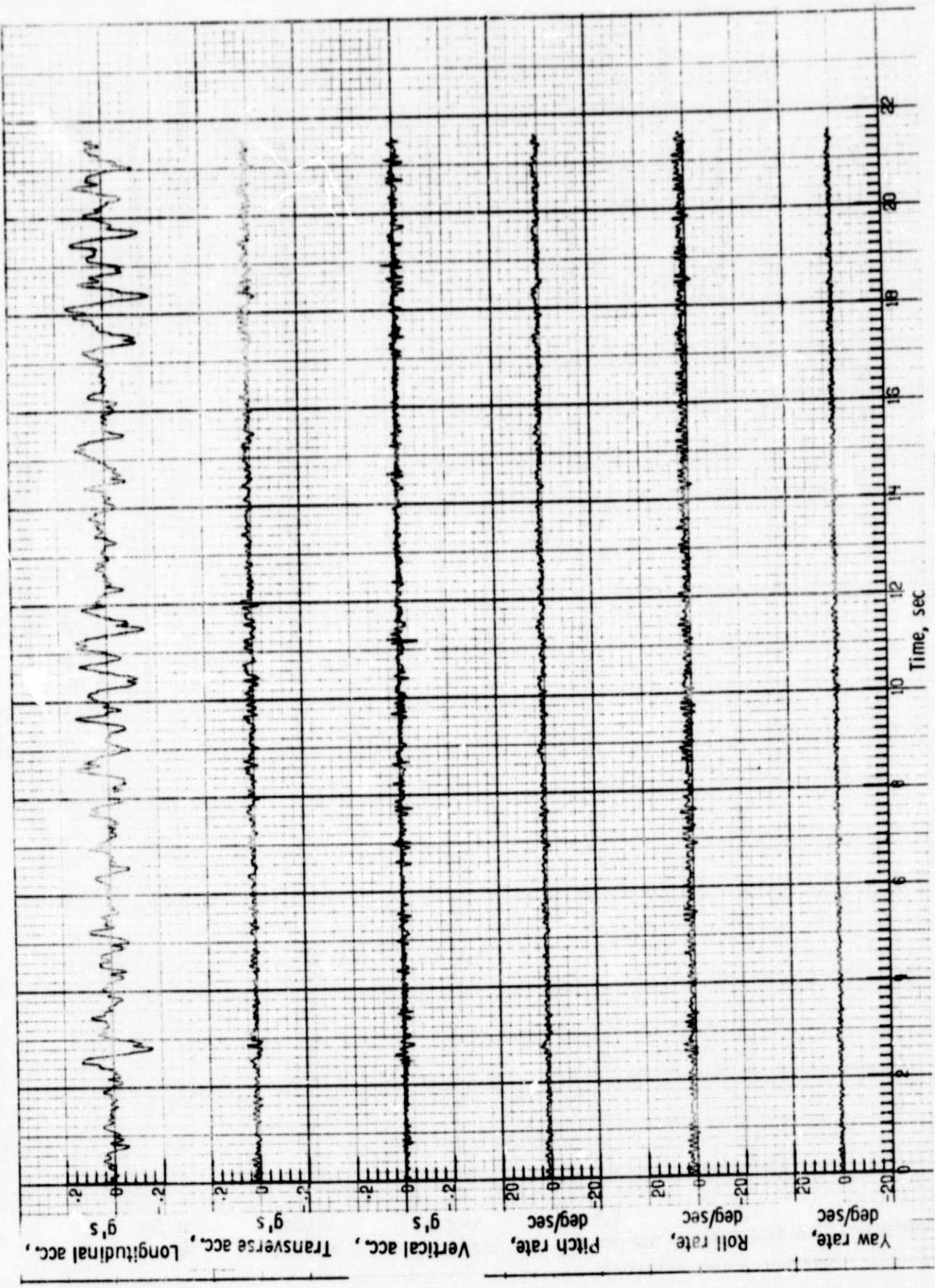
(a) Time histories (RMS longitudinal acc. 0.0098 g).

Figure 6. Measured motion characteristics using longitudinal acc. with typical 1-2 Hz inputs.



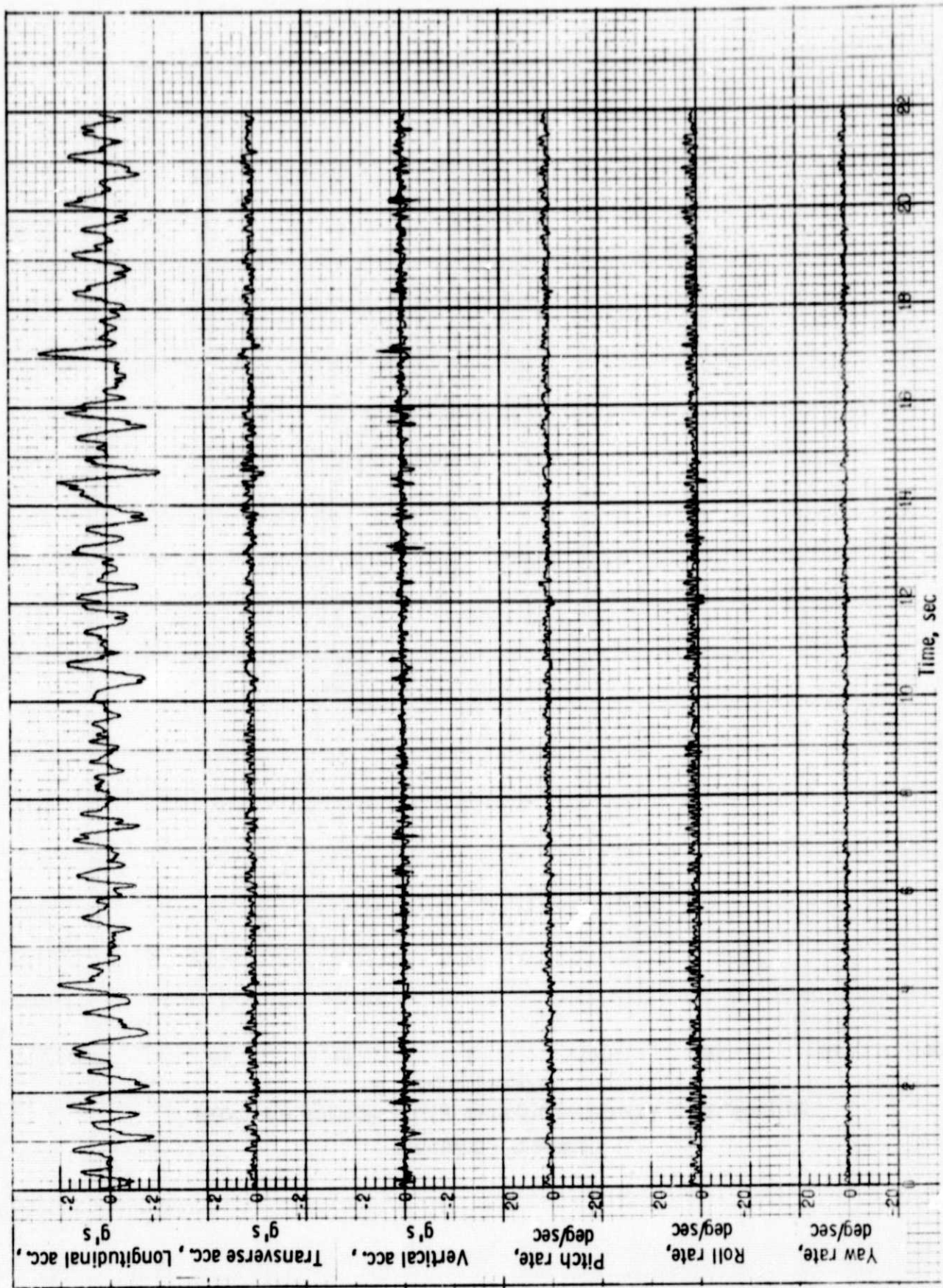
(a) Time histories (RMS longitudinal acc. 0.0291 g).

Figure 6 - Continued.



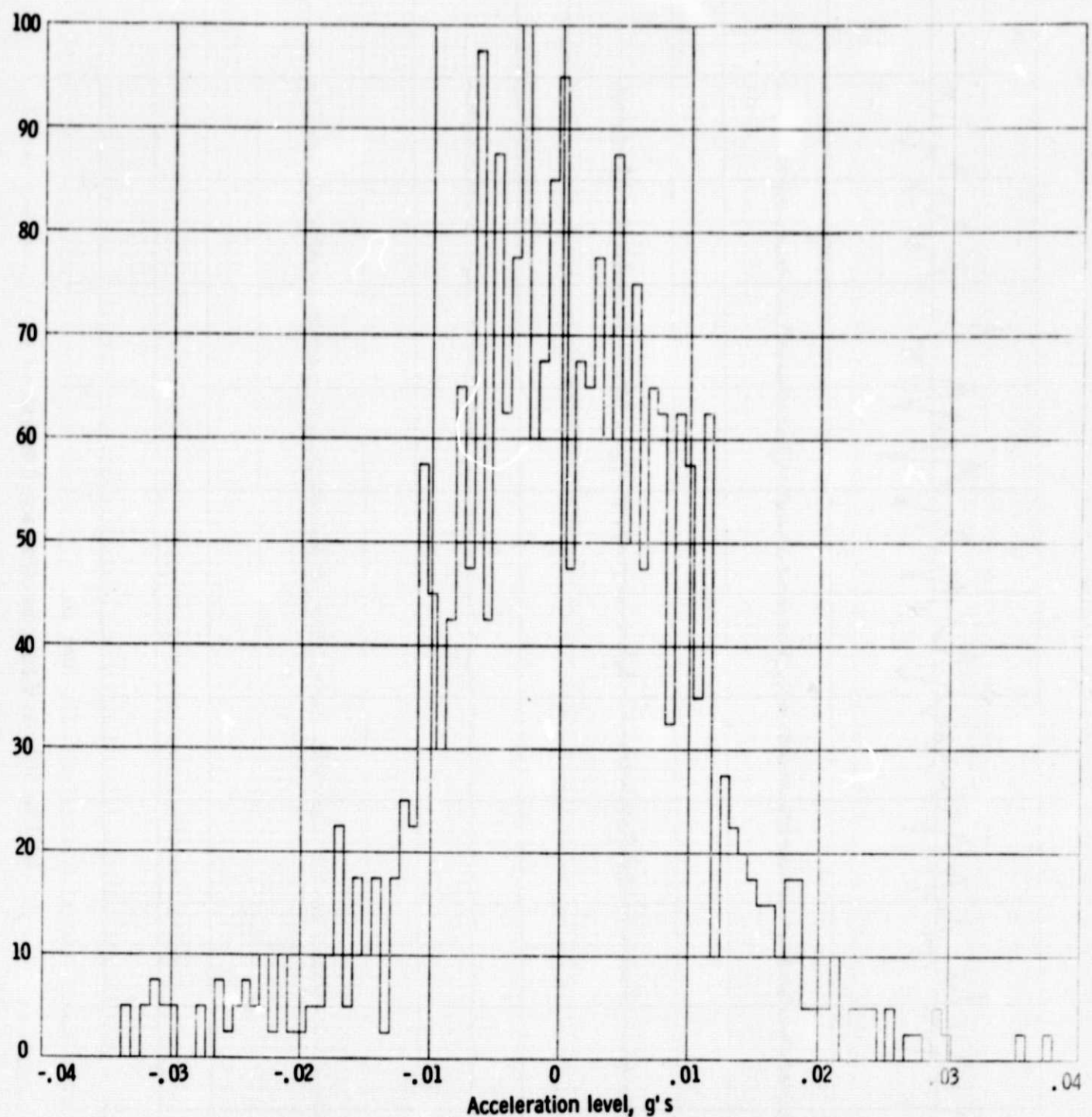
(a) Time histories (RMS longitudinal acc. 0.0545 g).

Figure 6 - Continued.



(a) Time histories (RMS longitudinal acc. 0.0798 g).

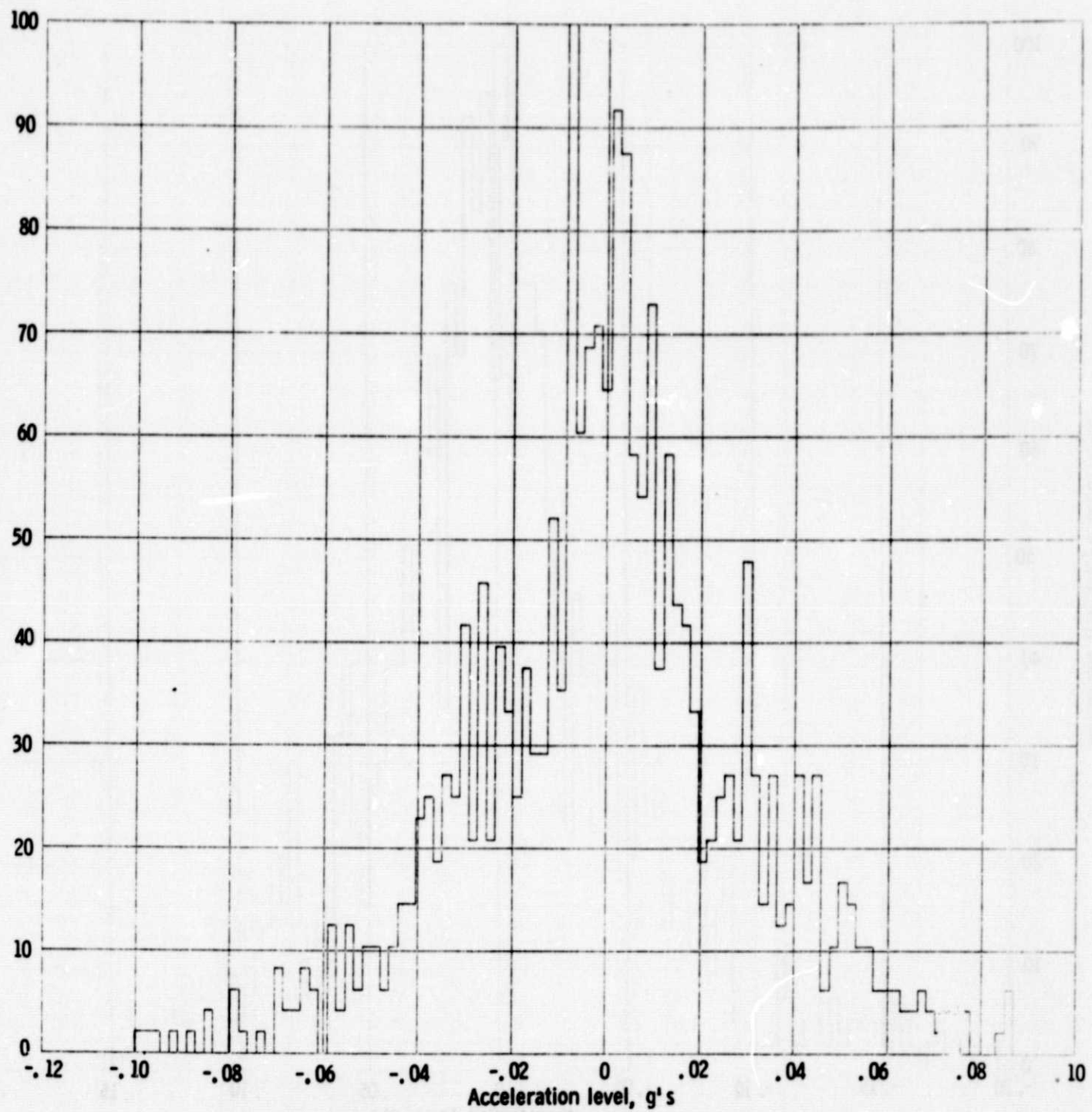
Figure 6 - Continued.



(b) Longitudinal acceleration histogram (RMS longitudinal acc. 0.0098 g).

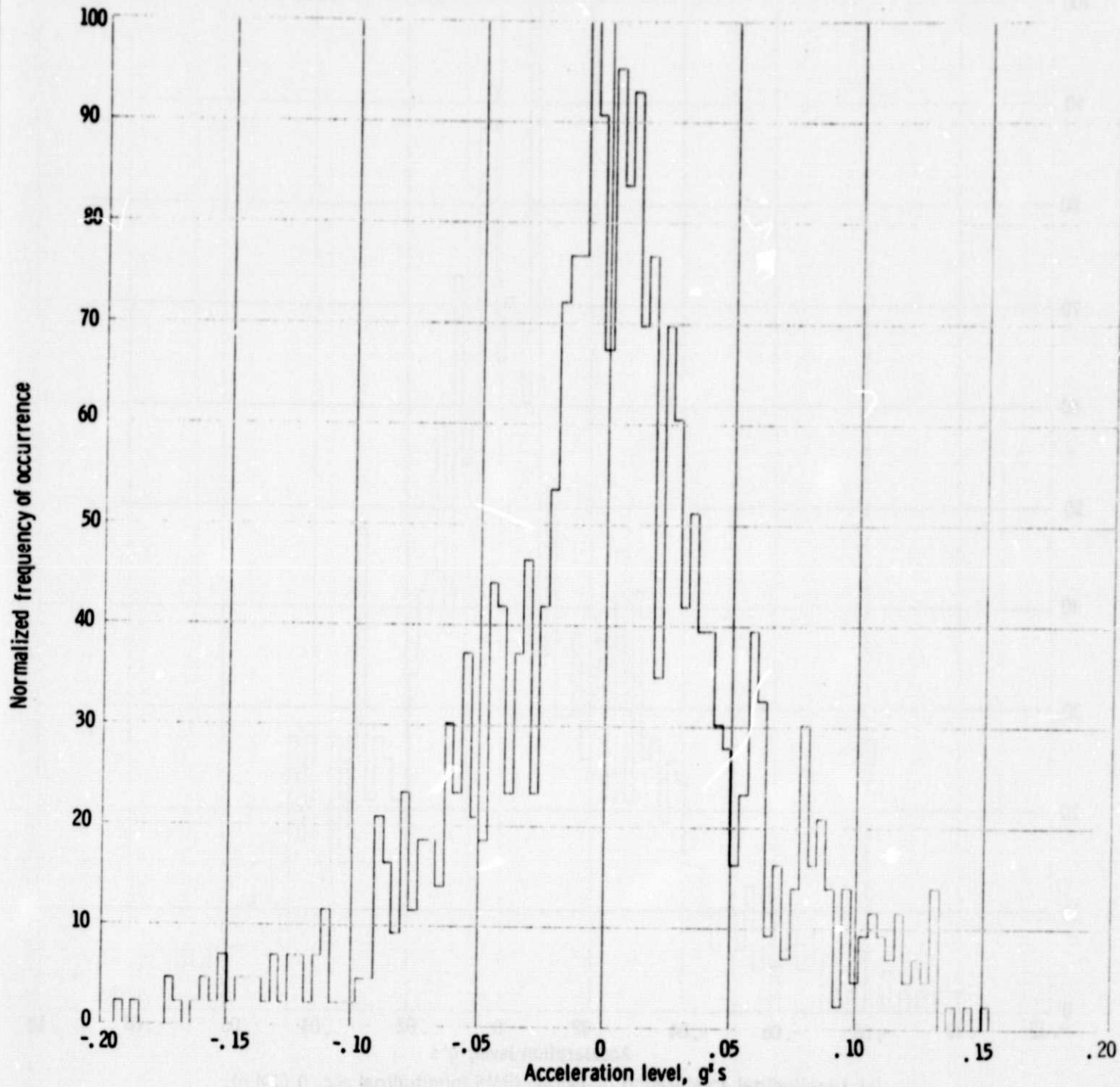
Figure 6. - Continued.

Normalized frequency of occurrence



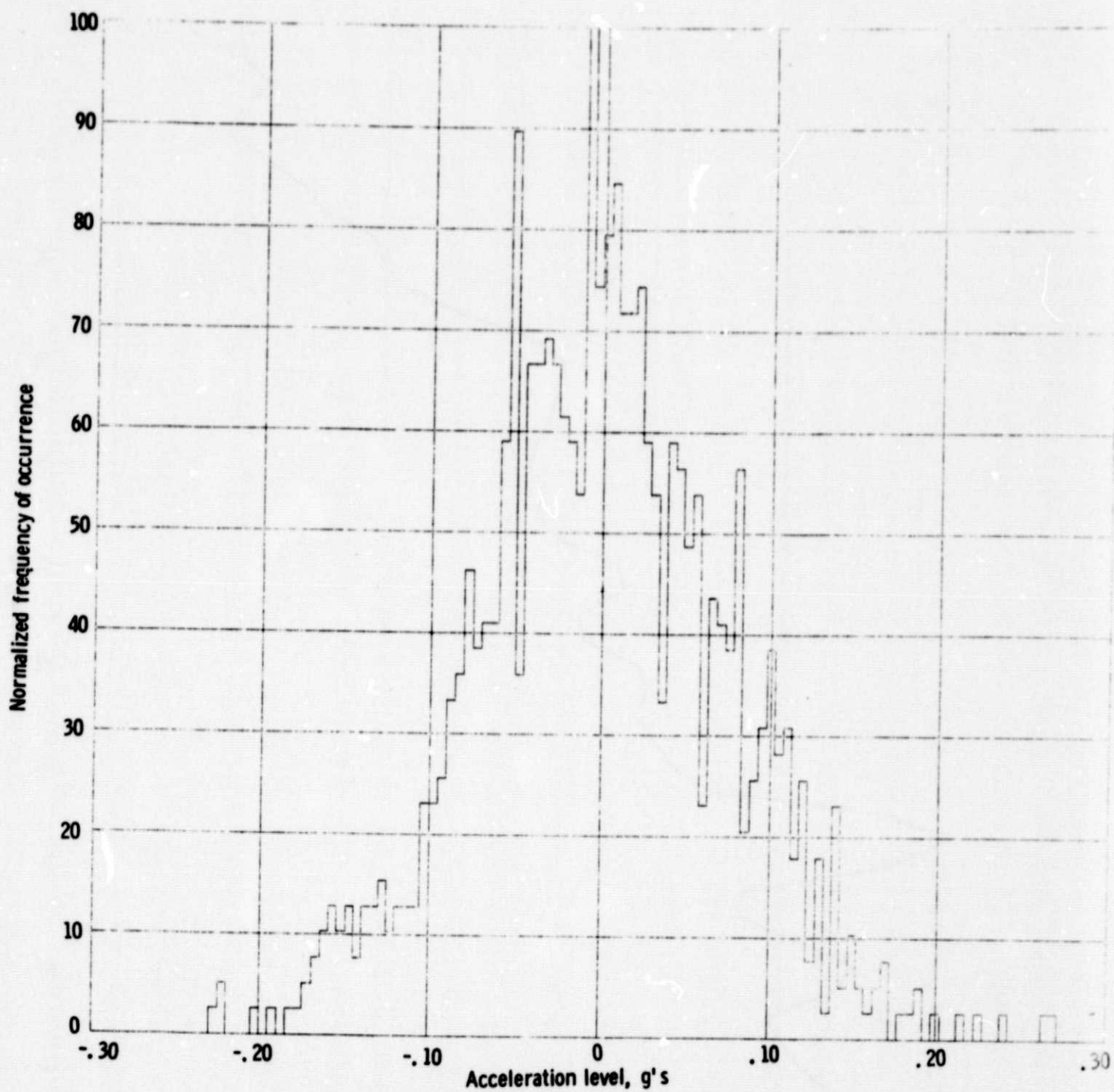
(b) Longitudinal acceleration histogram (RMS longitudinal acc. 0.0291 g).

Figure 6. - Continued.



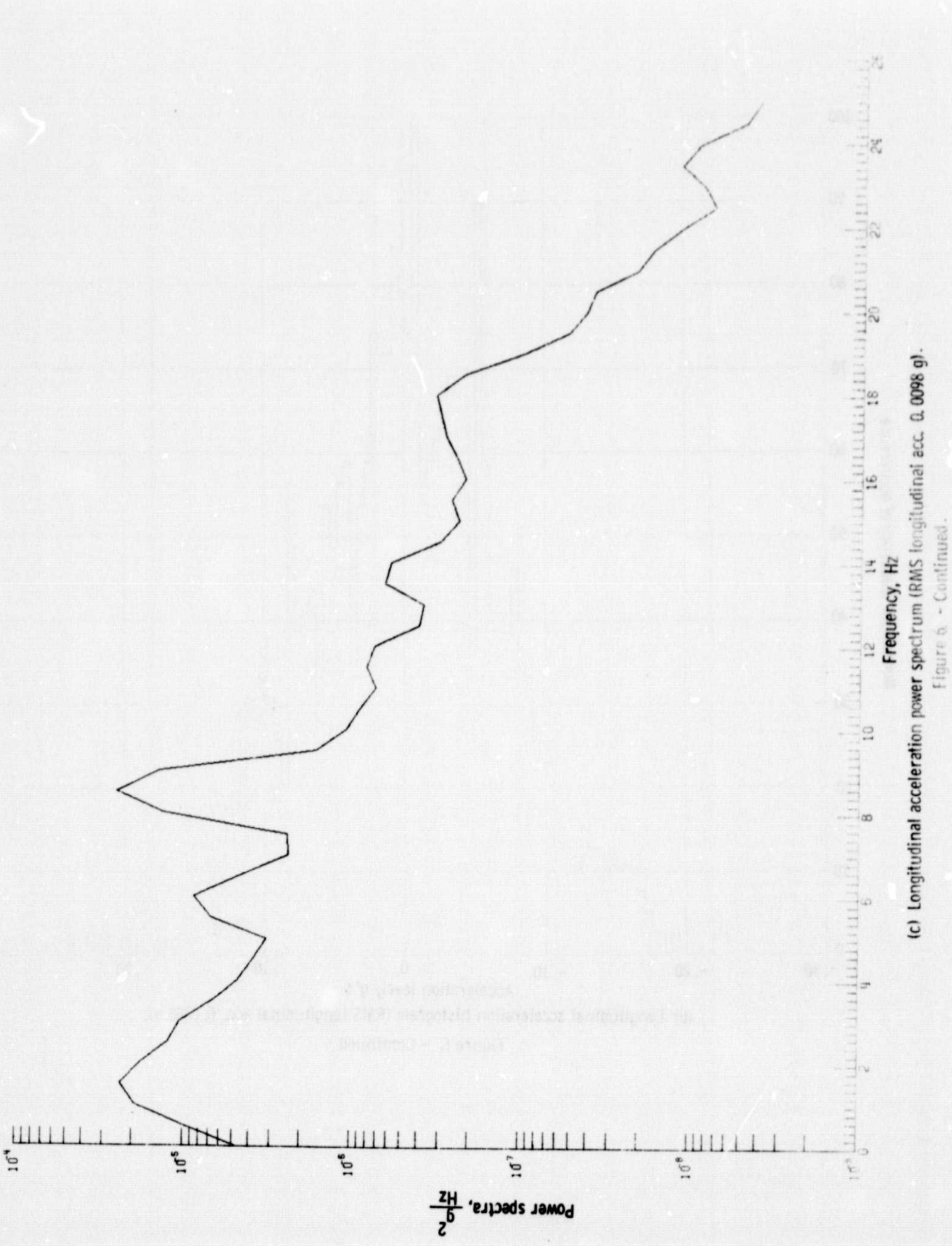
(b) Longitudinal acceleration histogram (RMS longitudinal acc. 0.0545 g).

Figure 6. - Continued.



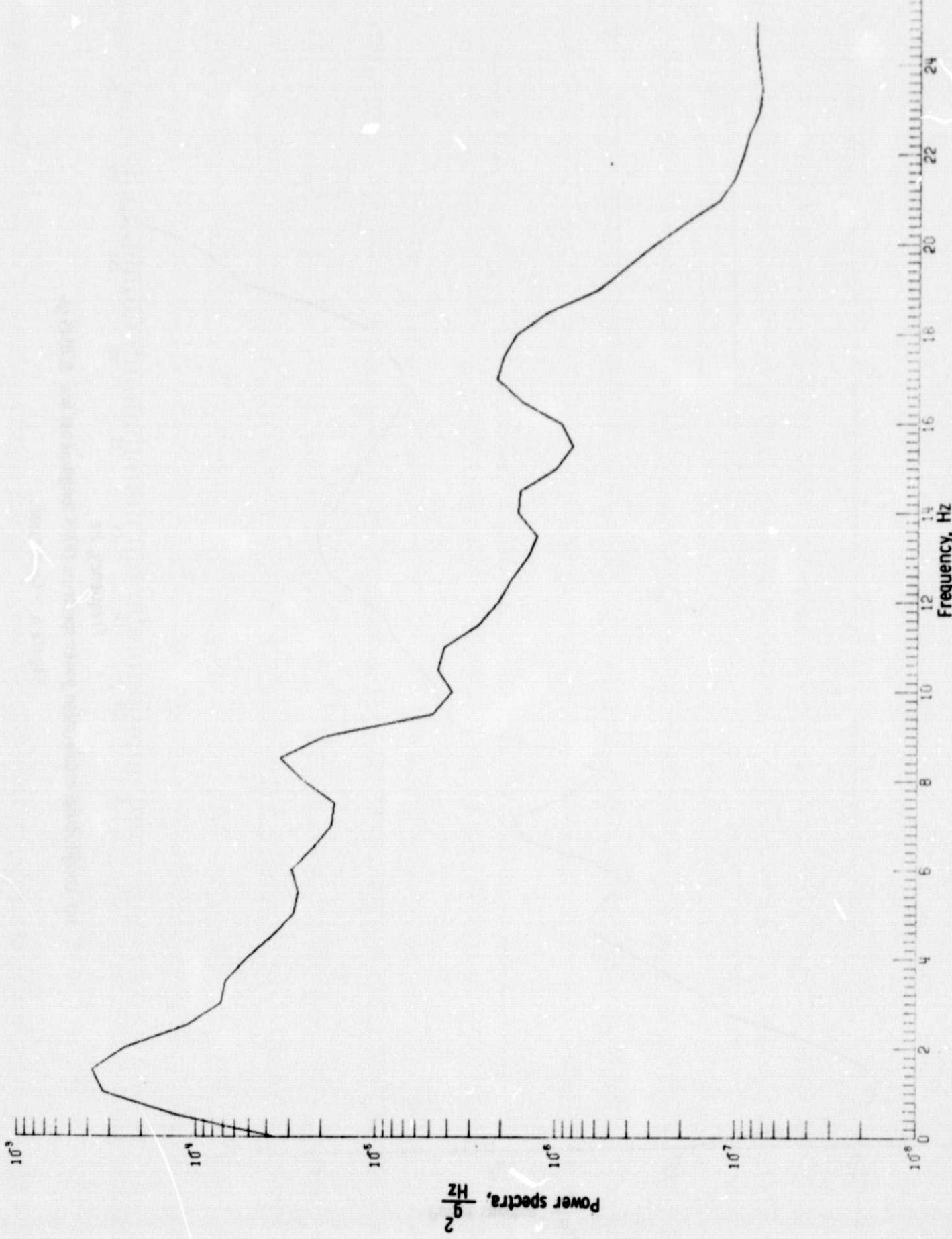
(b) Longitudinal acceleration histogram (RMS longitudinal acc. 0.0798 g.).

Figure 6. - Continued.



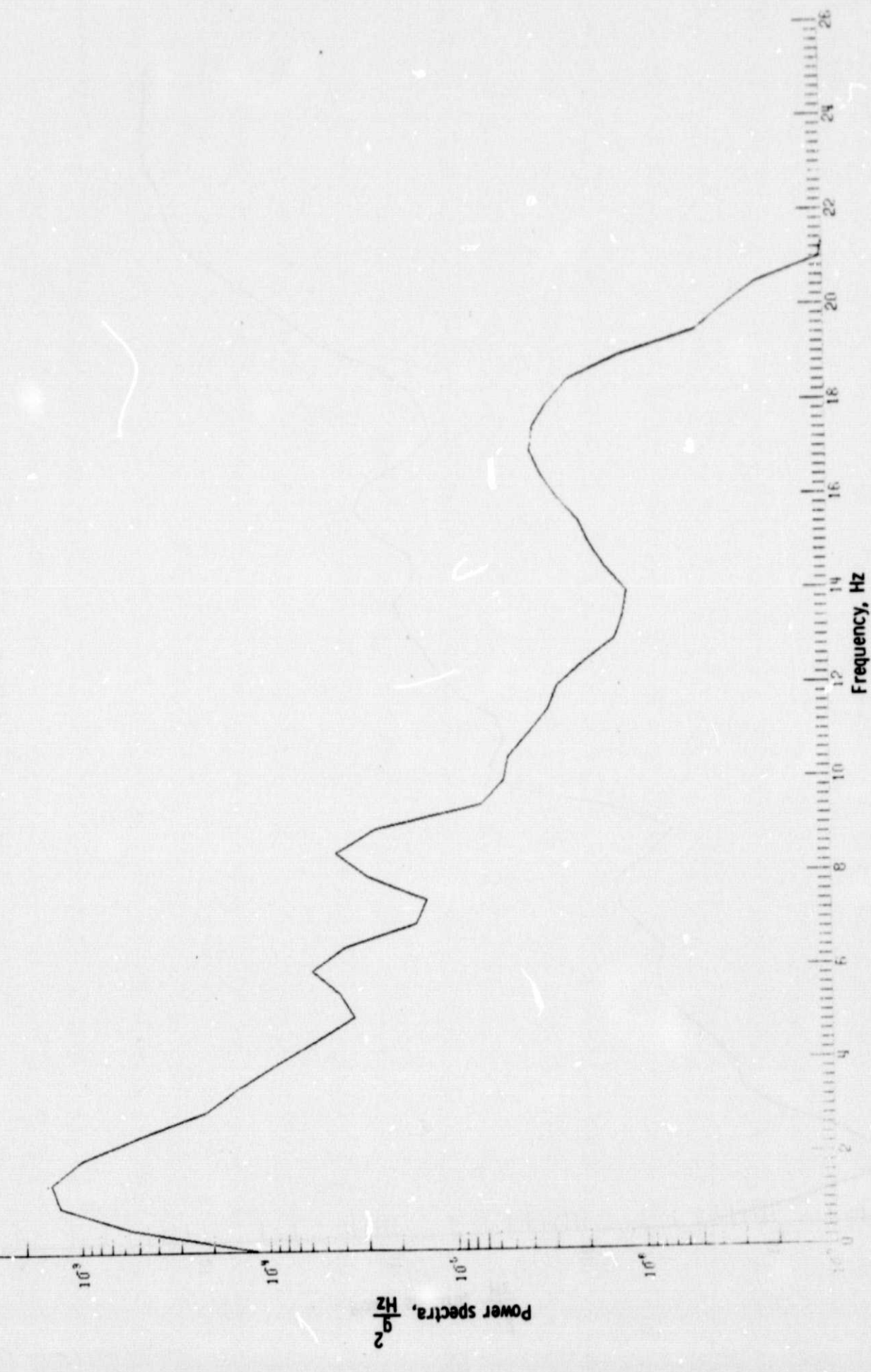
(c) Longitudinal acceleration power spectrum (RMS longitudinal acc. 0.0098 g).

Figure 6 - Continued.



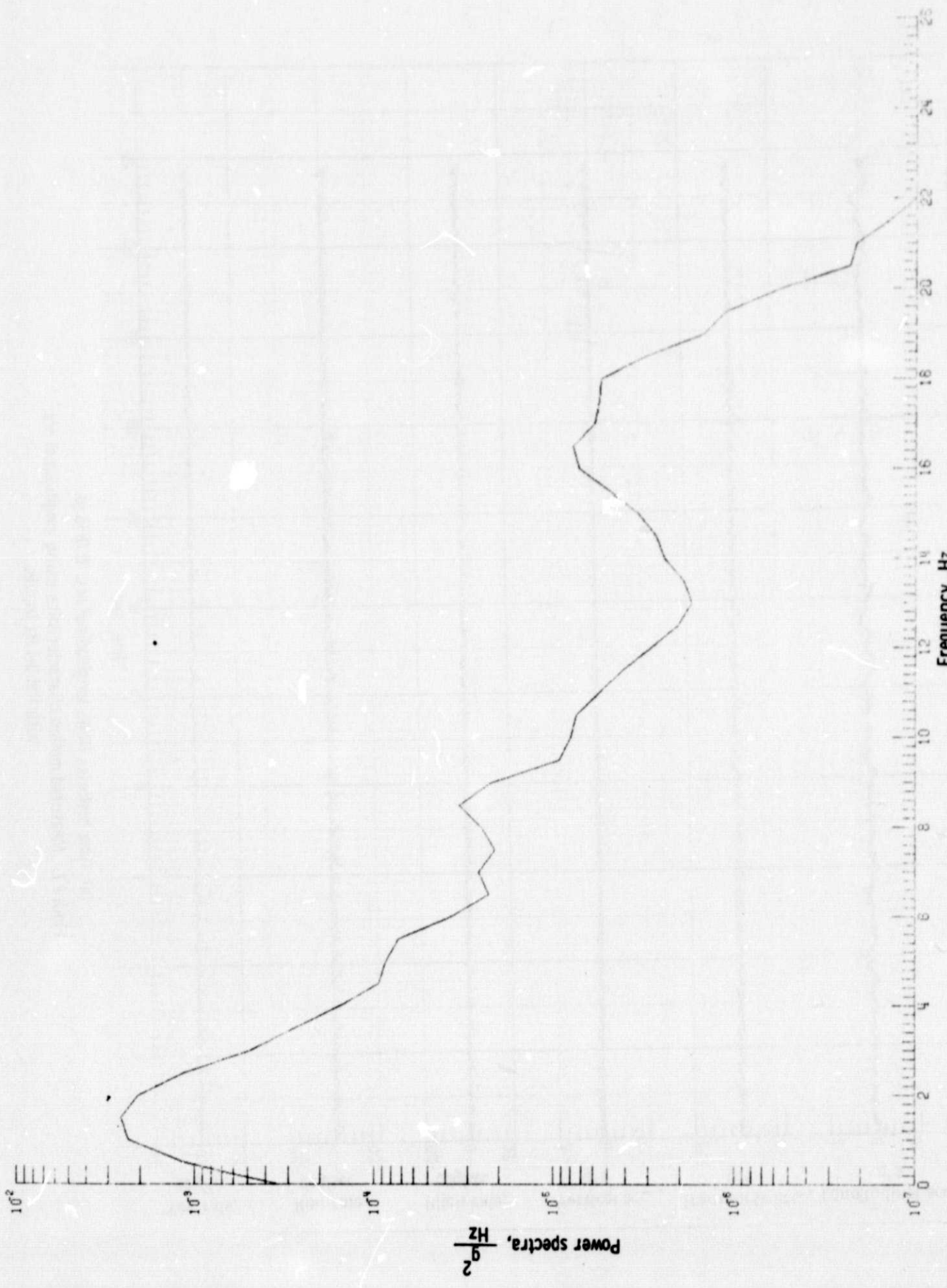
(c) Longitudinal acceleration power spectrum (RMS longitudinal acc. 0.029 g)

Figure 6 - Continued



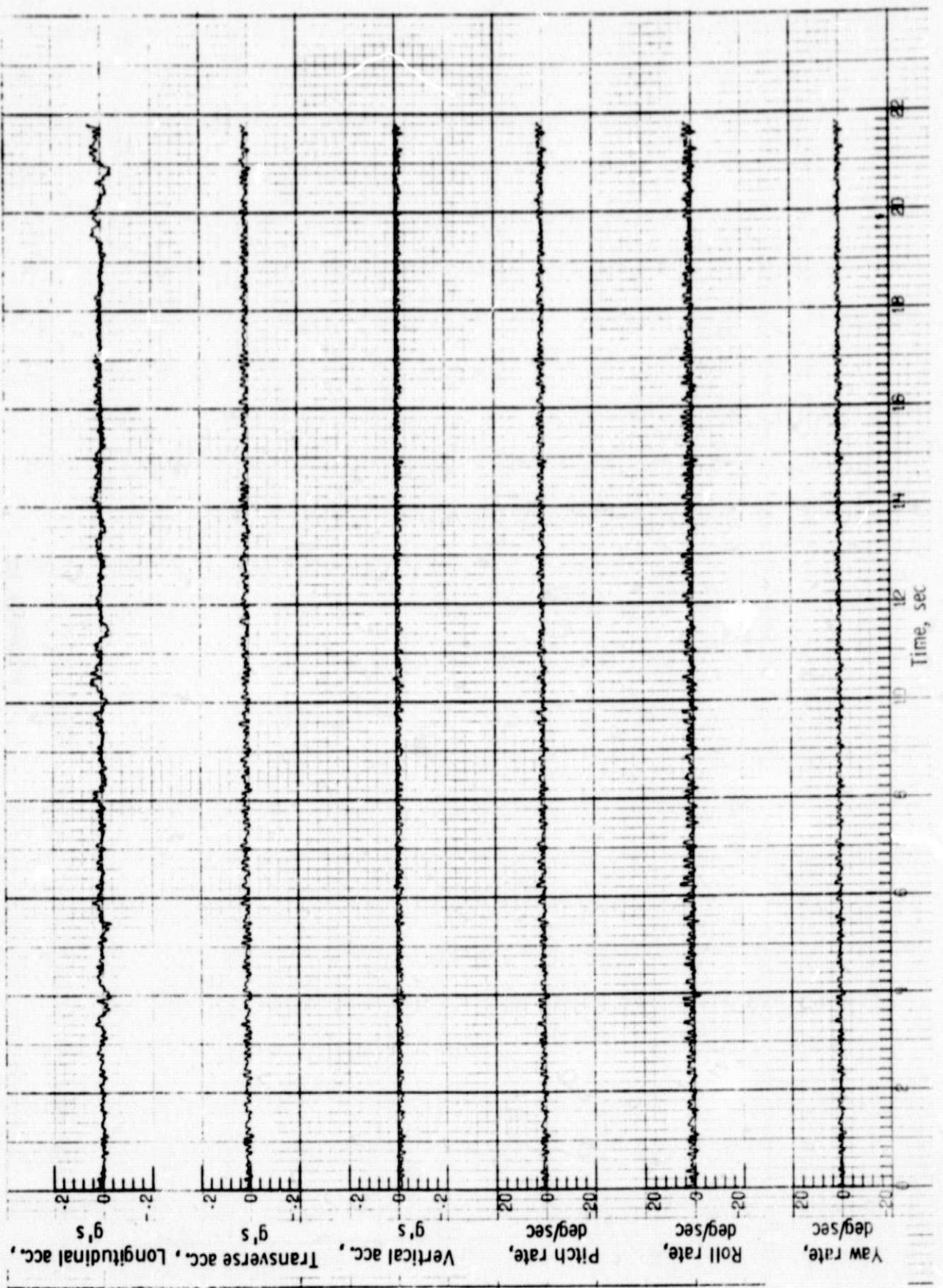
(c) Longitudinal acceleration power spectrum (RMS longitudinal acc. 0.0545 g).

Figure 6 - Continued.



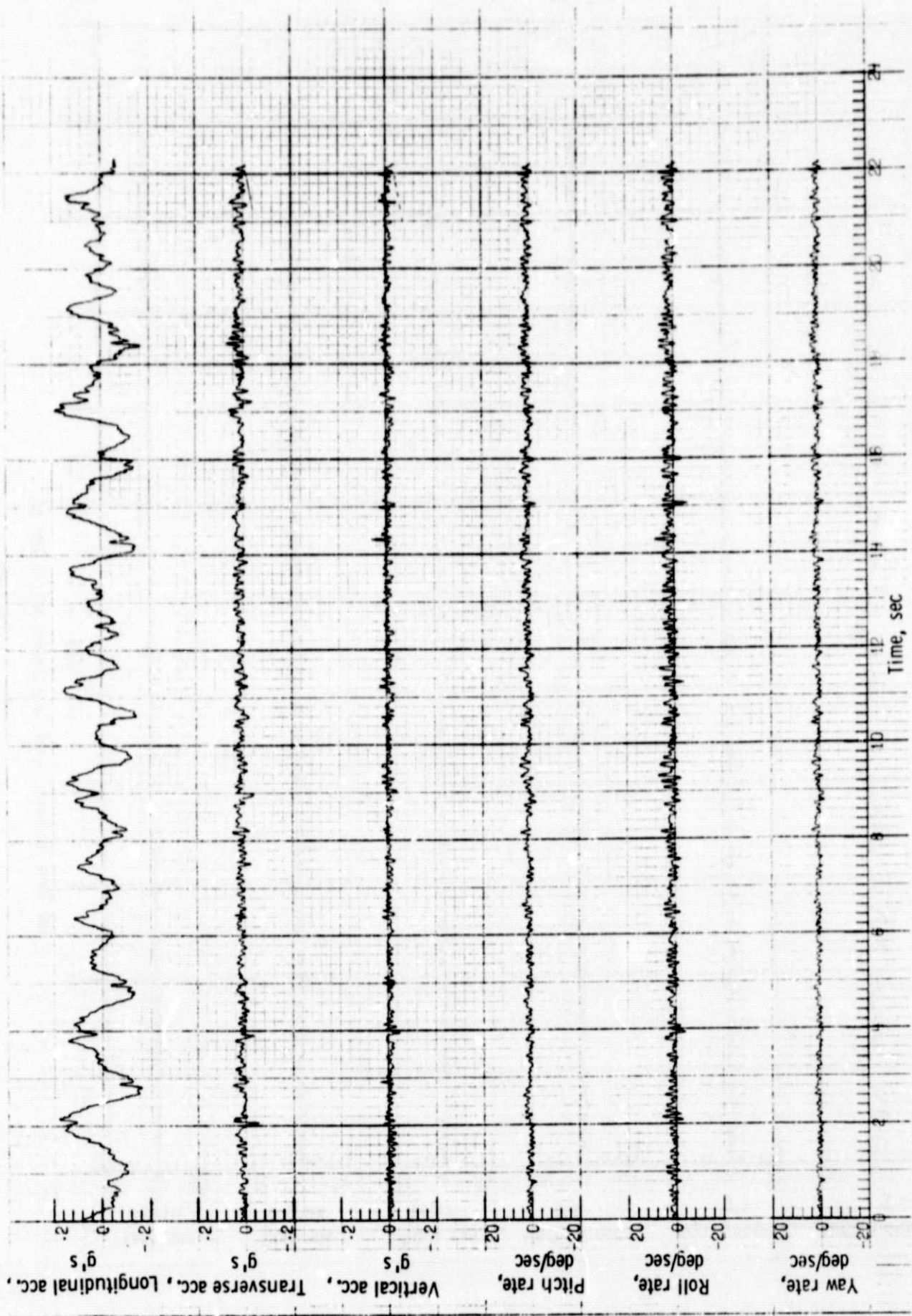
(c) Longitudinal acceleration power spectrum (RMS longitudinal acc.  $0.0798 \text{ g}$ ).

Figure 6 - Concluded.



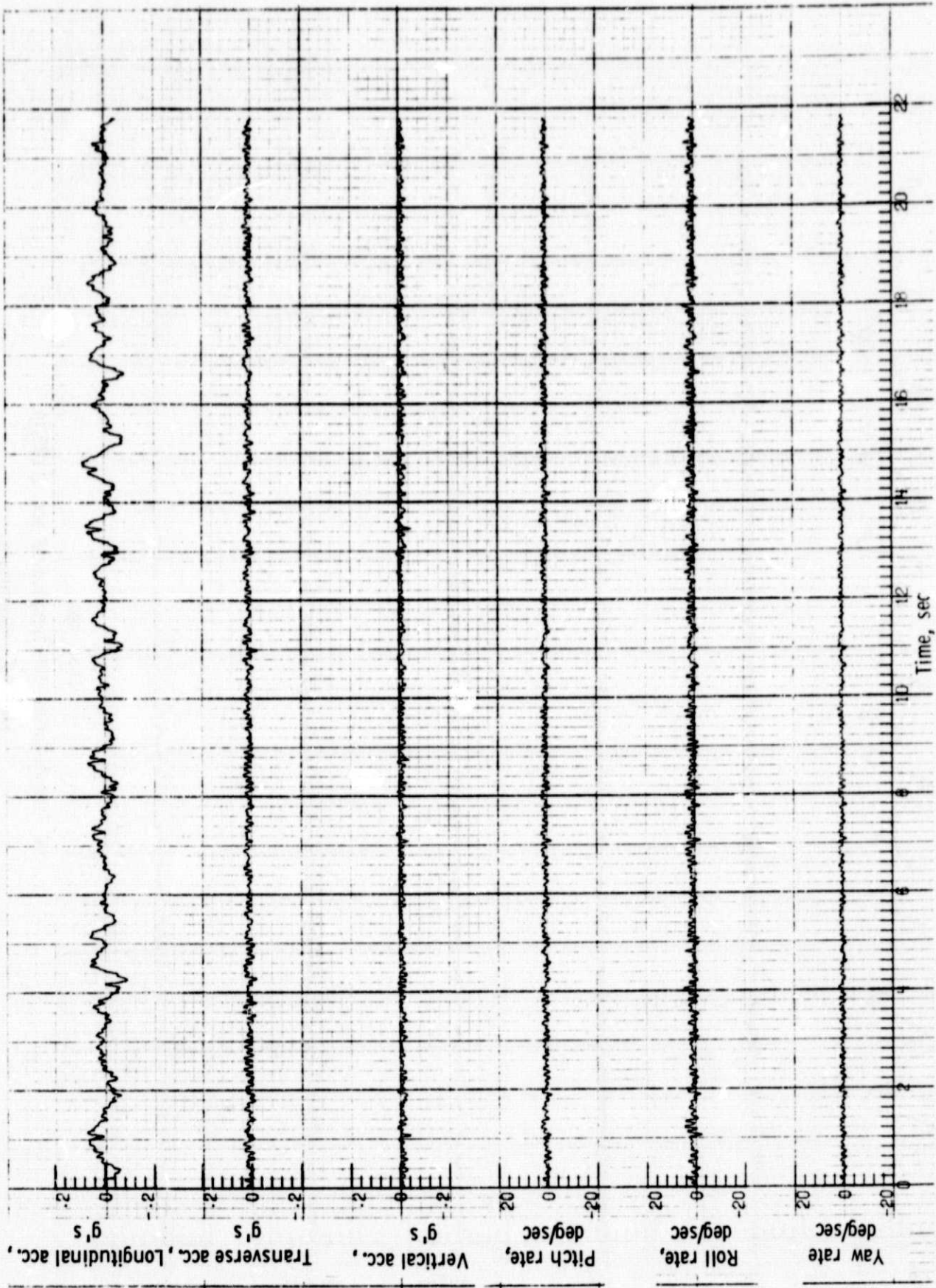
(a) Time histories (RMS longitudinal acc. 0.0138 g).

Figure 7. Measured motion characteristics using longitudinal acc.  
with flat 0-1 Hz inputs.



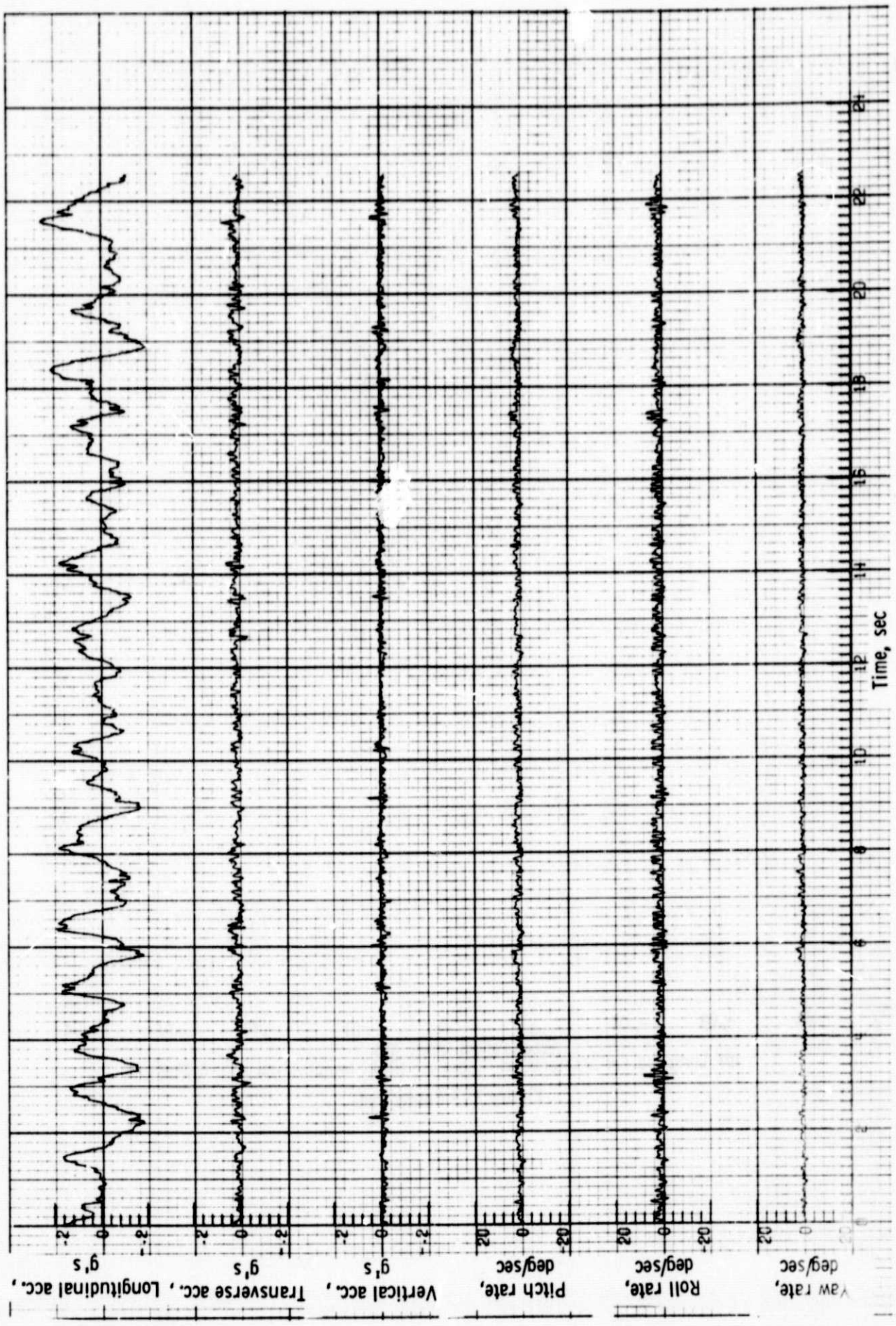
(a) Time histories (RMS longitudinal acc. 0.0727g).

Figure 7. - Continued.



(a) Time histories (RMS longitudinal acc. 0.0301 g).

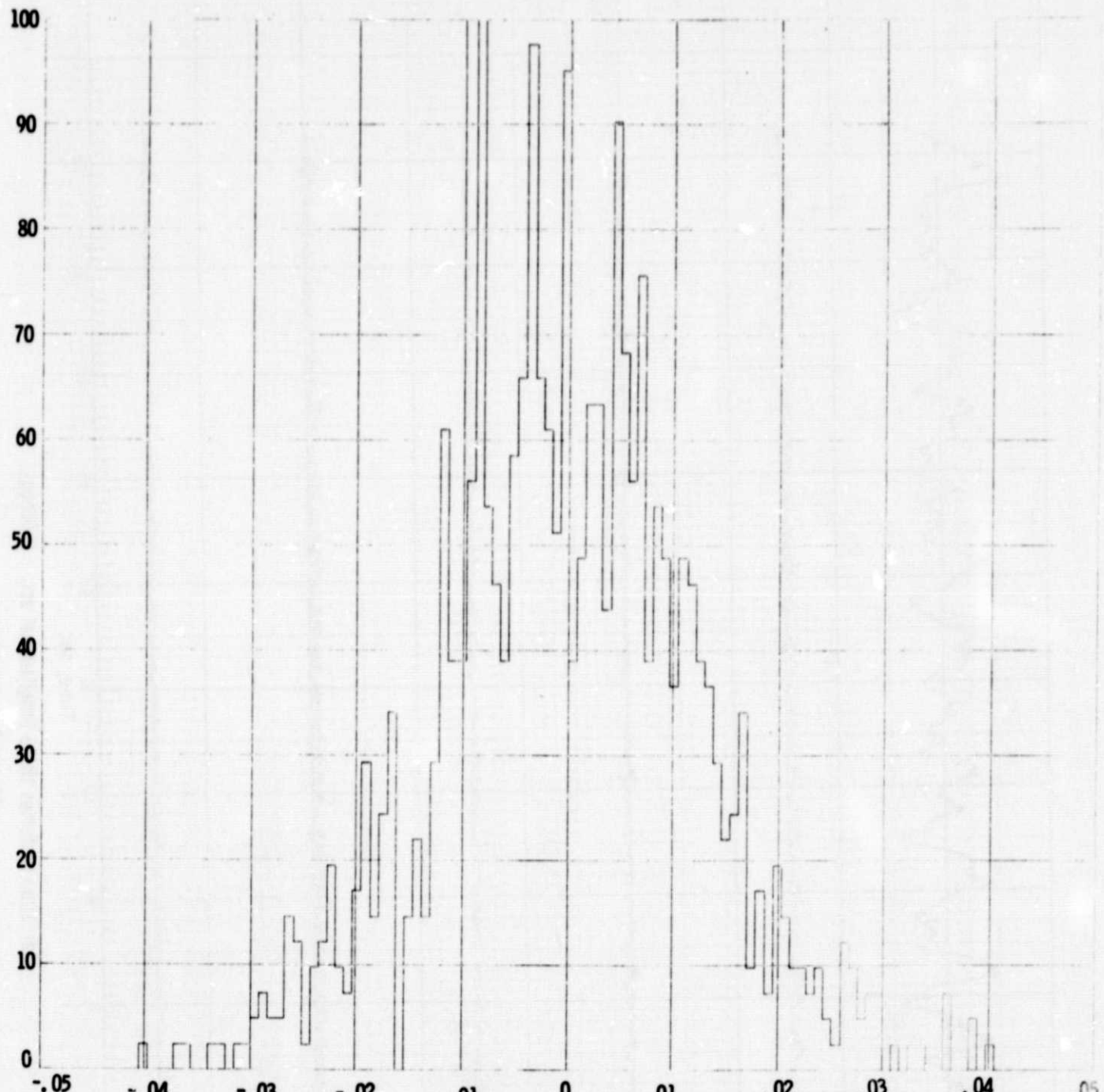
Figure 7. - Continued.



(a) Time histories; (RMS longitudinal acc. 0.0866g).

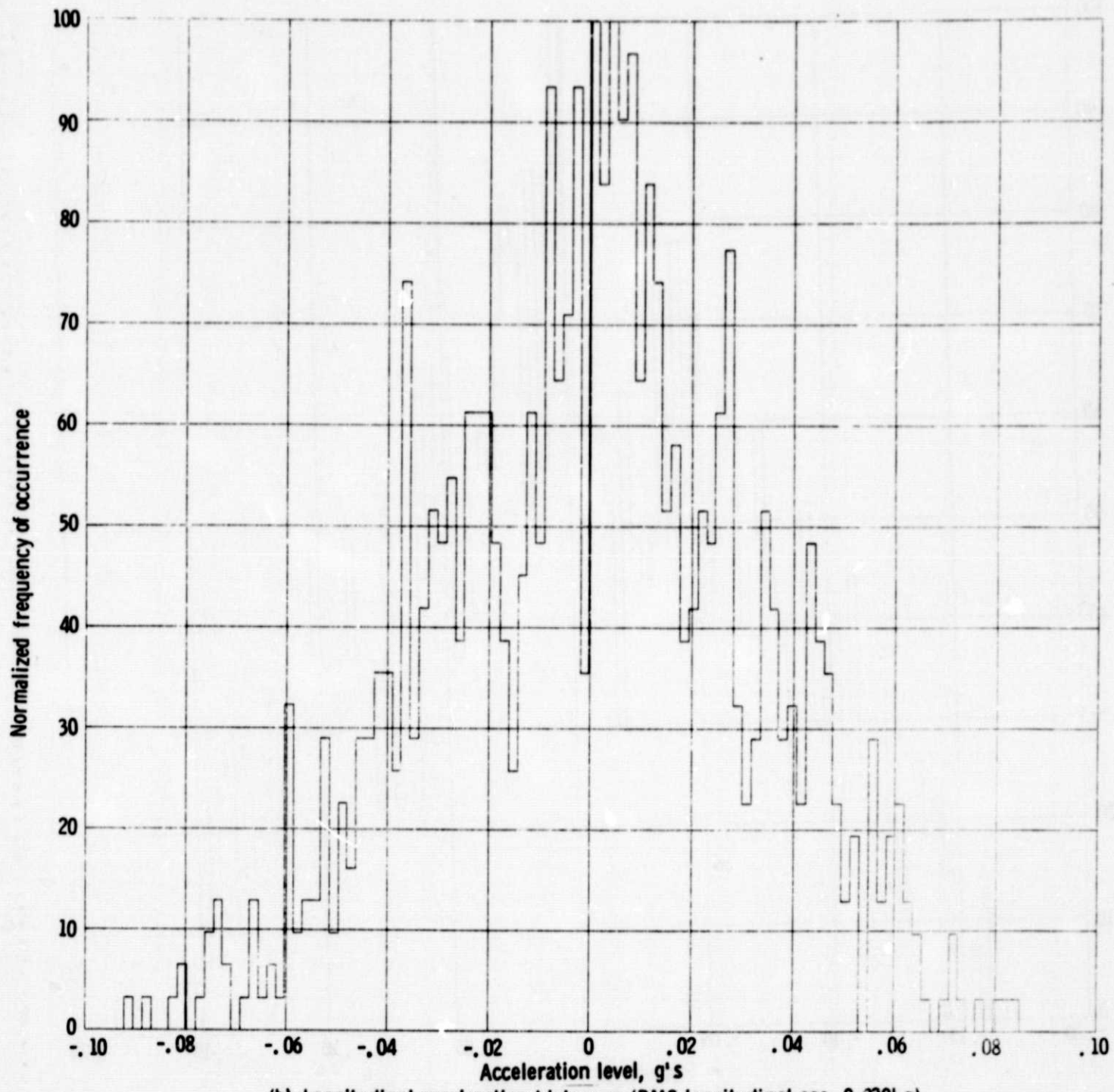
Figure 7. - Continued.

Normalized frequency of occurrence



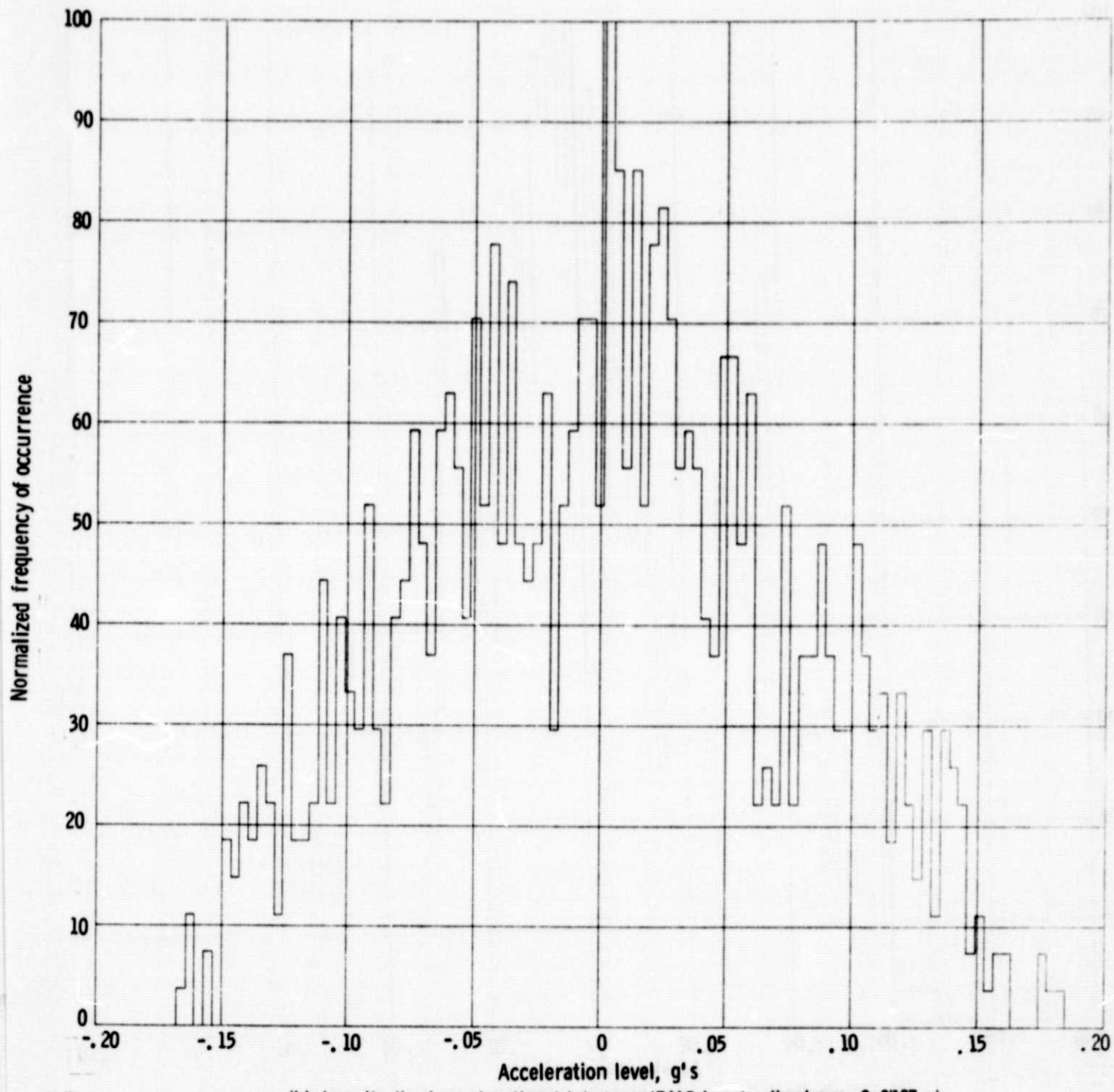
(b) Longitudinal acceleration histogram (RMS longitudinal acc. 0.0138 g).

Figure 7. - Continued.



(b) Longitudinal acceleration histogram (RMS longitudinal acc. 0.0301 g).

Figure 7. - Continued.



(b) Longitudinal acceleration histogram (RMS longitudinal acc. 0.0727 g).

Figure 7. - Continued.

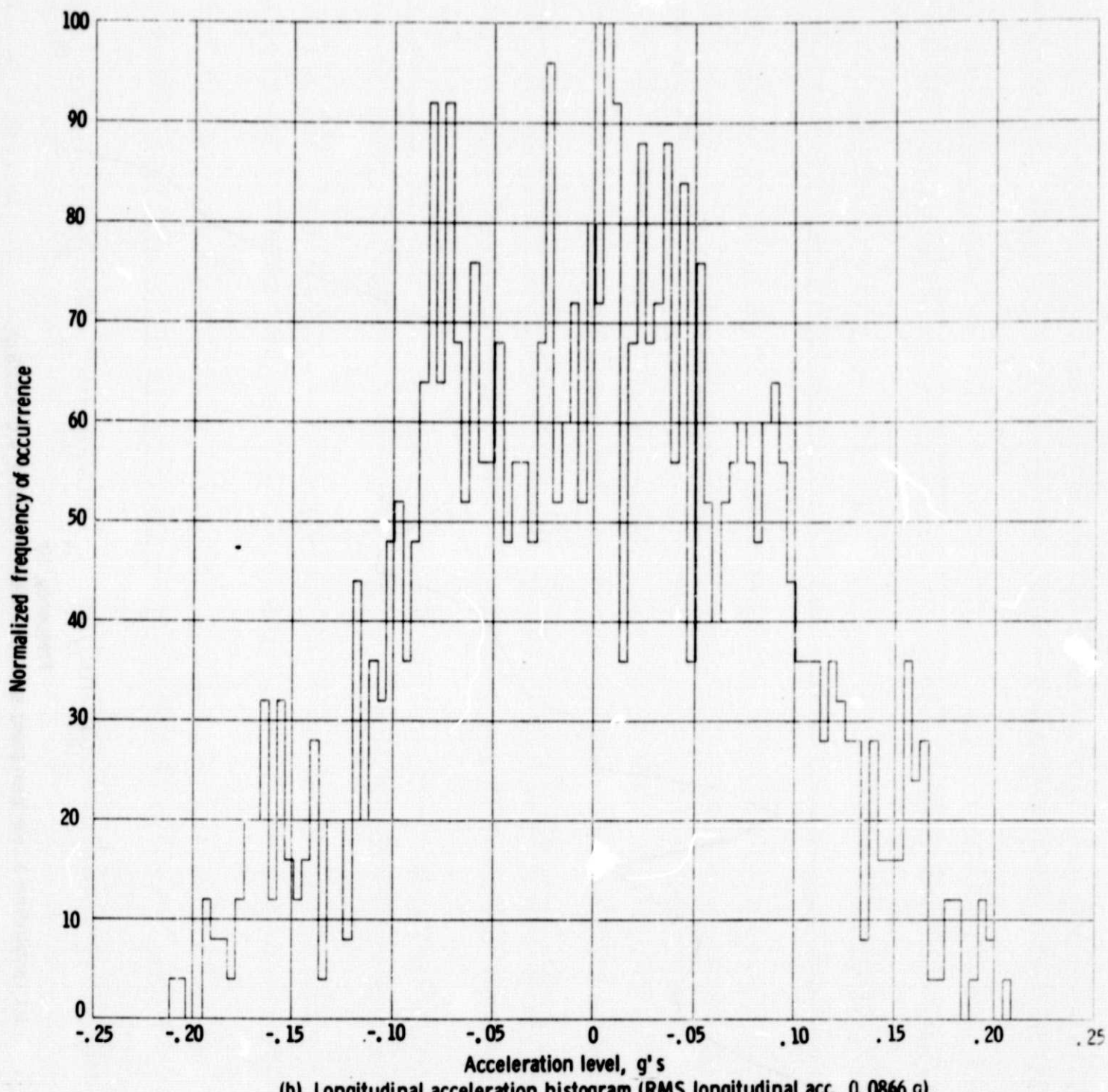
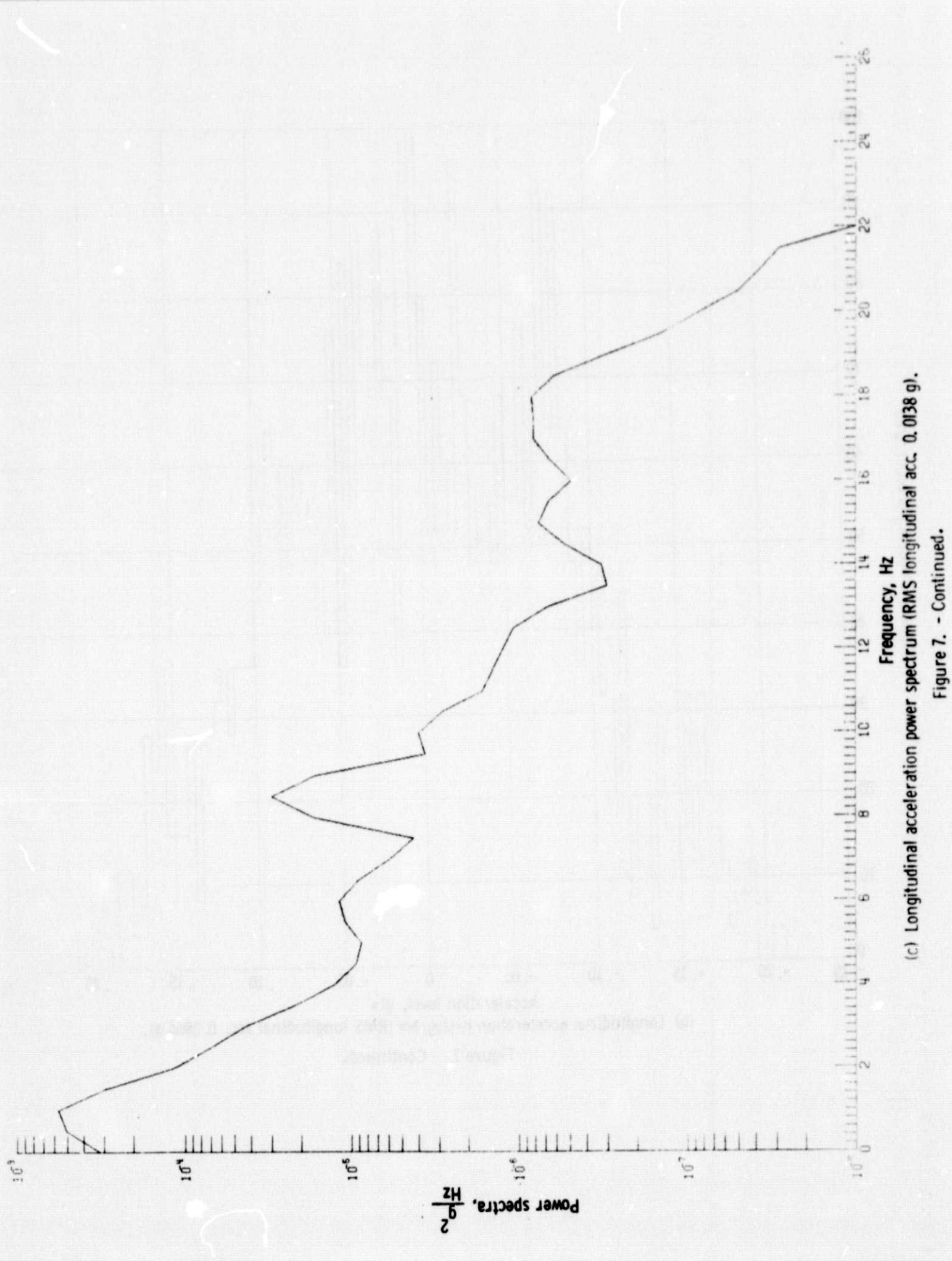
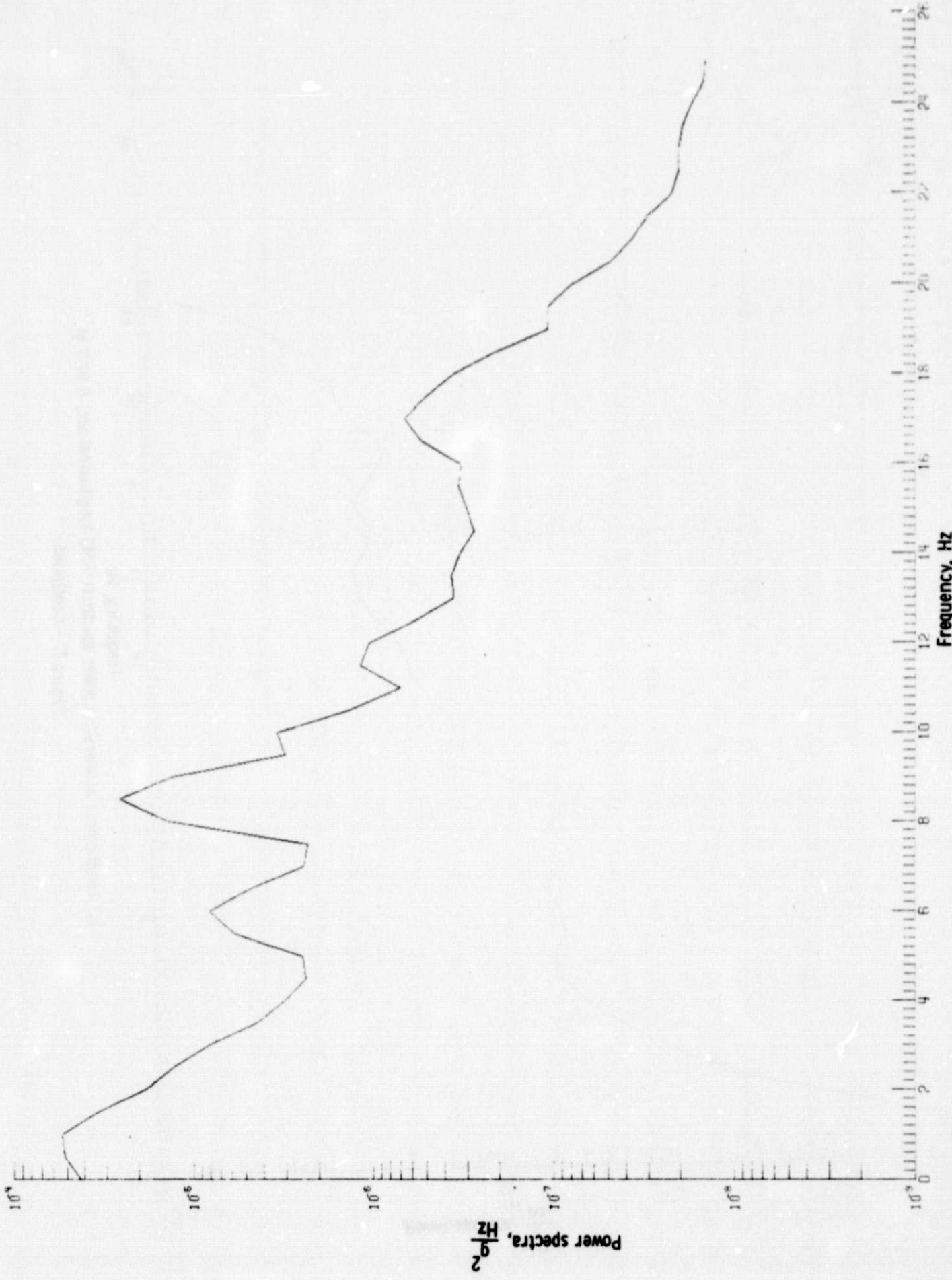


Figure 7. - Continued.



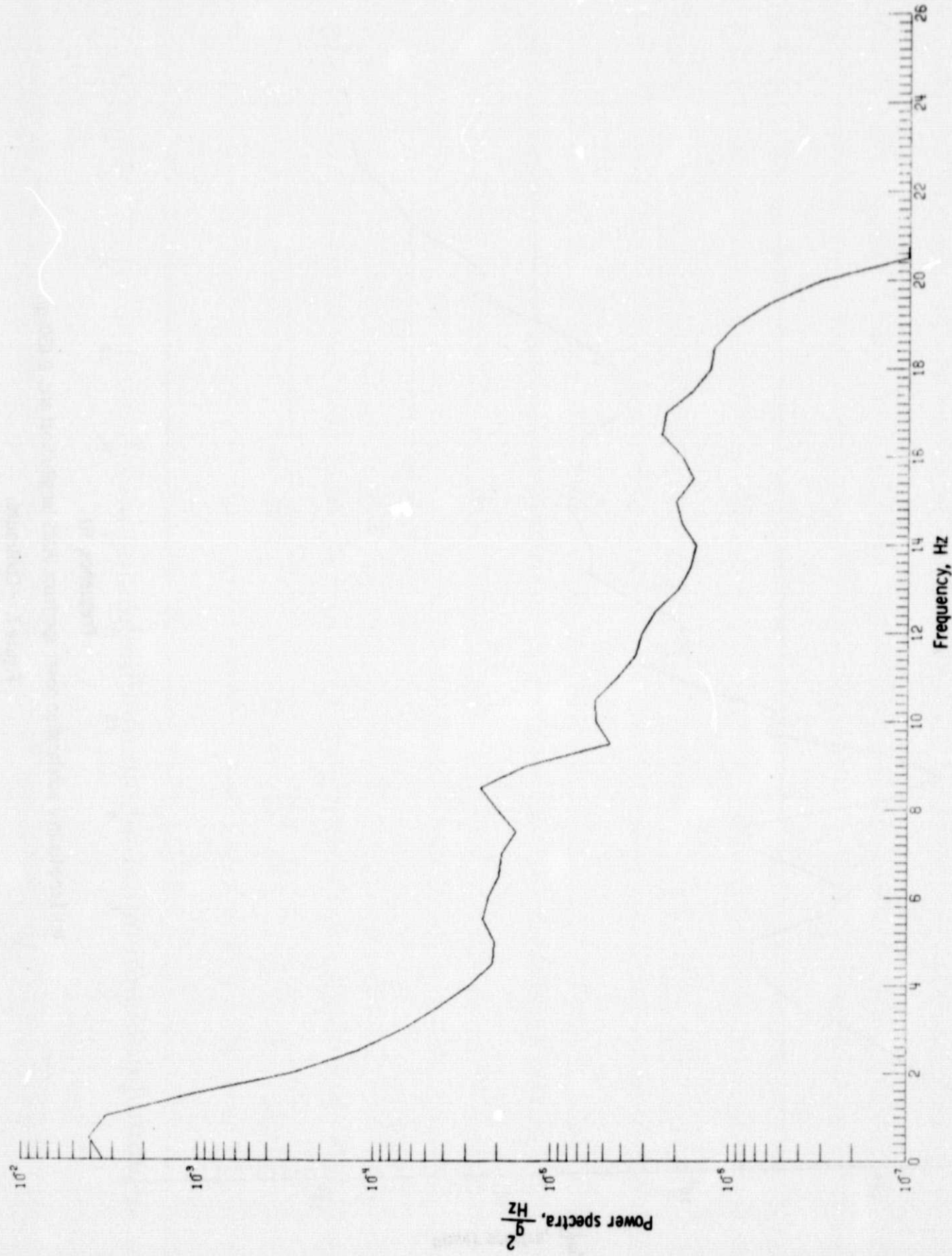
(c) Longitudinal acceleration power spectrum (RMS longitudinal acc. 0.0138 g).

Figure 7. - Continued.



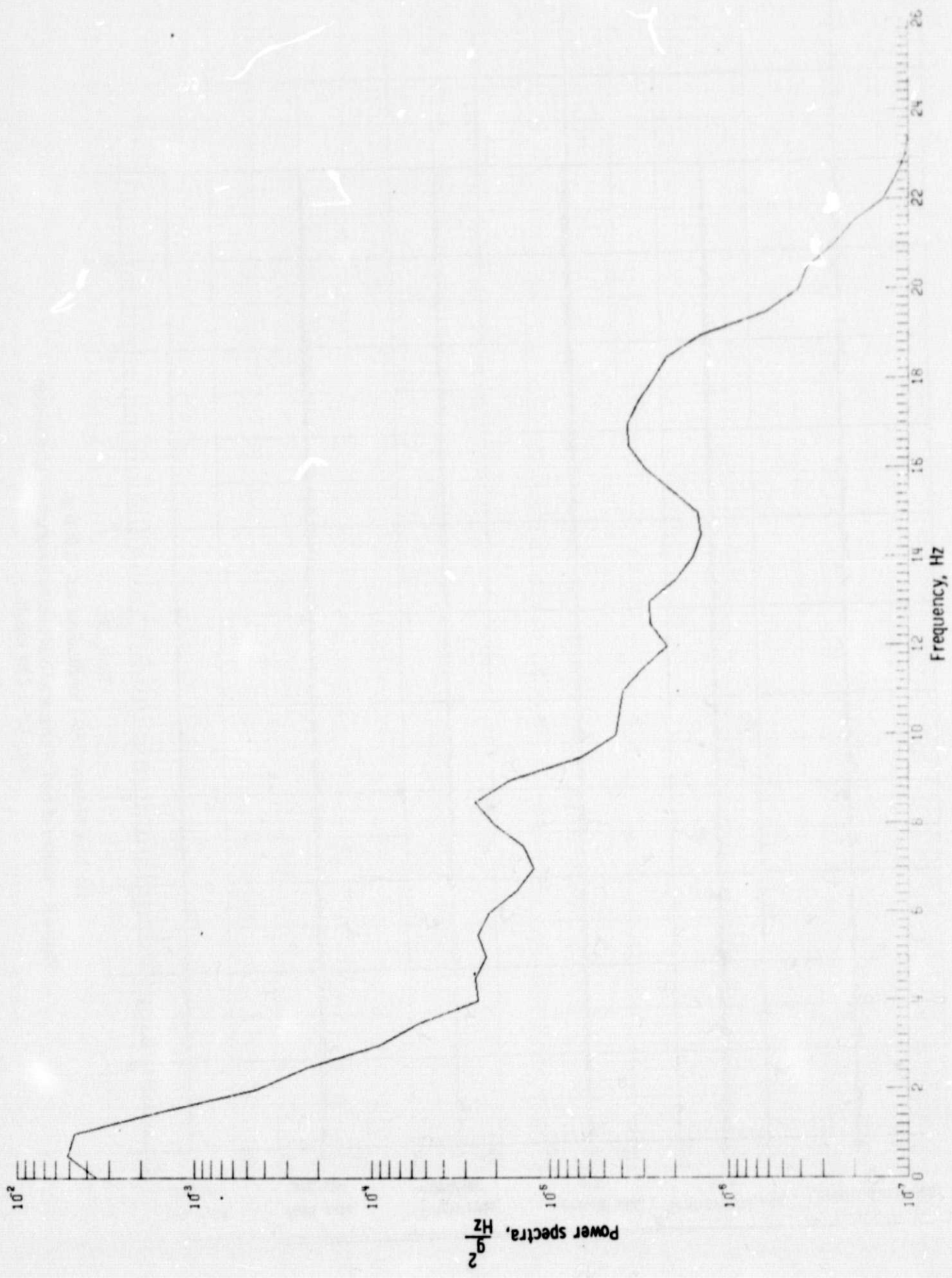
(c) Longitudinal acceleration power spectrum (RMS longitudinal acc. 0.0301 g).

Figure 7. - Continued.



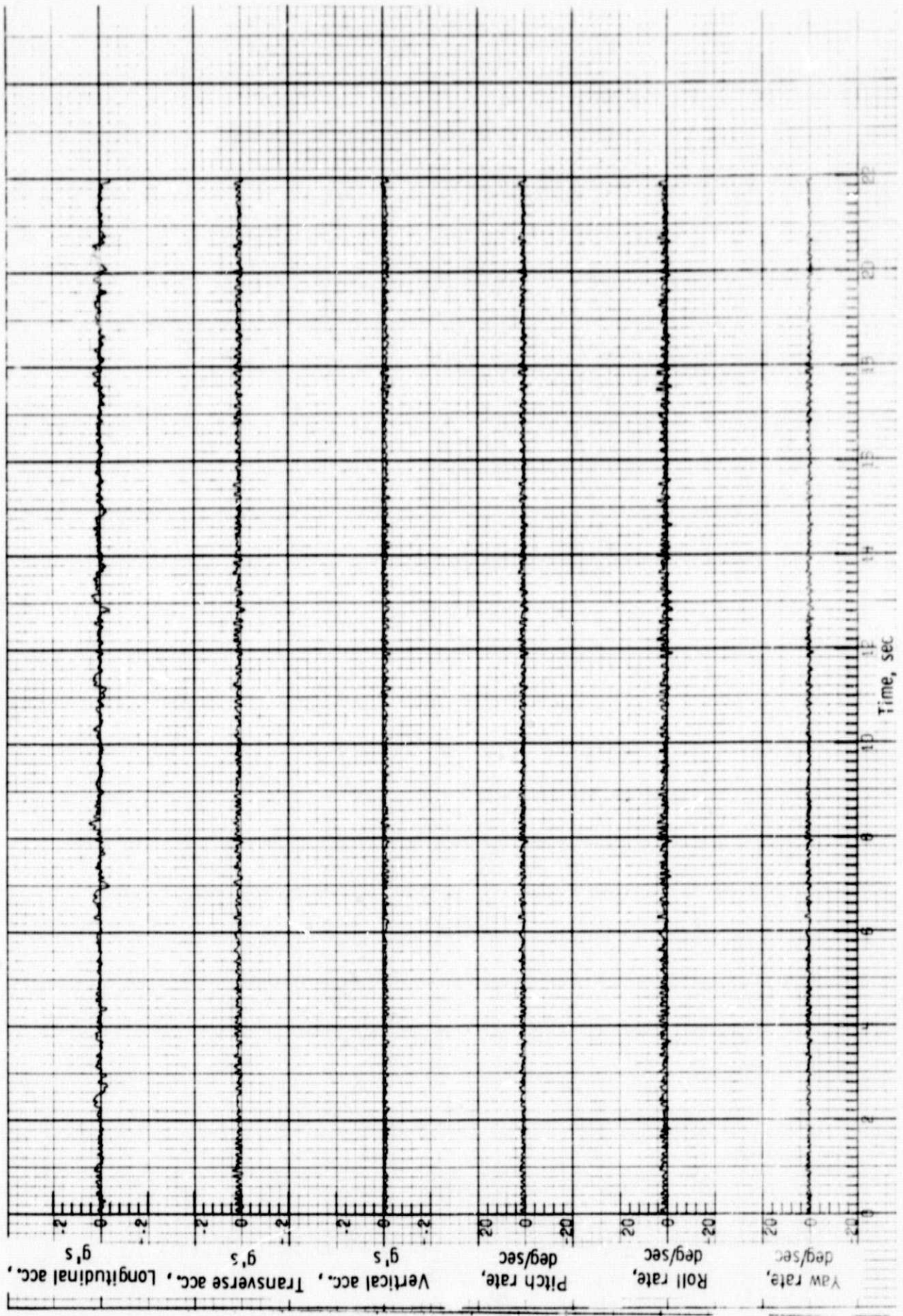
(c) Longitudinal acceleration power spectrum (RMS longitudinal acc. 0.0727 g).

Figure 7. - Continued.



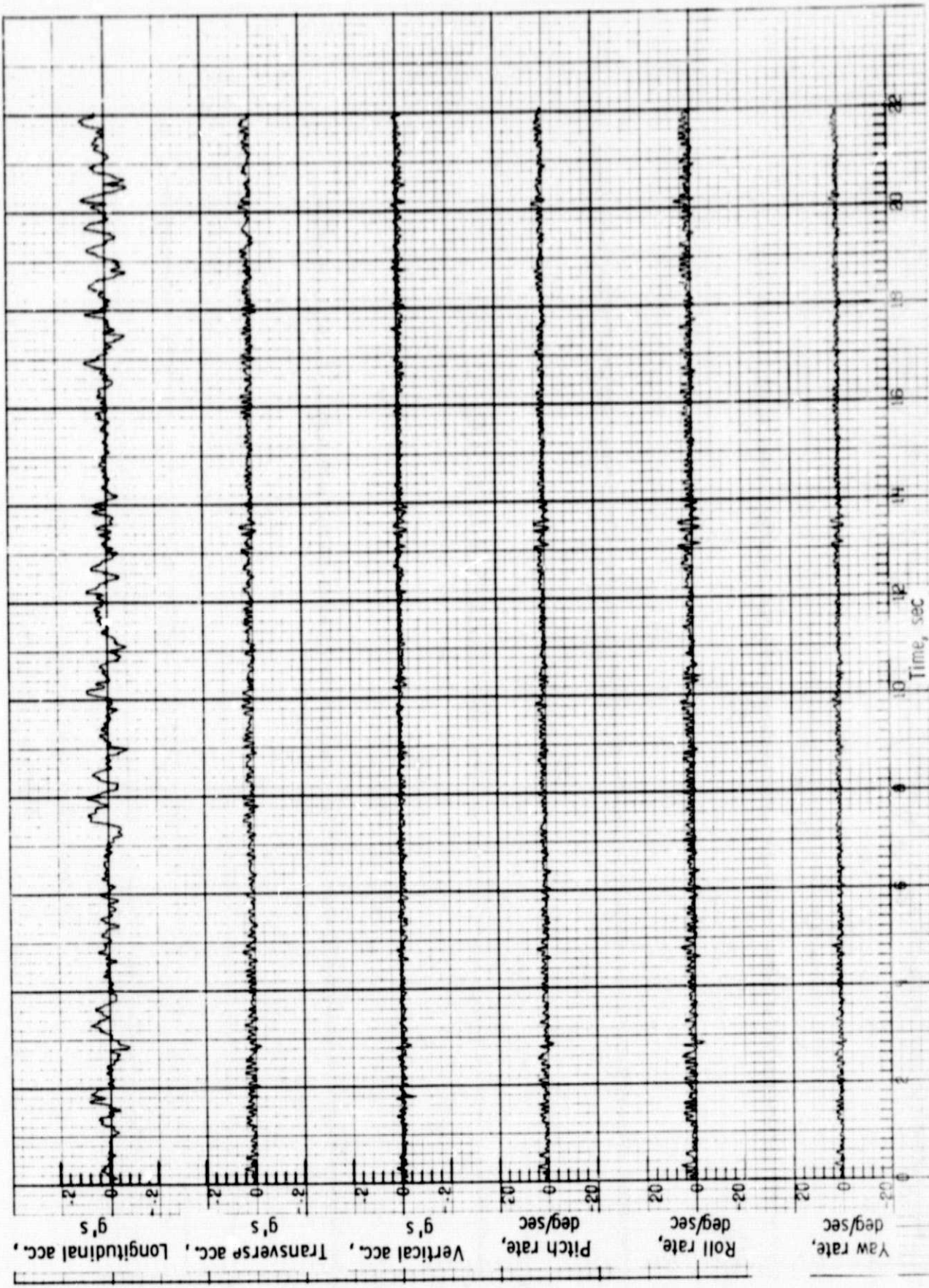
(c) Longitudinal acceleration power spectrum (RMS longitudinal acc. 0.0866 g).

Figure 7. - Concluded.



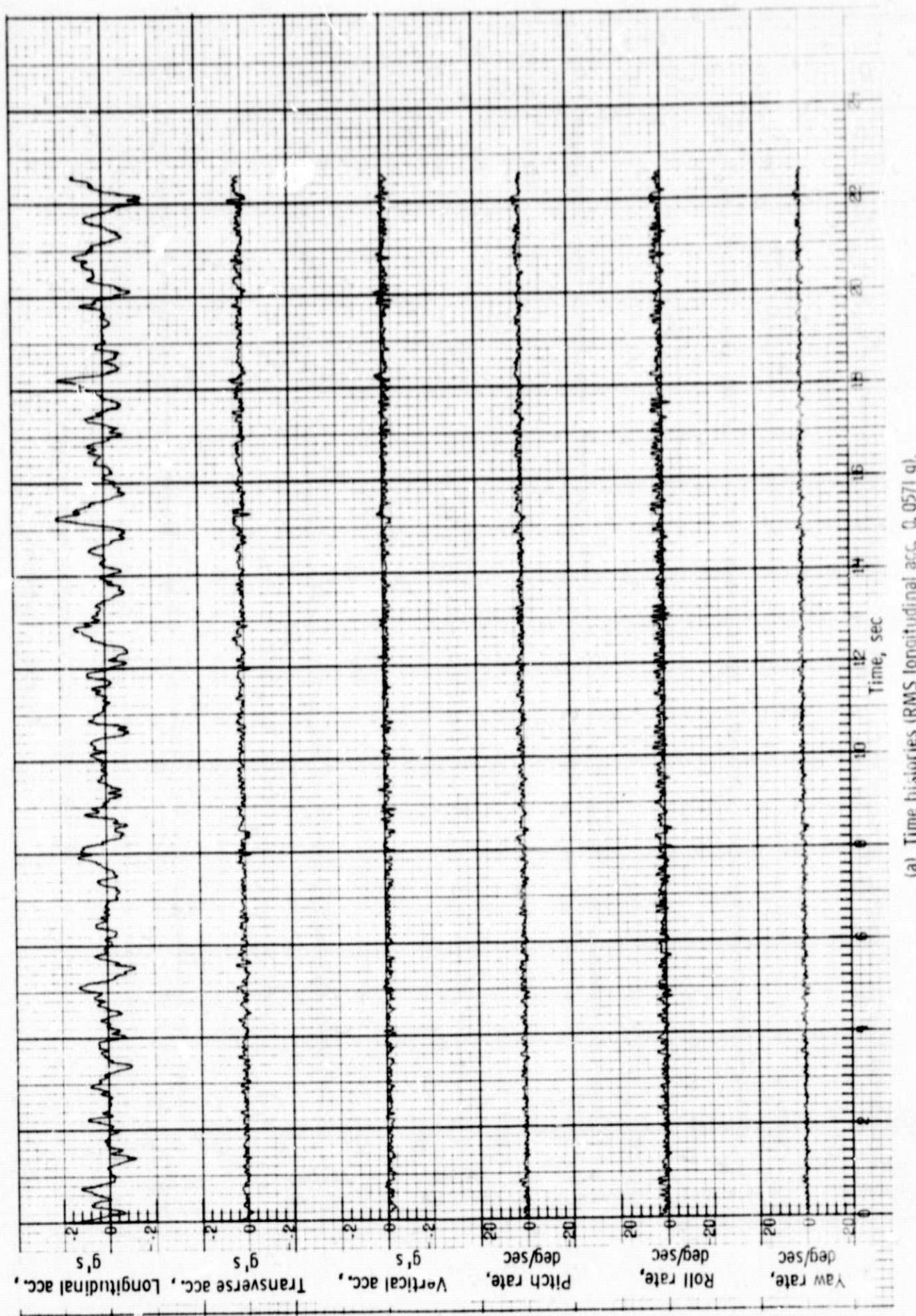
(a) Time histories (RMS longitudinal acc. 0.0120 g).

Figure 8. Measured motion characteristics using longitudinal acceleration with flat 0-2 Hz inputs.



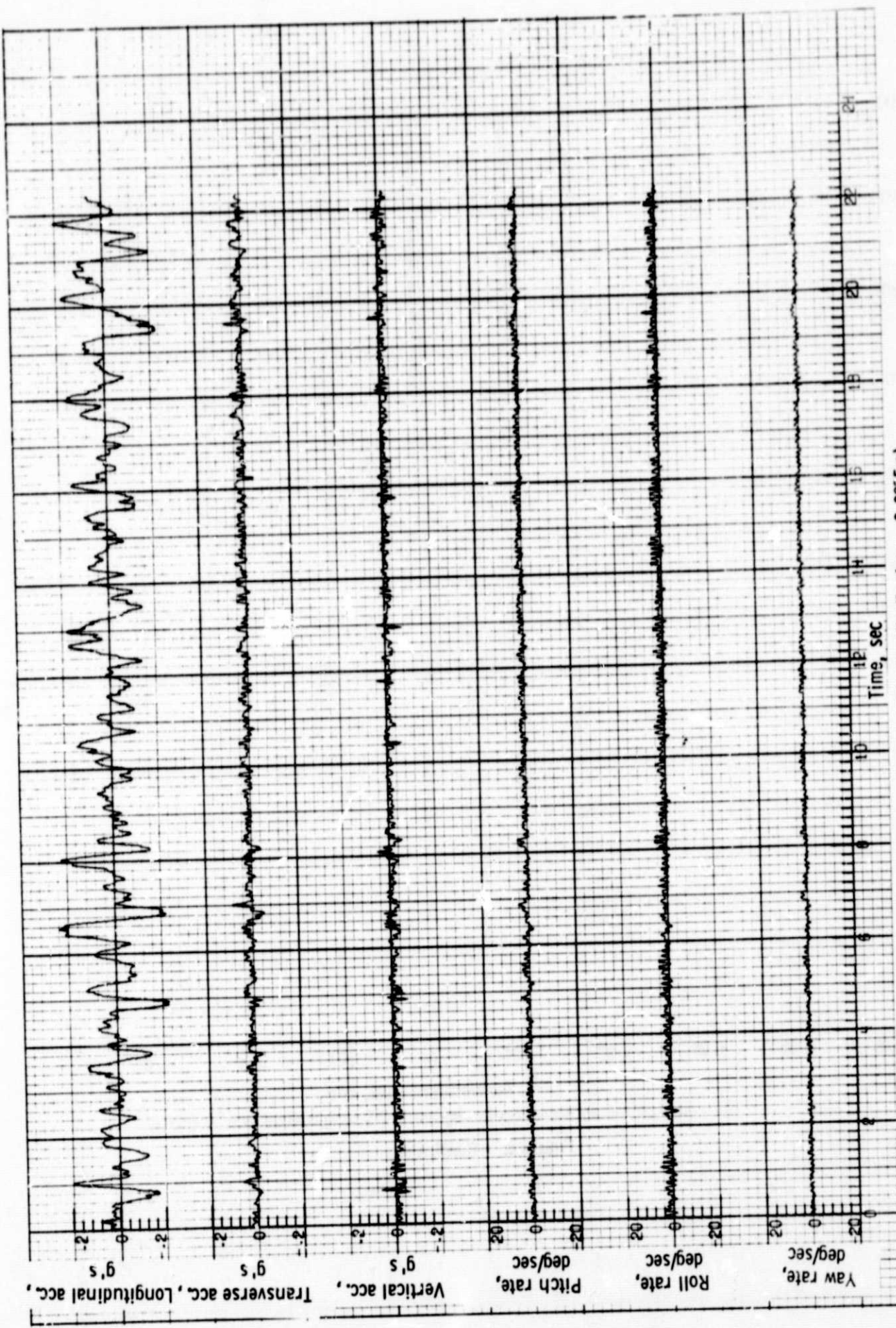
(a) Time histories (RMS longitudinal acc. 0.0315 g).

Figure 8 - Continued.



(a) Time histories (RMS longitudinal acc. 0.0571 g).

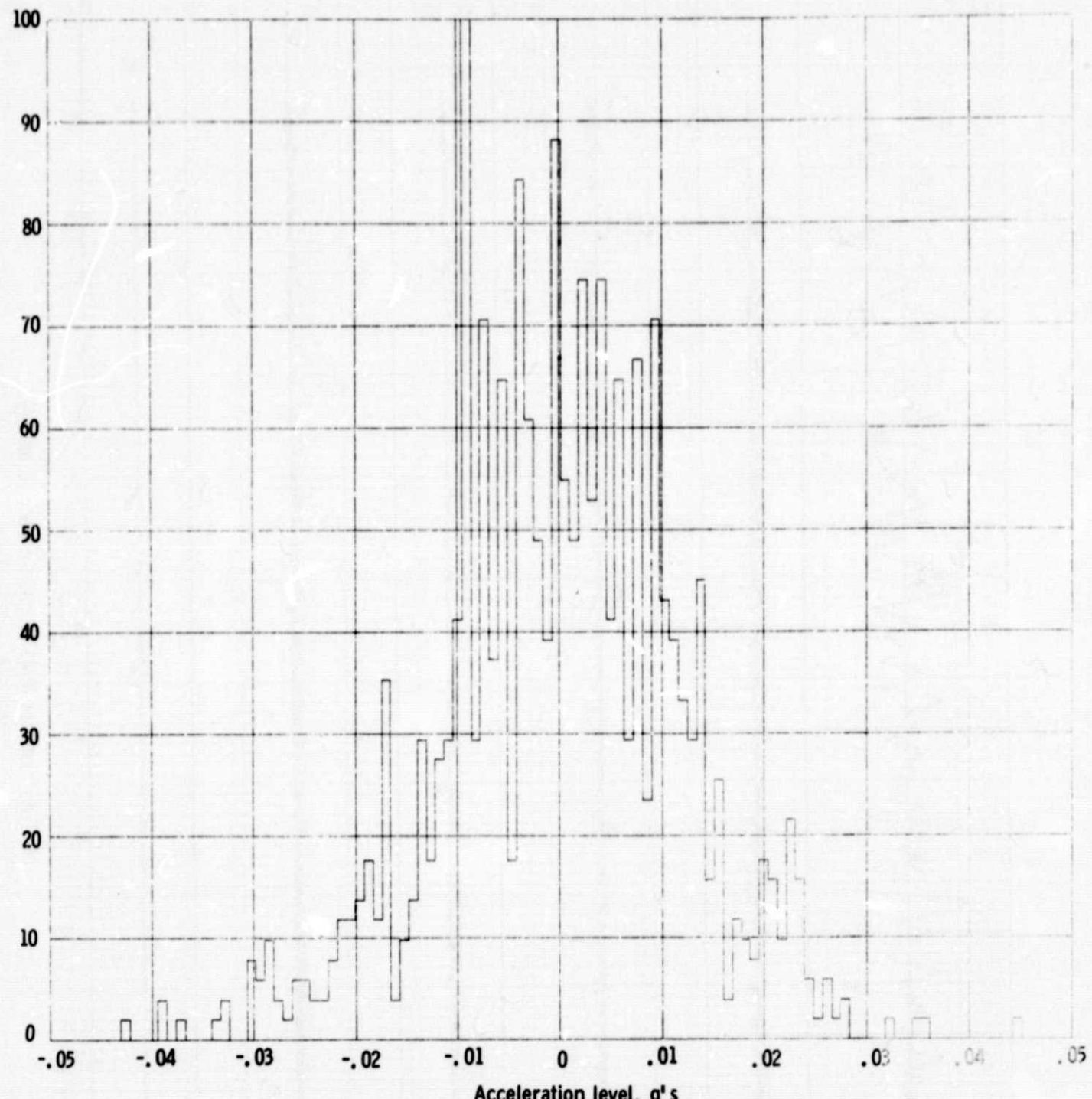
Figure 8 - Continued.



(a) Time histories (RMS longitudinal acc. 0.0855 g).

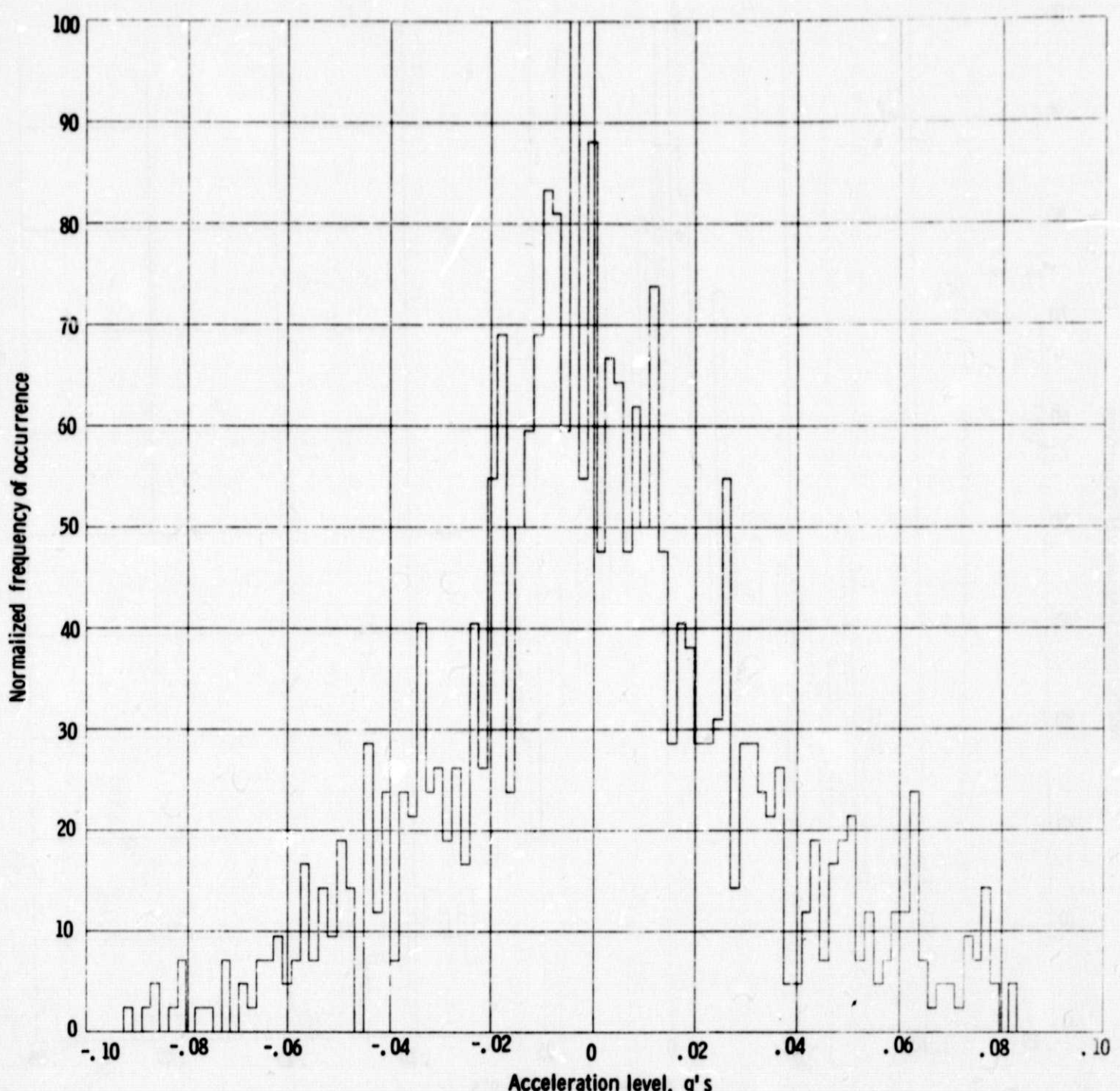
Figure 8 - Continued.

Normalized frequency of occurrence



(b) Longitudinal acceleration histogram (RMS longitudinal acc. 0.0120 g).

Figure 8. - Continued.



(b) Longitudinal acceleration histogram (RMS longitudinal acc. 0.0315 g).

Figure 8. - Continued.

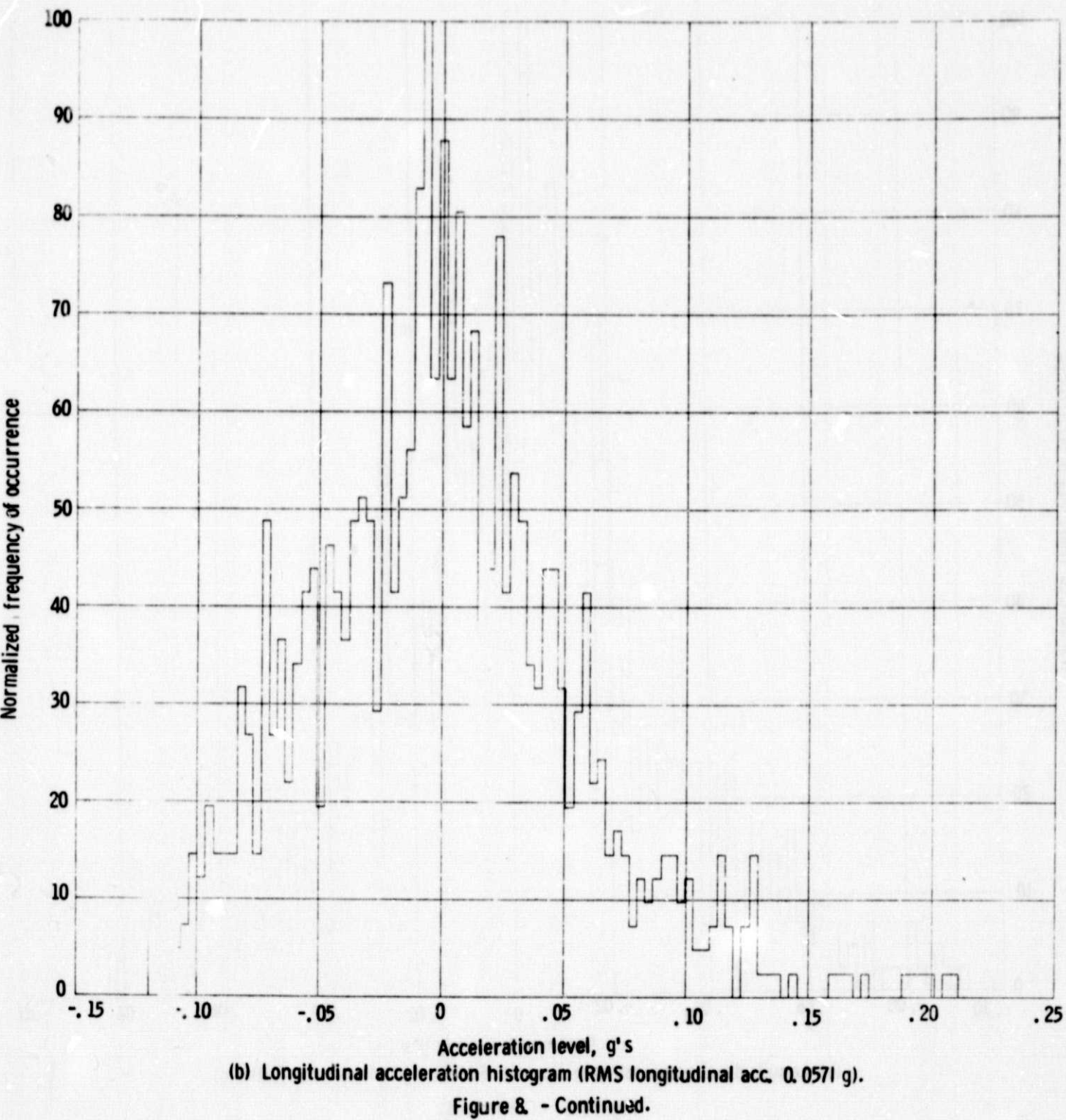
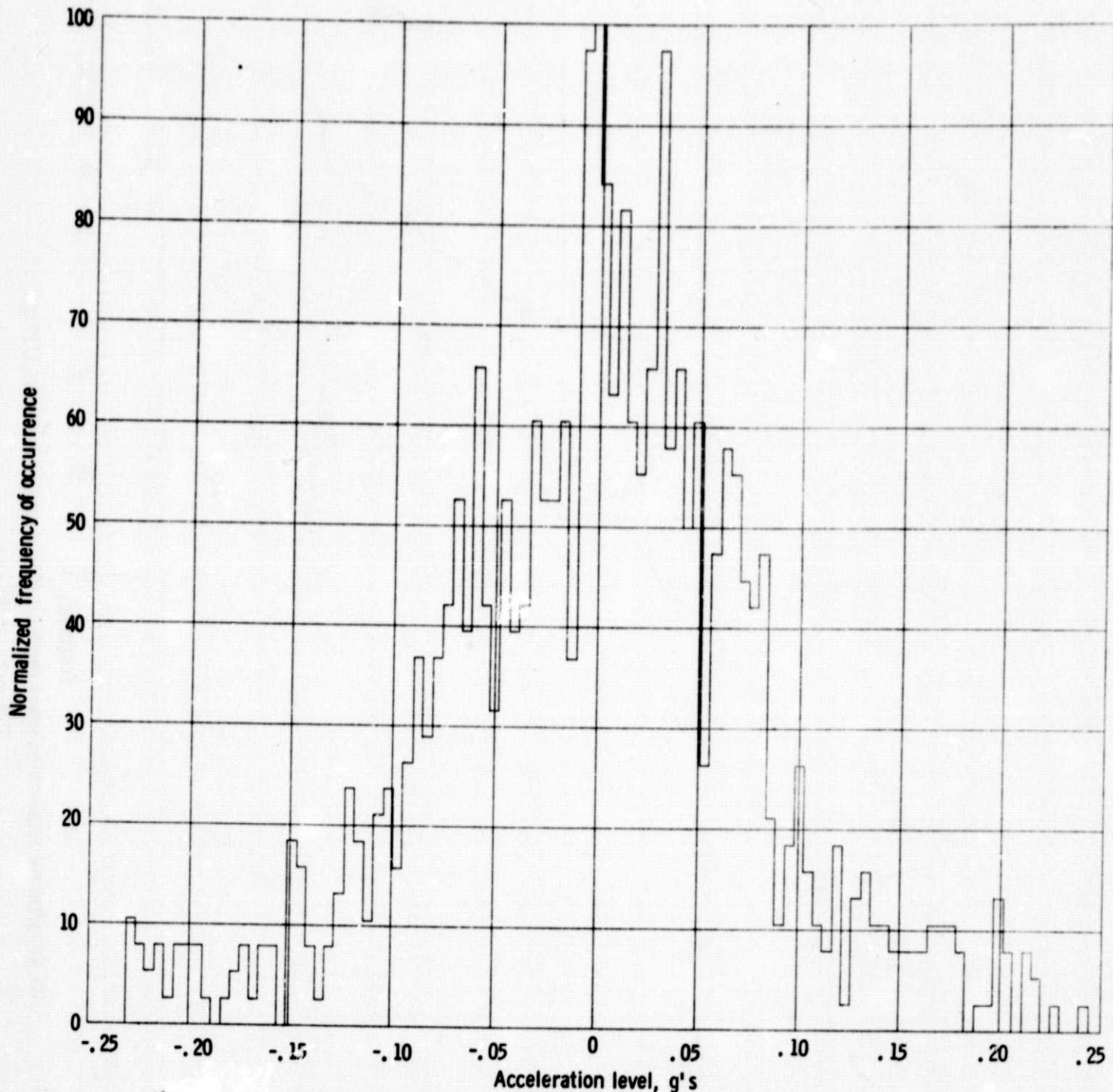
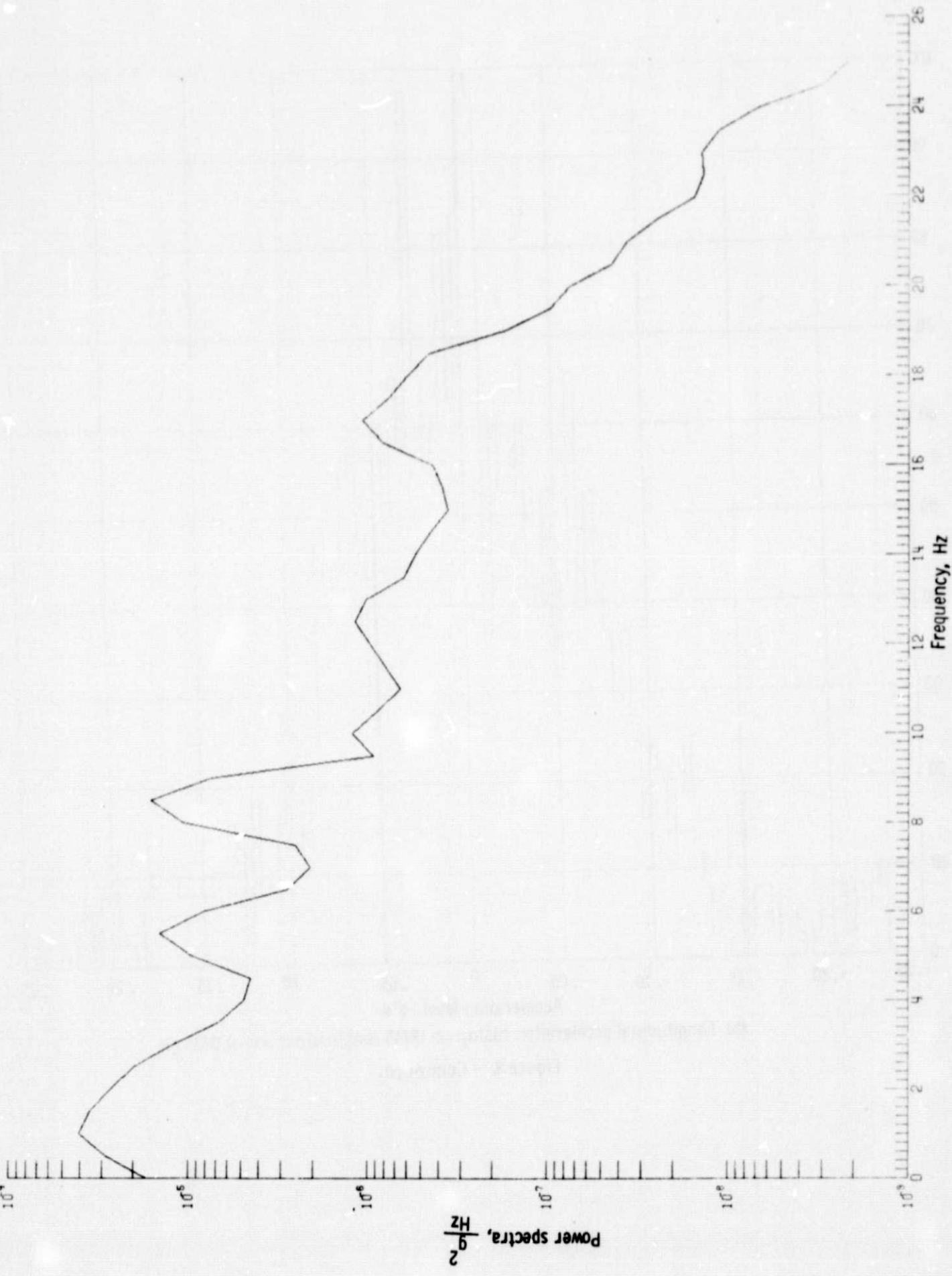


Figure 8 - Continued.



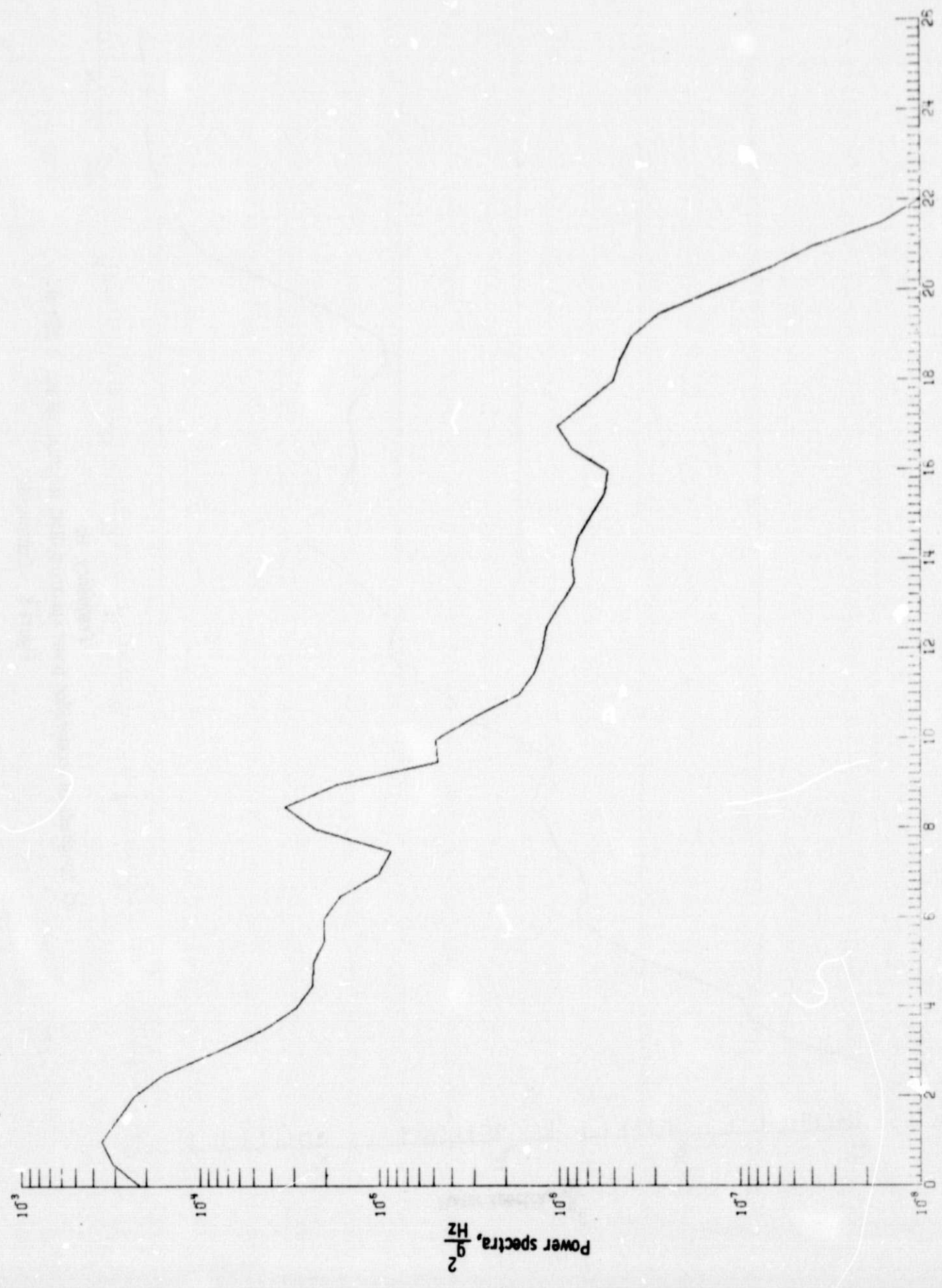
(b) Longitudinal acceleration histogram (RMS longitudinal acc. 0.0835 g).

Figure 8 - Continued.



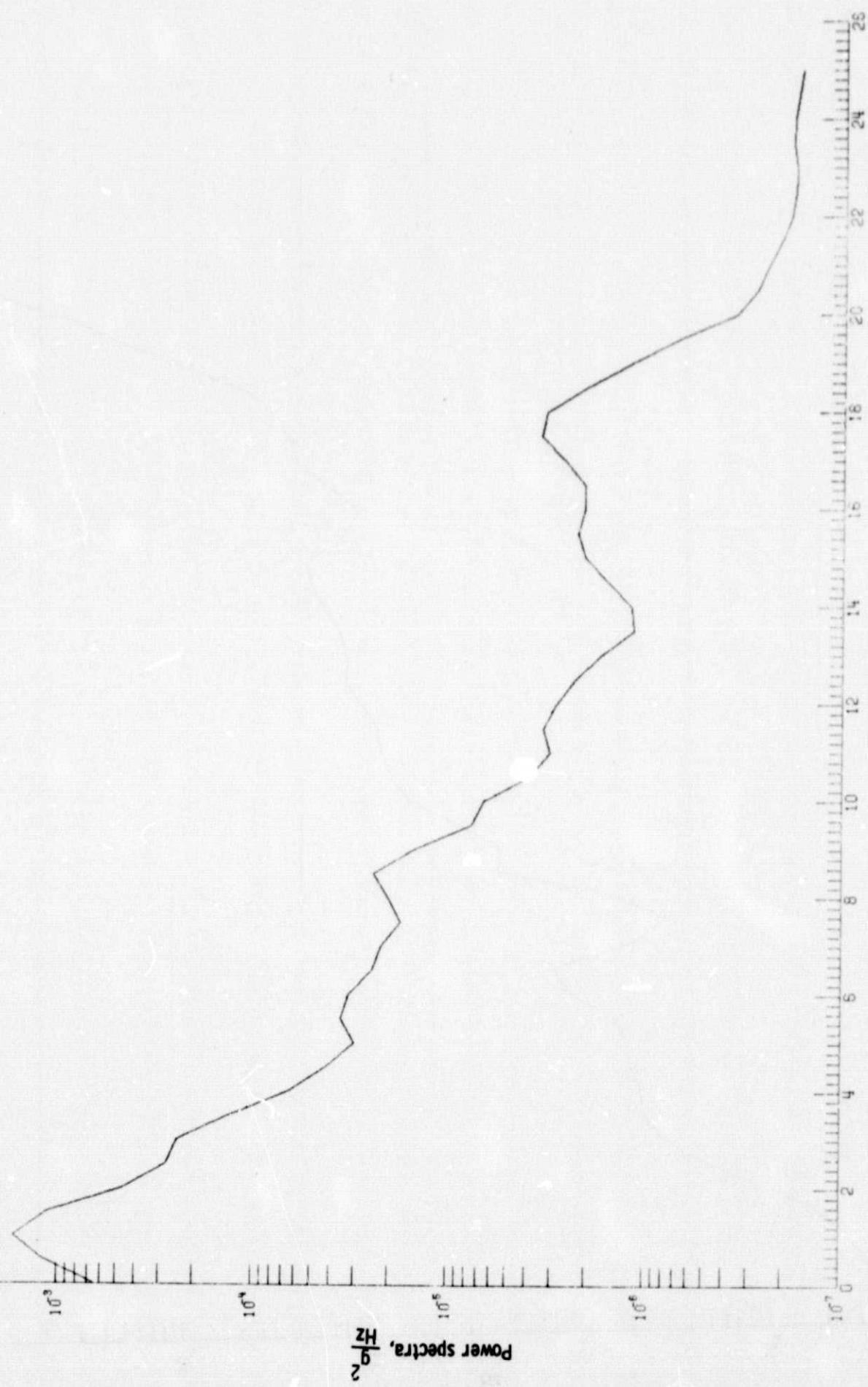
(c) Longitudinal acceleration power spectrum (RMS longitudinal acc. 0.0120 g).

Figure 8 - Continued.



(c) Longitudinal acceleration power spectrum (RMS longitudinal acc. 0.0315 g).

Figure 8 - Continued.



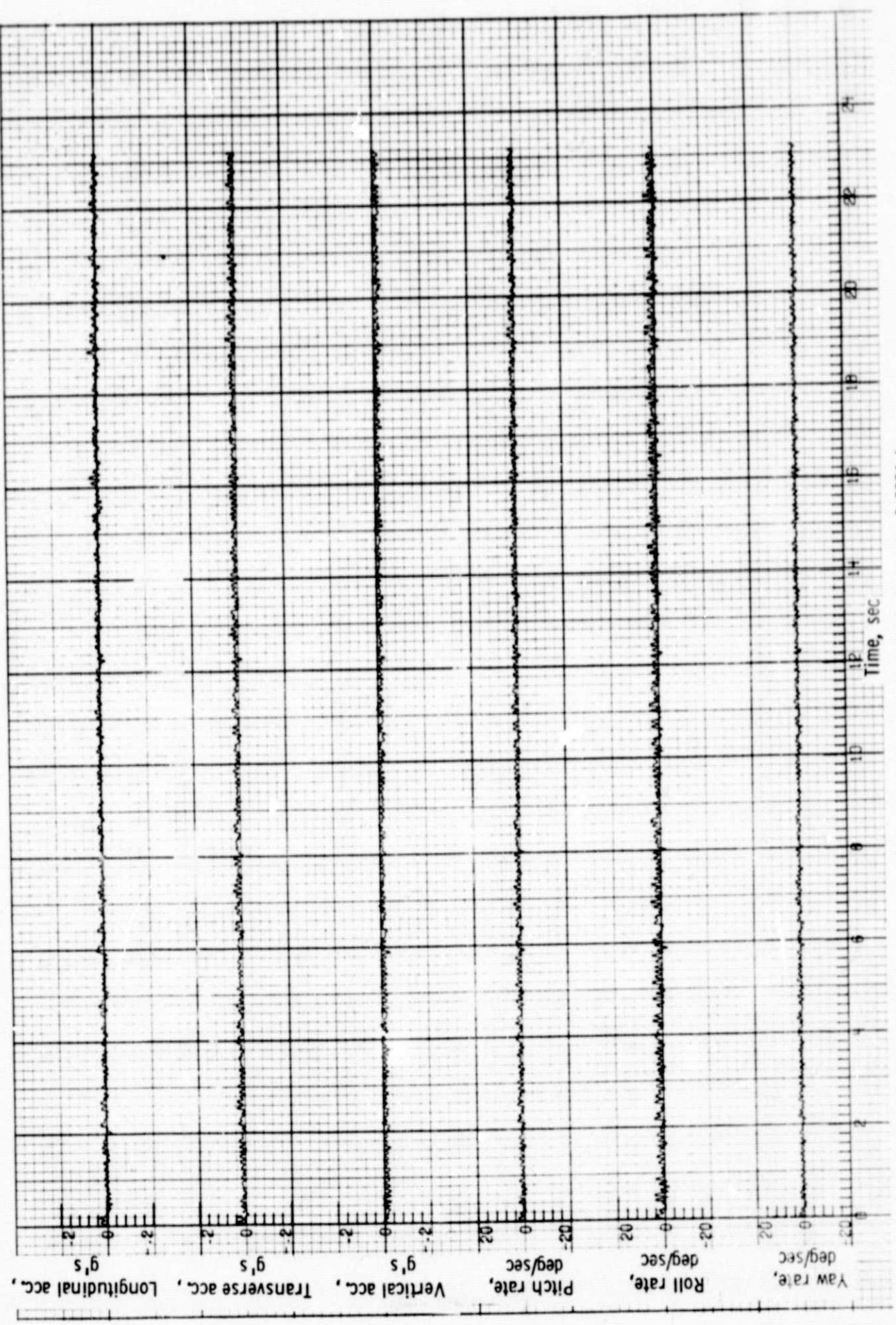
(c) Longitudinal acceleration power spectrum (RMS longitudinal acc. 0.0571 g).

Figure 8 - Continued.



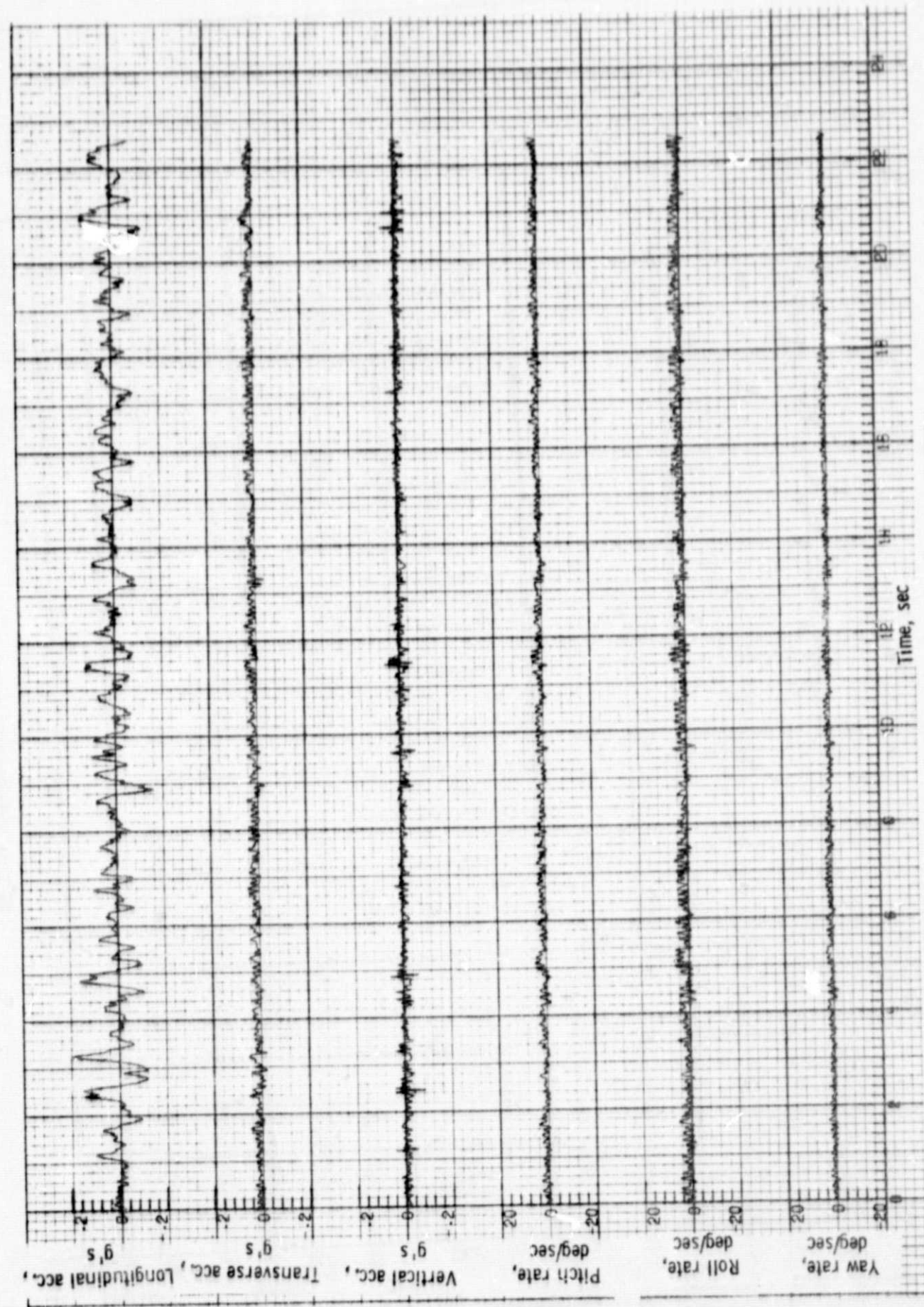
(c) Longitudinal acceleration power spectrum (RMS longitudinal acc. 0.0835 g).

Figure 8 - Concluded.



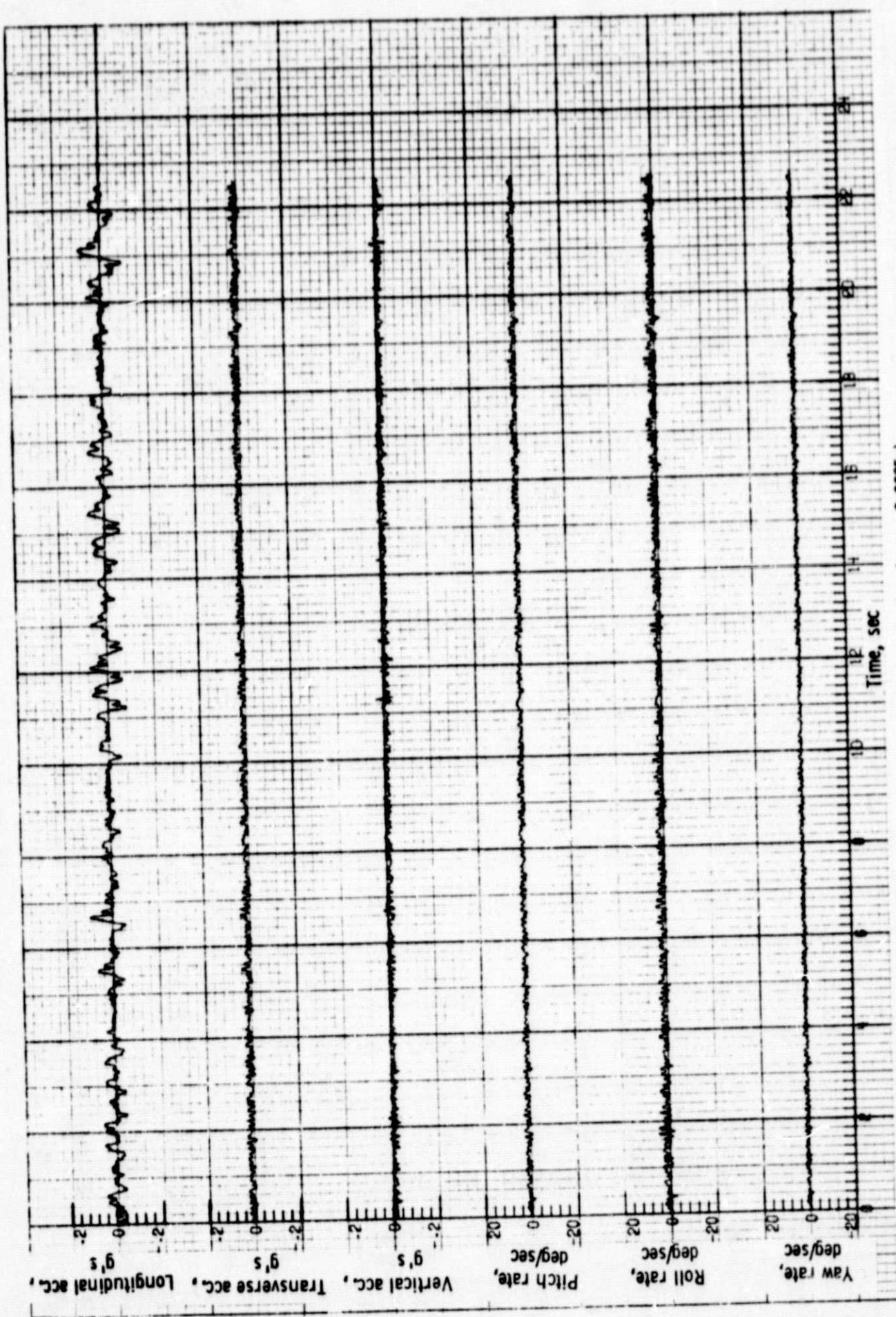
(a) Time histories (RMS longitudinal acc. 0.0086g).

Figure 9. Measured motion characteristics using longitudinal acceleration with flat 1-2 Hz inputs.



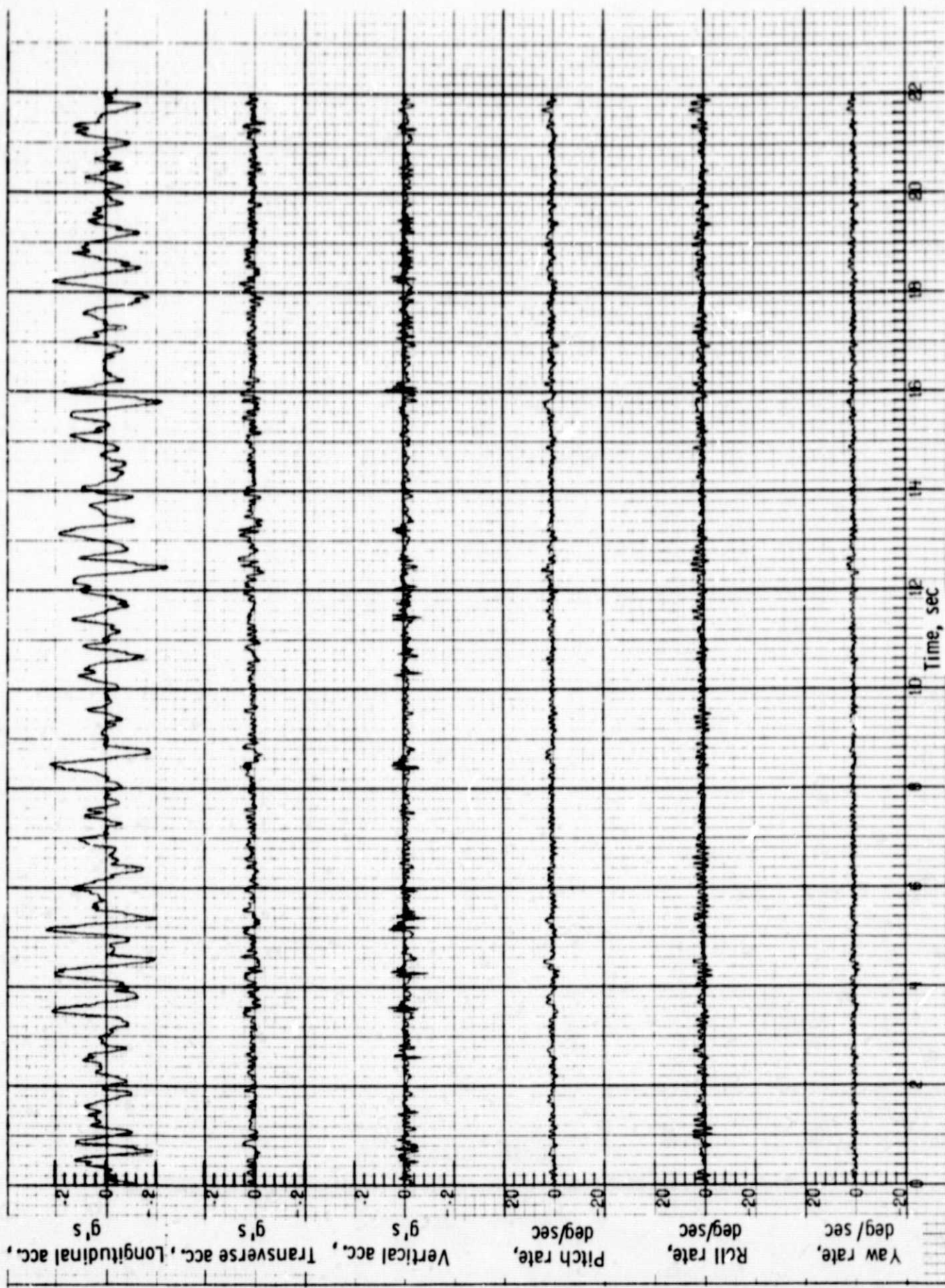
(a) Time histories(RMS longitudinal acc. 0.05(g)).

Figure 9. - Continued.



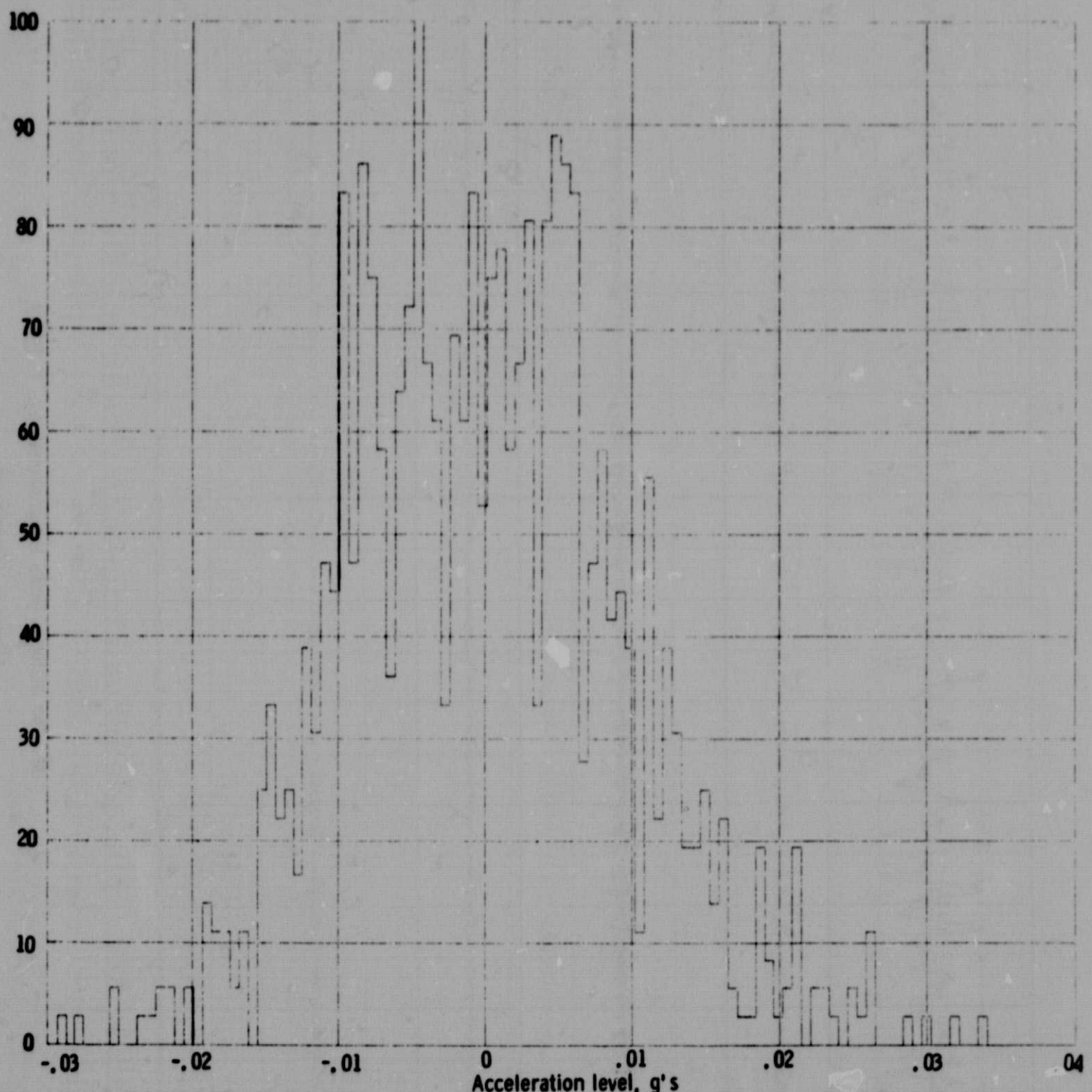
(a) Time histories/RMS longitudinal acc. 0.0225g.

Figure 9. - Continued.



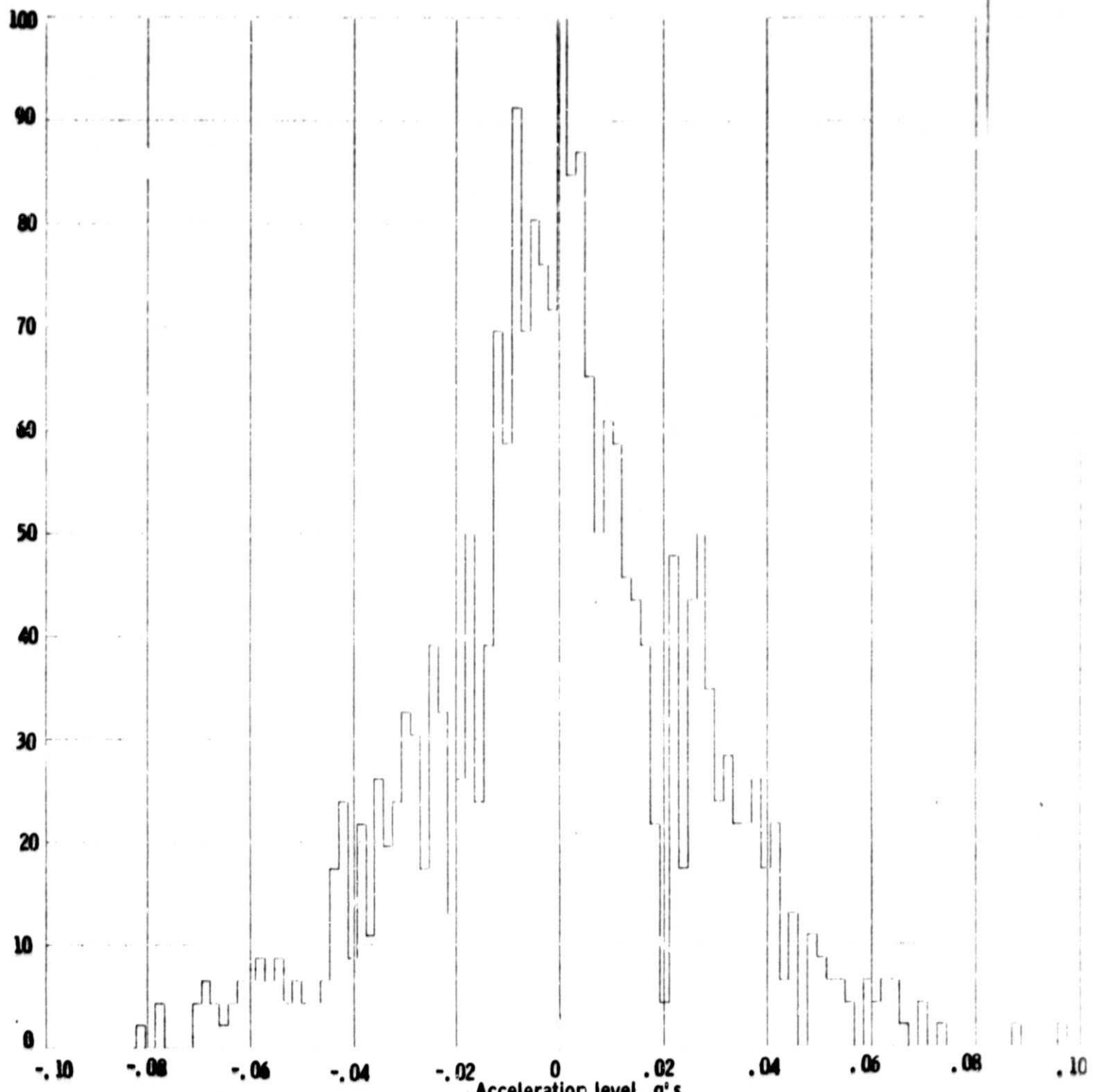
(a) Time histories (RMS longitudinal acc. 0.0790g).

Figure 9. - Continued.



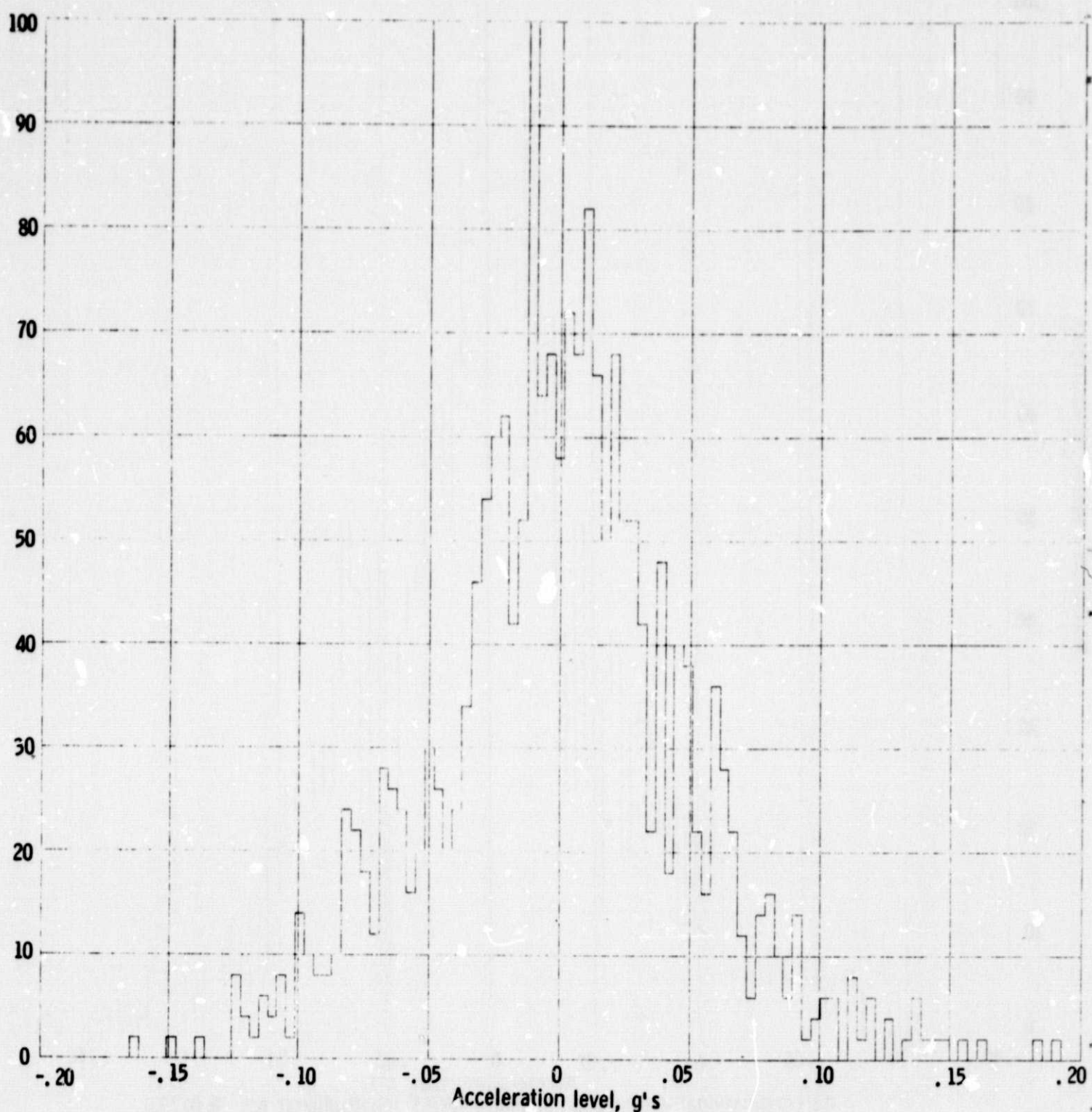
(b) Longitudinal acceleration histogram(RMS longitudinal acc. 0.0086 g).

Figure 9. - Continued.



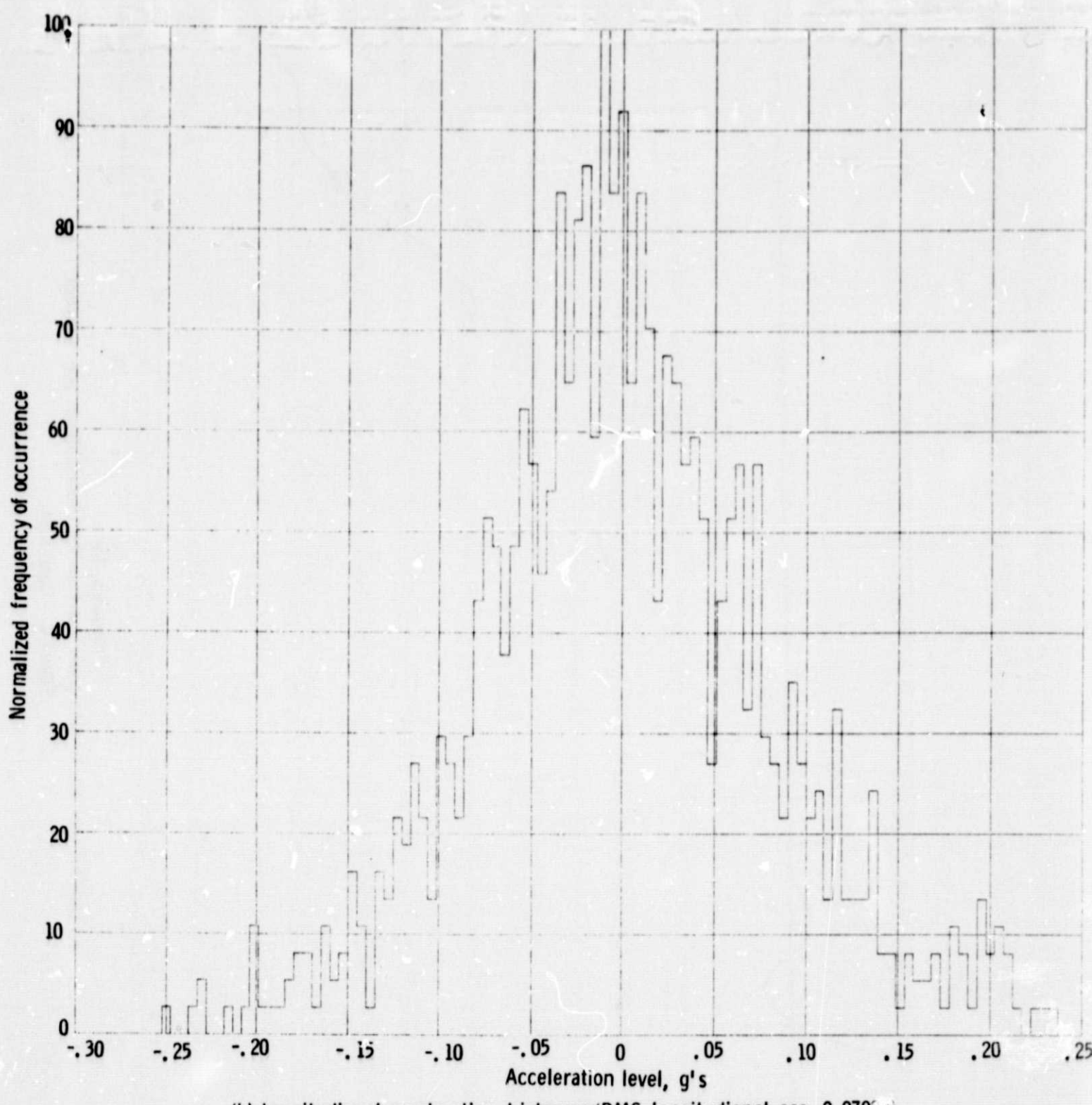
(b) Longitudinal acceleration histogram(RMS longitudinal acc. 0.0225g).

Figure 9. - Continued.



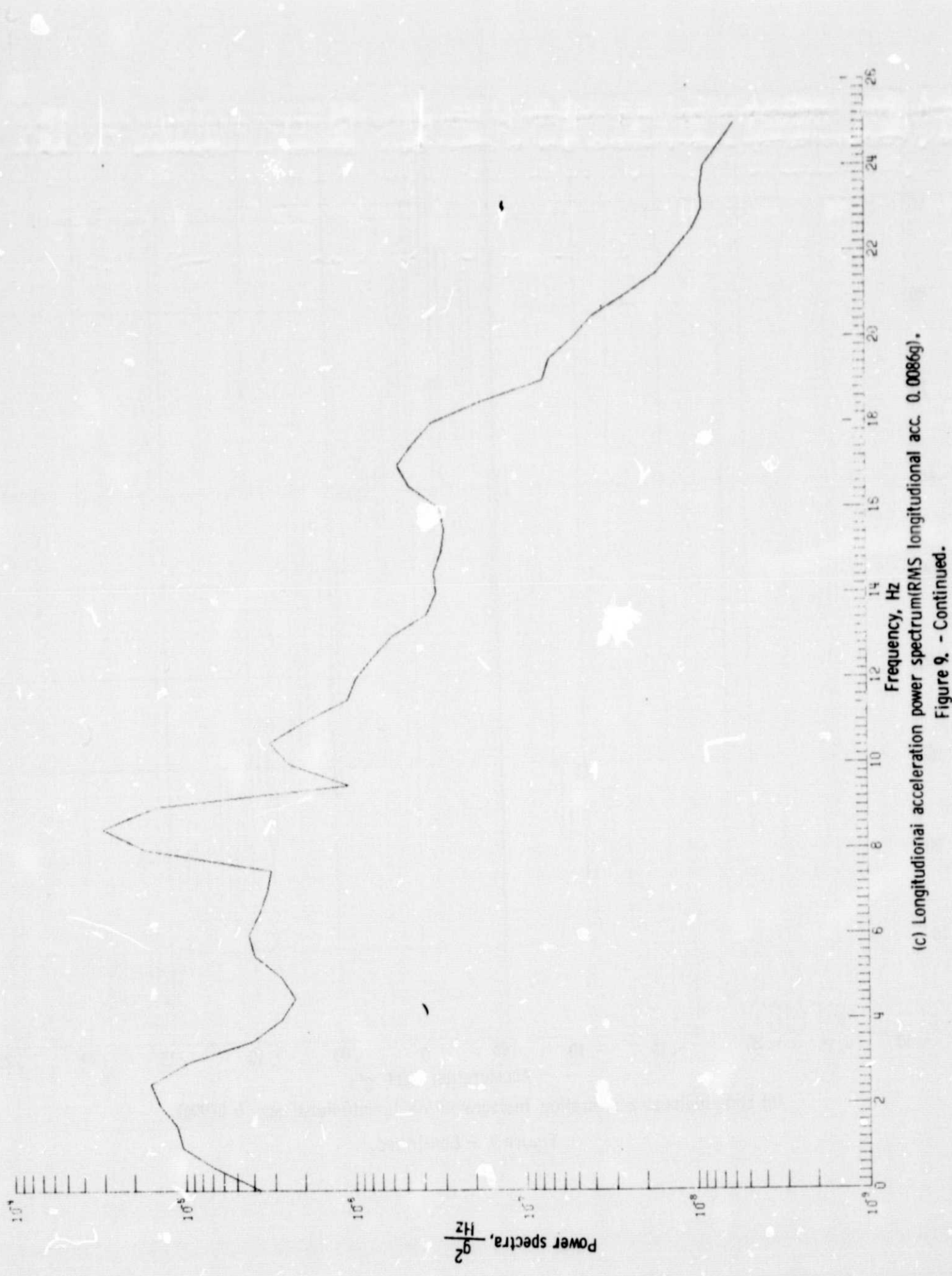
(b) Longitudinal acceleration histogram(RMS longitudinal acc. 0.0510g).

Figure 9. - Continued.



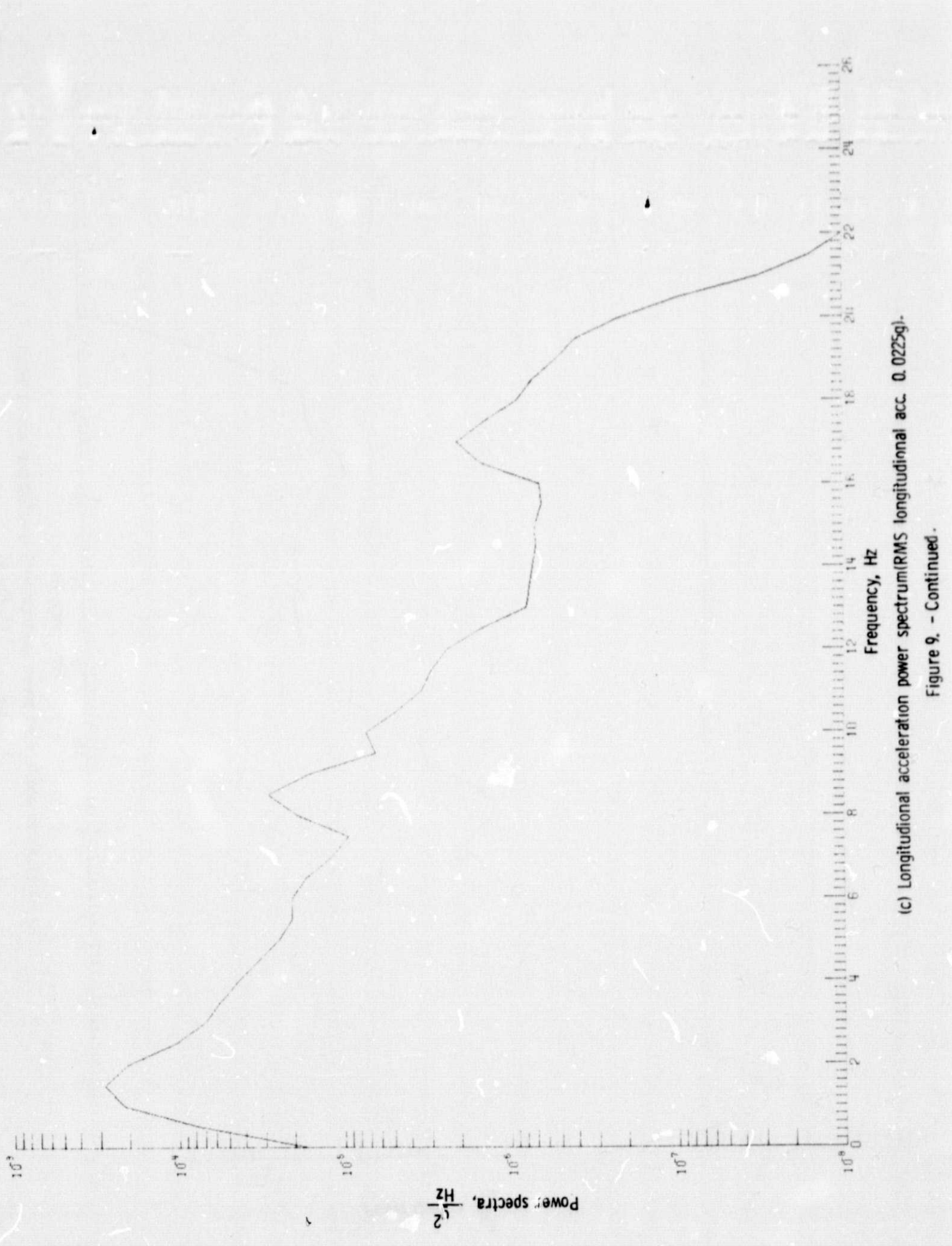
(b) Longitudinal acceleration histogram(RMS longitudinal acc. 0.079 $\text{g}_\text{J}$ ).

Figure 9. - Continued.



(c) Longitudinal acceleration power spectrum(RMS longitudinal acc. 0.0086g).

Figure 9. - Continued.

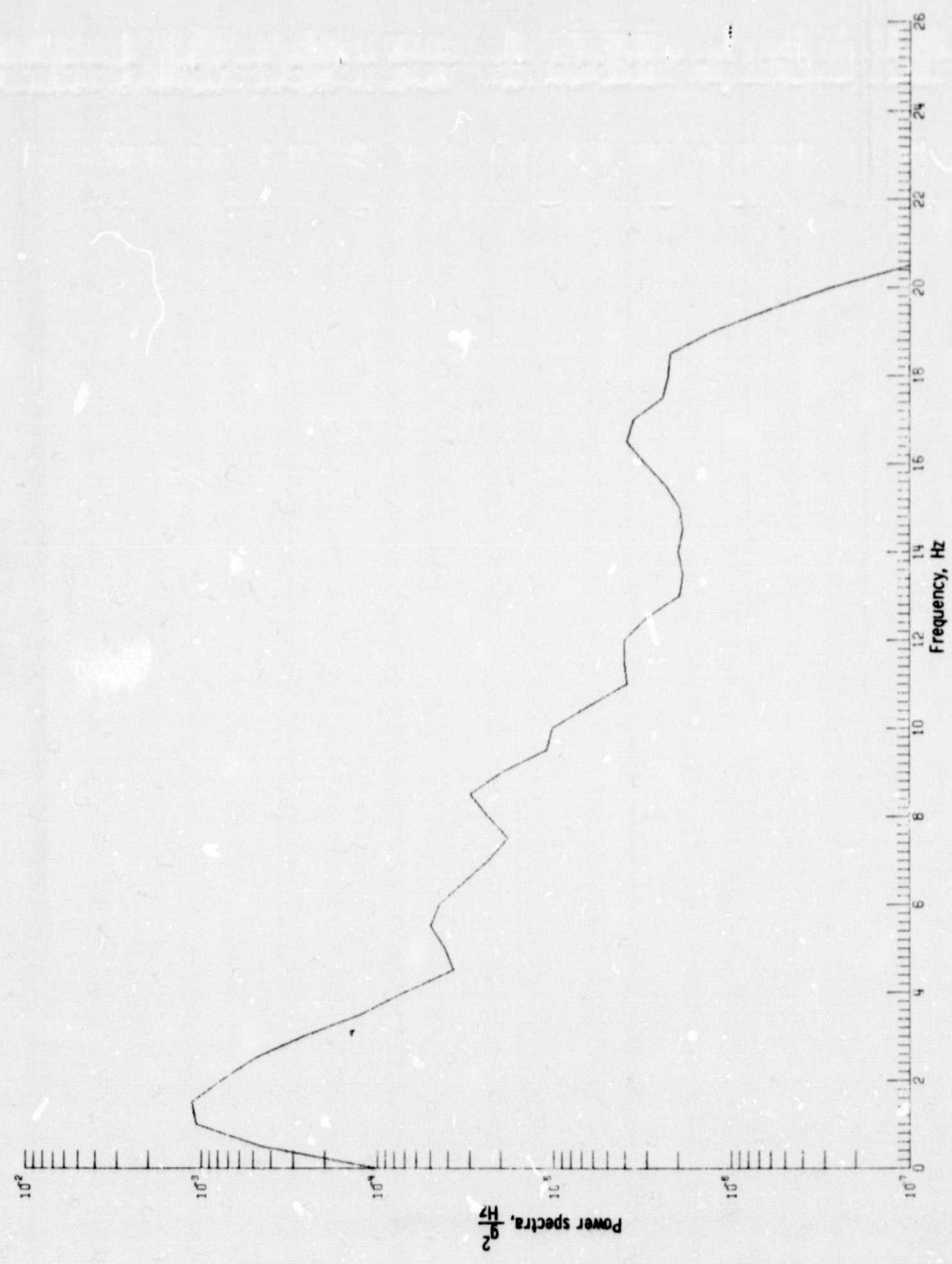


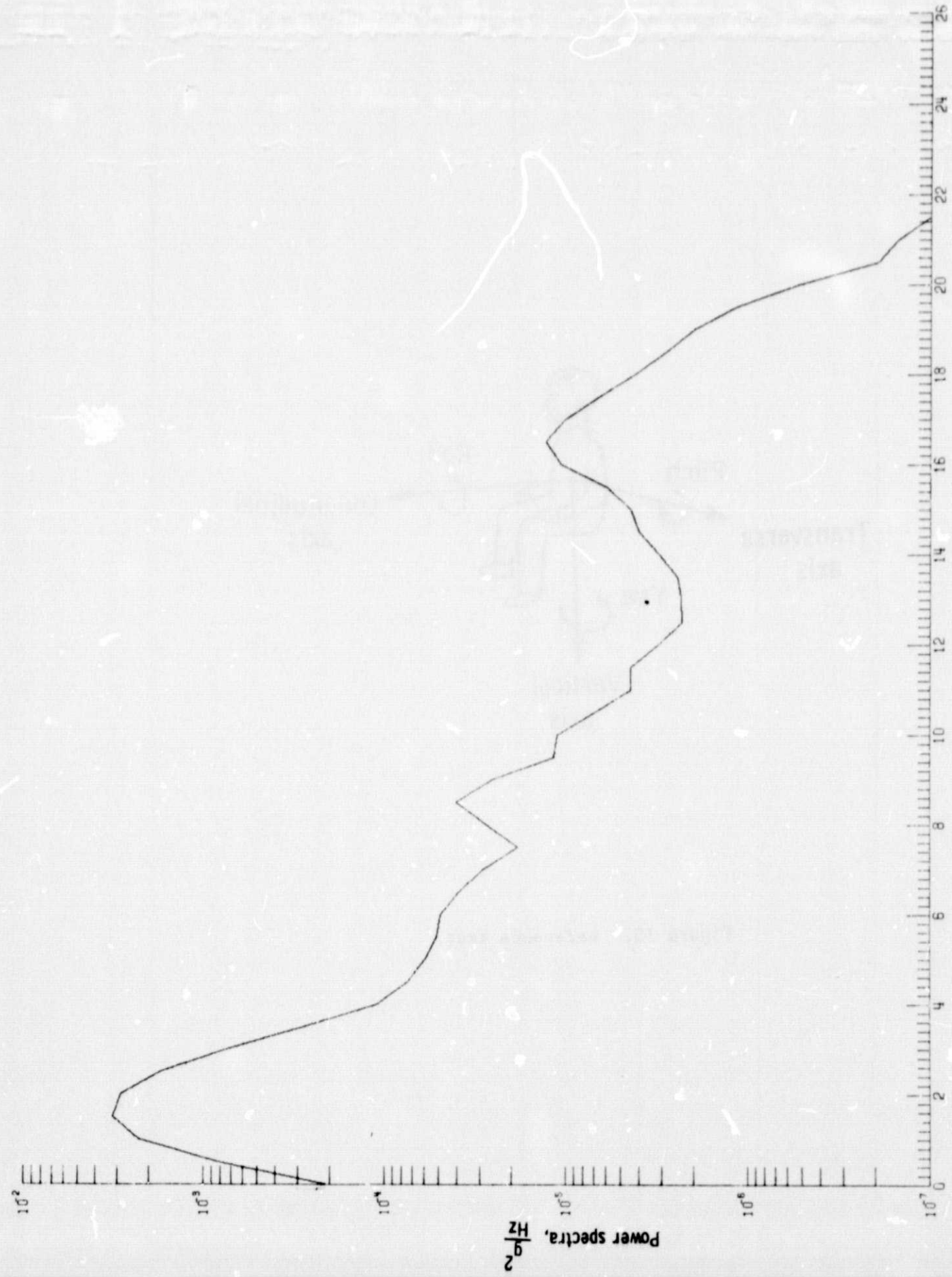
(c) Longitudinal acceleration power spectrum/RMS longitudinal acc. 0.025g).

Figure 9. - Continued.

Figure 9. - Continued.

(c) Longitudinal acceleration power spectrum(RMS longitudinal acc. 0.05log).





(c) Longitudinal acceleration power spectrum (RMS longitudinal acc. 0.0790g).

Figure 9. - Concluded.

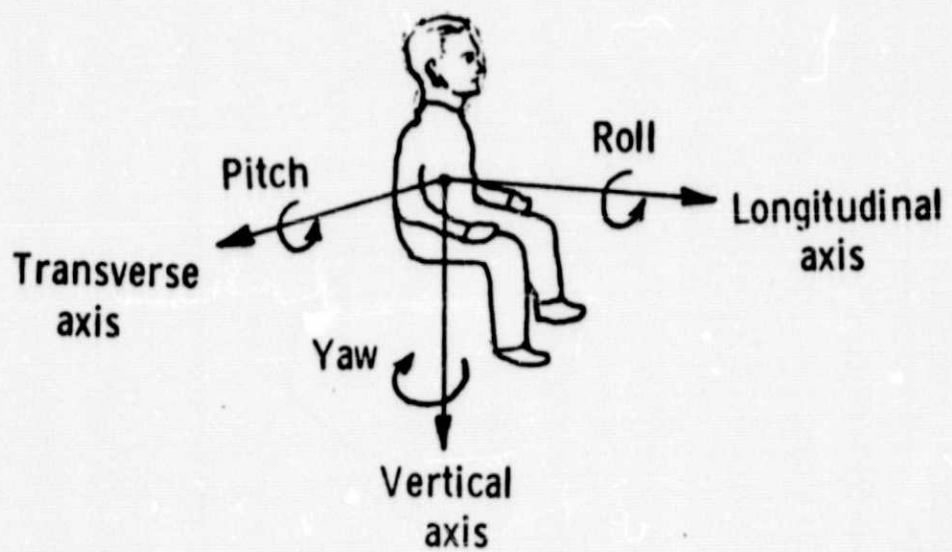


Figure 10.- Reference axes.

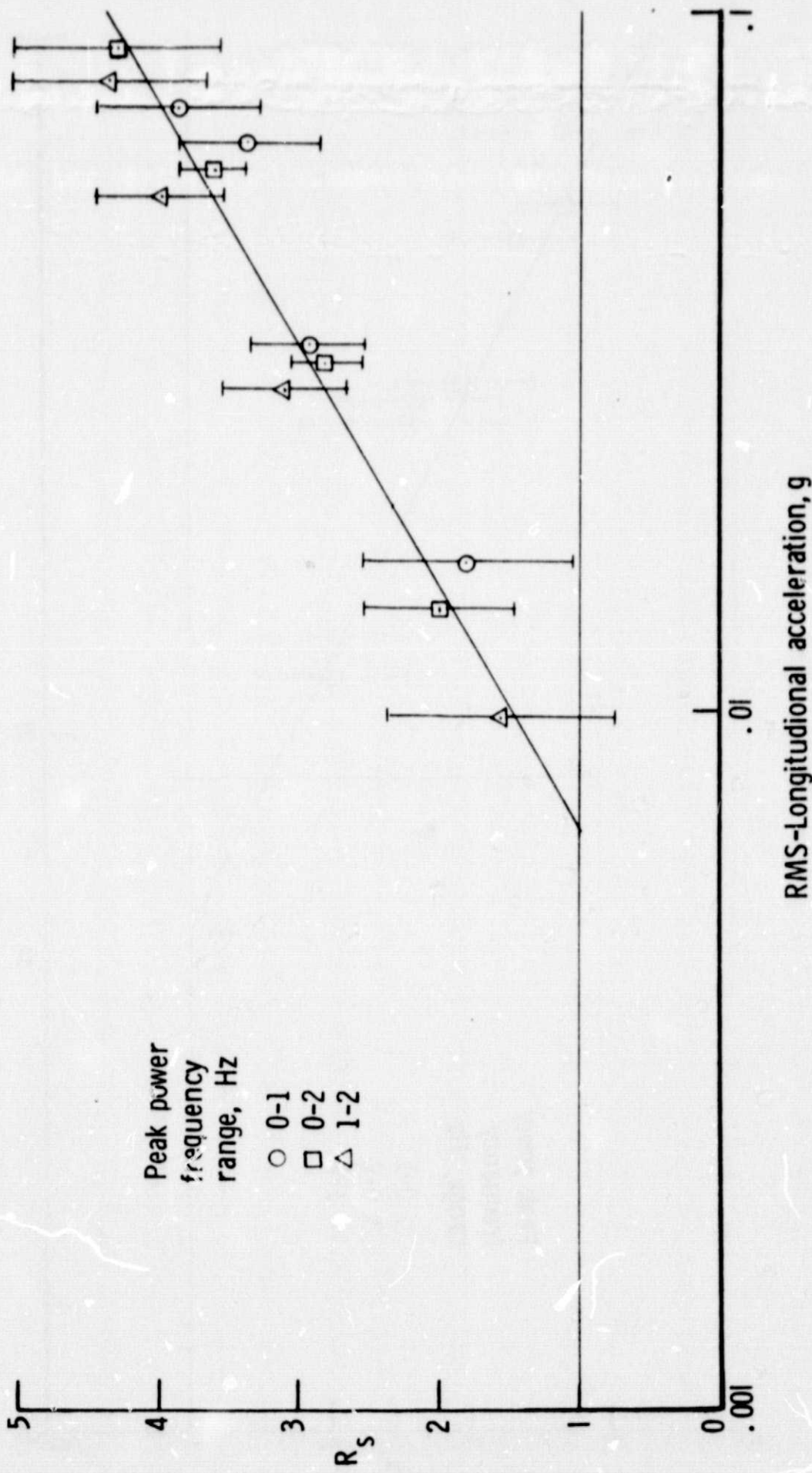


Figure 11.- Variations of ride comfort response with RMS longitudinal accelerations having typical power spectra.

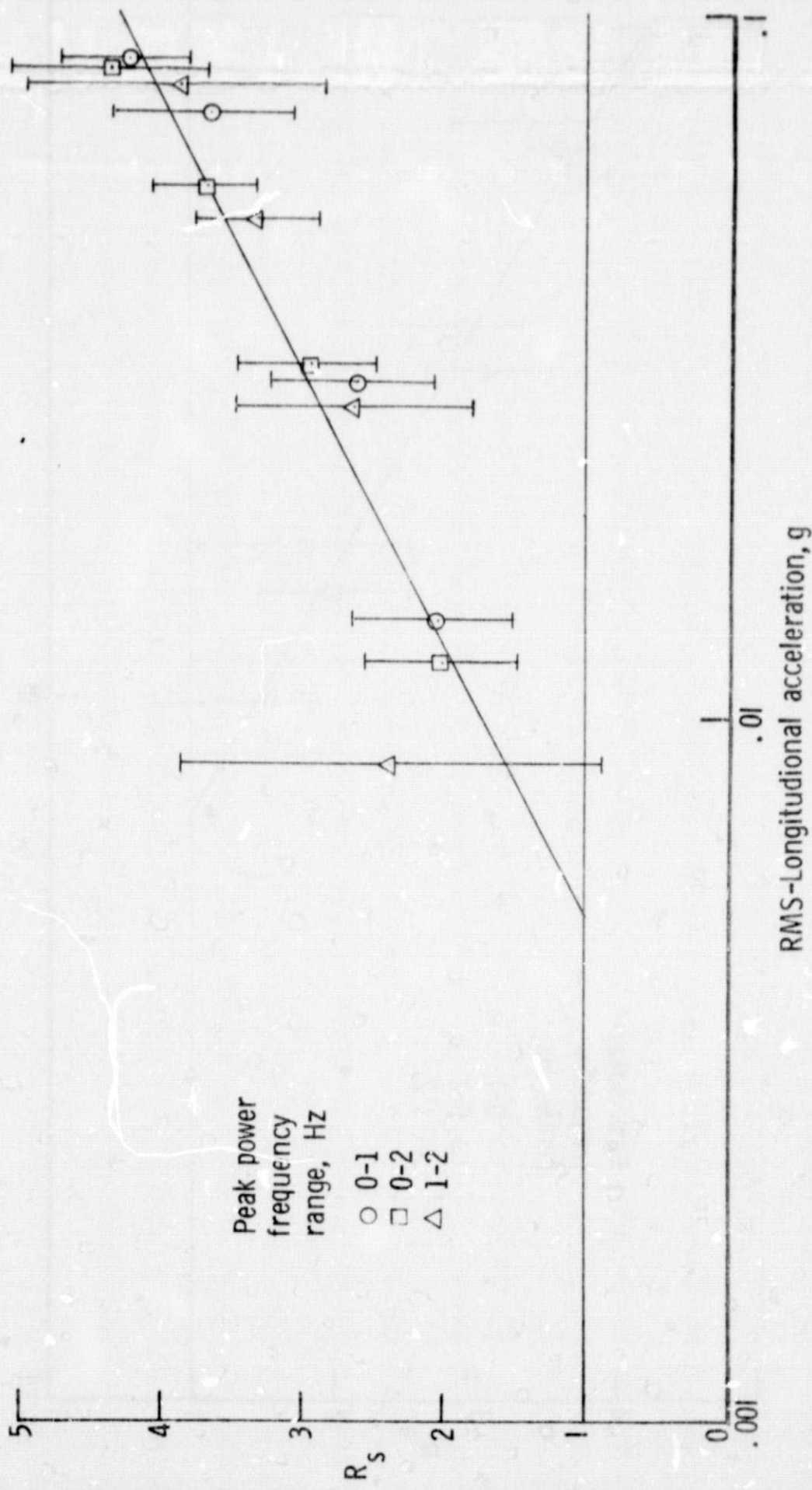


Figure 12.- Variations of ride comfort response with RMS longitudinal accelerations having flat power spectra.